Charles University in Prague
Faculty of Mathematics and Physics

HABILITATION THESIS

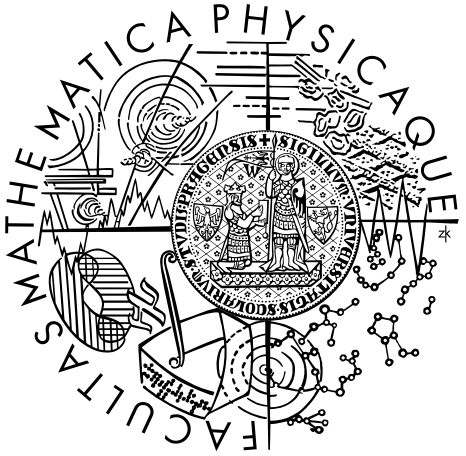

Mgr. Michal Žák, Ph.D.

Urban climate in Central Europe

Department of Atmospheric Physics

Prague 2021

Contents

Introduction

Cities are home to over 50 percent of the world population, and the urbanization has accelerated in the last decades. The change of natural environment in cities – especially use of artificial materials like concrete, asphalt, glass, metals, etc. leads to change of its atmosphere and even creation of its climate. Traditionally, air pollution has been the main hallmark of the urban atmosphere, as found in antiquity cities. This problem increased in the Middle Ages when coal-burning became widely used in larger cities, London being one of the best examples. And it was London that first appeared in the cornerstone of urban climatology. Luke Howard published the earliest book dealing with urban climate, i.e, with unique features of the city's climate, in 1818. Howard [1818] recognized a significant alteration of meteorological elements. The most important finding of Howard was identification of the warmer temperatures in the urban center compared to the surrounding rural areas. His studies laid the foundations of urban climatology and especially its main feature – the urban heat island. In the next decades of the 19th century, a number of monographic studies dealing with the climate of different cities appeared. This was supported by an increasing number of meteorological stations in city centers and in the countryside. For example, Johann Gregor Mendel is known as an outstanding geneticist. But he was involved in meteorology and climatology, too, and intensely focused on the climate of Brno, the second-largest city of Czechia (see, e.g, Dubec and Orel [1980]).

The rapid increase in urban areas' size after World War II led to deterioration of air quality, meteorological visibility and the alteration of other meteorological parameters. That supported a growing number of studies focussing on urban climate after 1950s. Among them, some remarkable comprehensive monographies can be found, like, e.g, Oke [1979] or Landsberg [1981].

As the cities become more extensive, the impact of urbanized areas on the environment becomes crucial. We can find many ways in which cities influence atmospheric conditions. Urban development modifies the radiative and thermal balance and moisture and aerodynamic properties of the surface. Fluxes and balances of heat, mass, and momentum are influenced by urban surfaces, too, creating a distinct urban boundary layer. This modification of local conditions in metropolitan areas can manifest in many meteorological elements and phenomena, like temperature, humidity, wind, clouds, fogs, sunshine, precipitation.

The main feature of the urban climate is urban heat island (UHI). The concept of the UHI was introduced already some 50-60 years ago Oke and Maxwell [1975]. Different radiative, thermal, hydrological and aerodynamical properties are the reason why city centres have a few degrees higher temperature than the outskirts of the city. This difference can be found in daily average temperatures, but the difference varies throughout the day. The differences are usually larger during the evening and night hours. In the morning, the so-called urban cold island (the situation reversed to UHI, e.g, Goncalves et al. [2018]) can build up for a few hours. The development of the UHI is strongly influenced by synoptic circulation (large-scale atmospheric conditions).

When studying the UHI, we usually talk about the intensity of the UHI, the temperature difference between the city center and the surrounding rural

areas – but sometimes it's not easy to compute this parameter since suitable meteorological stations are not always available (both, in the city centers and surrounding (Chapter 1)). The lack of surface observation can be partly solved by using remote measurement techniques, especially the satellite measurements (Chapter 2).

The UHI intensity is greatly correlated with the population of inhabitants and the city size. An increasing UHI intensity can be expected due to increasing number of the population living in the cities in the coming decades. But the UHI can have negative effects on the city's inhabitants, especially older people. For example, we can observe higher night-time temperatures making it difficult to achieve a comfortable temperature for sleeping and resting of inhabitants without air-conditioning. Uncomfortable conditions can occur during hot sunny days in outdoor spaces with artificial surfaces increasing heat stress, especially to vulnerable people. Finally, the higher energy demands caused by higher need of air-conditioning should be considered among the negative effects of UHI.

The adverse effects of the UHI will be very likely amplified during the heat waves that are expected to become more frequent due to global warming (e.g, Founda and Santamouris [2017]). For this reason, many studies and projects have been dealing with counteracting the negative effect of UHI, or generally of the urban climate, in the last few decades (see Chapter 3). To find the best solution for mitigating the UHI effect, modeling its impact in a combination with field measurement campaigns where possible is needed.

The above-mentioned main points of urban climate research, focused on the central Europe region, especially on Prague, are the basis of this thesis. It has been created as a summary and evolution of materials published in selected papers during my research career. The core is built up upon four stand-alone publications with my major or great participation, provided in the appendices and dealing in large part (though not exclusively) with urban heat island and climate and methods of their study:

- Zak, M, Nita, I, Dumitrescu, A, Sorin, C, 2020: Influence of synoptic scale atmospheric circulation on the development of urban heat island in Prague and Bucharest, *Urban Climate*, 34, DOI: https://doi.org/10.1016/j.uclim.2020.100681

  Appendix A (p. 37)

- Zak, M, Miksovsky, J, Pisoft, P, 2015: CMSAF Radiation Data: New Possibilities for Climatological Applications in the Czech Republic, *Remote Sensing*, 7 (11), DOI: https://doi.org/10.3390/rs71114445

  Appendix B (p. 51)

- Zak M, Zahradnicek P, Skalak P, Halenka T, Ales D, Fuka V, Kazmukova M, Zemanek O, Flegl J, Kiesel K, Jares R, Ressler J, Huszar P, 2016: Pilot Actions in European Cities – Prague. In: Musco F. (eds) Counteracting Urban Heat Island Effects in a Global Climate Change Scenario. Springer, Cham, DOI: https://doi.org/10.1007/978-3-319-10425-6_14

  Appendix C (p. 65)

- Karlicky, J, Huszar, P, Halenka, T, Belda, M, Zak, M, Pisoft, P, Miksovsky, J, 2018: Multi-model comparison of urban heat island modelling approaches, *Atmospheric Chemistry and Physics*, 18, DOI: https://doi.org/10.5194/acp-18-10655-2018

Appendix D (p. 94)

Additional supporting materials have been adapted from the following publications, too, though they are not enclosed within the thesis:

- Halenka, T, Belda, M, Huszar, P, Karlicky, J, Novakova, T, Zak, M, 2019: On the comparison of urban canopy effects parameterization, *International Journal of Environment Protection*, 65, 177-194.

- Huszar, P, Karlicky, J, Doubalova, J, Sindelarova, K, Novakova, T, Belda, M, Halenka, T, Zak, M, Pišoft, P, 2020: Urban canopy meteorological forcing and its impact on ozone and PM2.5: role of vertical turbulent transport, *Atmospheric Chemistry and Physics*, 20, 1977–2016

Finally, to provide a complete picture of the discussed topics, selected fragments of yet unpublished analyses or those currently under preparation were also included.

While the topics covered in this thesis vary substantially in terms of used methods, examined datasets, and sometimes even in the purpose of the particular analyses, joint themes can be highlighted. The general subject of urban heat island study pervades in my past research, from connection to synoptic-scale circulations (Zak et al. [2020]) through observing and detecting methods of the UHI, the problem of stations availability including remote sensing methods for climatological analyses (Zak et al. [2015]), to study of the adverse UHI effects on urban inhabitants (Zak et al. [2016], Zahradnicek et al. [2014]). The issue of modeling the UHI effects and its connections to air quality issues also permeates through some of my past work (Huszar et al. [2020], Halenka et al. [2019], Karlicky et al. [2018]).

Despite the obvious topical diversity of the problems addressed here and the resulting specificity of the conclusions reached, general insight regarding the specific features of the urban climate in central Europe can be found. These are provided in the following chapters of this thesis. As already mentioned above, four main themes are discussed in four topically focused (though still partly overlapping and interrelated) segments. Chapter 1 shows the specifics of urban heat island in central Europe, including a discussion of station selection for urban climate study. Chapter 2 deals with remote sensing methods possibilities in climatology, with a focus on UHI analyses. Chapter 3 addresses the adverse effects of the UHI, focusing on thermal comfort, and briefly describes the possibilities of UHI mitigation or counteraction with a description of experiences gained for the city of Prague. The modeling approach of the UHI evolution and its effects on urban weather conditions are explored in Chapter 4. Finally, summarizing and concluding remarks are provided in Conclusion, together with some thoughts on our related ongoing and future research.

1. Urban heat island in Central Europe

Urban heat island (UHI) is relatively common phenomenon of metropolitan areas and a typical feature of their climate. UHI is manifested by significantly higher temperatures in urban areas compare to their surroundings (with either rural or non-urban characteristics). There are many reasons for the UHI occurrence, most of them are relatively well understood (e.g. Landsberg [1981], Oke [1982], Arnfield [2003]).

The main cause is connected with the modified physical characteristics of materials used in the urban areas. The artificial surfaces (of e.g. concrete or asphalt) are absorbing much more solar radiation compared to the natural surfaces. This lead to surplus heating of the surfaces. Therefore surfaces emit long-wave radiation, especially during nocturnal hours. Another factor leading to the increase of temperature is antropogenic heating. It is created by waste heat released during energy consumption (cooling, heating, transportation, industry etc.), called anthropogenic heating. It can be mathematically described through the surface energy balance model (Oke [1988]):

$$R_n + F = H + LE + S + A \tag{1.1}$$

where R_n is the net all wave radiation; F stands for the anthropogenic heating; H stands for sensible heat (that heats the air in the city); LE is the latent heat (i.e. the heat required to convert a solid into a liquid or vapour); S represents heat storage (absorbed e.g., by building materials); and A is the advective heat flux . Heat and energy (left side of 1.1) is mostly stored in materials with low albedo and higher roughness (e.g. asphalt), while lawn, parks, trees etc. act as a heat sink. Therefore, urban areas with artificial materials experience higher temperatures than vegetated areas.

The UHI effect can be explored in three ways according to their measurement altitudes: boundary UHI, canopy UHI, and surface UHI (Zhang et al. [2009]). Boundary UHI can be understand from the rooftop's level to the atmosphere (Mirzaei and Haghighat [2010]). It investigates the UHI effect at mesoscale point of view (from 1 to 10 000 km^2) and can be for example studied by help of radiosondes (Voogt [2007]).

Canopy UHI is considered from the surface to the rooftop (Krayenhoff and Voogt [2007]). Analyses of the canopy UHI are usually the object of microscale studies and the main input data are obtained from weather stations (Kato and Yamaguchi [2007]). Surface UHI is a feature of the earth's surface level and is usually explored by satellite images (see Chapter 2) to derive the surface UHI effect.

The magnitude of the UHI effect can be expressed in terms of Urban Heat Island intensity. This parameter is obtained as the temperature difference (usually in °C) between urban and rural (or non-urban) temperatures measured simultaneously. The intensity of UHI is greatly influenced by e.g., land-use, population density, vegetation, density of built-up area (e.g., Landsberg [1981], Oke [1982, 1988]). Meteorological conditions can also influence UHI magnitude, as was con-

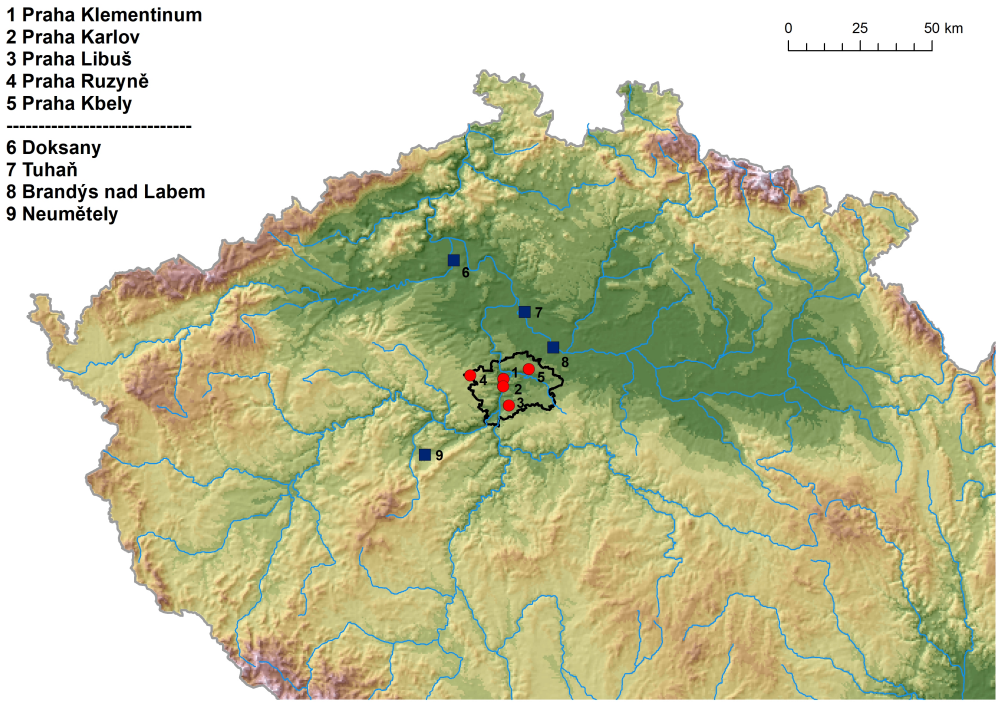

Figure 1.1: Locations of surface climatological stations traditionally used for studying the UHI of Prague.

firmed by many papers (e.g., Sakakibara and Matsui [2005], van Hove et al. [2015]).

Our research focused on central Europe, especially on Prague, the Czech Republic's capital city. Prague's urban heat island has been studied several times, usually using the traditional comparison of urban-rural long-term station pairs. These results have provided information about the UHI of Prague's intensity, its annual course, and long-term changes under climate change. For the city of Prague, such pair of stations usually involves Prague, Klementinum station situated in the very city centre, being one of the stations with the longest continual temperature records in Europe (world), starting in 1775. Of course, as many old urban stations are situated in the heart of a city, its location is not representative of the WMO (World Meteorological Organization) guidelines (placing of the screen with thermometers). But it mirrors the influence of densely built-up area of the city center very well. Before automatization in 2013, only three measurements per day were carried out (7, 14, and 21 o'clock local time); after automatization, 10-minutes observations are available. Another station suitable for UHI study in Prague is the Karlov station, which can be found approximately 2 kilometers from Klementinum (in the building where the office of Dean of the Faculty of Mathematics and Physics of Charles University is situated). This is a so-called synoptic station providing hourly measurement, not only of temperature, but full range of meteorological parameters and phenomena (including wind, cloudiness, sunshine duration, radiation, humidity etc.), i.e., variables needed for calculation of the thermal comfort parameters (see Chapter 3).

As a "rural" station of the stations-pair, either airport stations (typically Ruzyne, sometimes Kbely) are used – both of them being synoptic stations and

therefore providing the hourly data with the full range of meteorological parameters; or some of the stations outside of the city of Prague – usually any of the following climatological stations: Dobřichovice, Brandys nad Labem – Stara Boleslav, Tuhaň, Neumětely or Doksany (see Fig. 1.1). All the stations are operated by the Czech Hydrometeorological Institute, that is also responsible for quality checks.

When analyzing the UHI based on station-pairs, it is not always easy to find the best-suited combinations; therefore, more stations have sometimes been used. Besides the question of sufficient data record (full length, all parameters needed), we have to deal with different altitudes of the station used. Another point to be mentioned is the suitability of station selection based on how the UHI effect is mirrored in the measurement. Regarding the effect of the UHI on the day-to-day temperature variability, the Czech Republic area has been (to our best knowledge) for the first time studied in Zak et al. [2019b]. For this purpose, the difference between the day-to-day variation of daytime maximum temperatures and night-time minimum temperatures has been used. Statistical methods based on Anderson et al. [2018] paper were applied, with day-to-day (DTD) temperature variability expressed as follows:

1) absolute difference between the ambient temperatures of adjacent days:

$$DTD = \frac{\Sigma_{i=1}^{N}(T_i - T_{i-1})}{N-1} \tag{1.2}$$

2) the difference between the DTD variation of daytime temperatures and night-time temperatures:

$$\triangle DTD = DTD(T_{max}) - DTD(T_{min}) \tag{1.3}$$

Urban sites are characterized by positive (i.e., daytime DTD(Tmax) exceeds night-time DTD(Tmin)), or less negative values, while rural sites are characterized by negative (i.e., night-time DTD(Tmin) exceeds daytime DTD(Tmax)), or less positive values. DTD values show seasonality with peak for minimum temperature in winter months (when the highest albedo of surfaces occurs, leading to less energy storage) and minimum in July (opposite conditions). When applied to Prague's stations, urban effects can be clearly detected for Karlov and Klementinum stations. On the other hand, some stations usually classified as rural when performing UHI analysis of Prague do not exhibit the $\triangle DTD$ metric's variation expected to be associated with a typical rural station (Fig. 1.2).

The development of the UHI phenomenon is strongly influenced by large-scale (synoptic) circulation. Under high pressure areas, the conditions are generally more favorable due to smaller cloudiness (i.e., higher direct radiation) and usually weak winds (Morris et al. [2001]). The mutual position of the city and anticyclone is important for the UHI development, since it influences the prevailing wind direction. Especially during winter season the low cloudiness under high pressure area conditions can develop and obscure the radiation weather development in the city. This can apply to wind, too. If the wind becomes too strong, the development of the UHI is hindered or suppressed. For Prague, the wind field over the city was simulated with the help of Calmet Modell (Scire et al. [2000]). This simulated wind speed and direction are much more convenient to

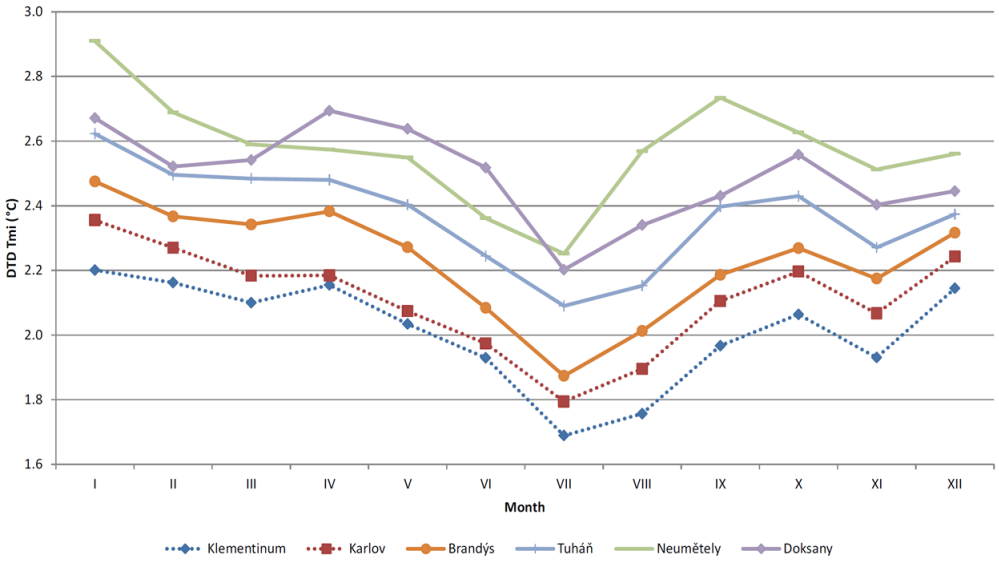

Figure 1.2: Monthly values of DTD for minimum temperatures.

study the connection between UHI development and wind speed because station measurements of wind in the urban area usually suffer from a lack of representativity. Based on these simulations, it was found that Prague's UHI vanishes when windspeed surpass 8 $m.s^{-1}$ (e.g., Zak and Skachova [2010]).

The lowest UHI intensity occurs under cloudy and windy conditions, but not necessarily under cyclonic influence. Many studies focus on UHI development's during clear sky and weak wind, i.e. under optimal conditions. In contrast, the number of papers deeply studying relationship between the UHI intensity and different synoptic conditions is much smaller (e.g., Beranova and Huth [2005] for Prague; Polrolniczak et al. [2017] for Poznan, Poland; Beck et al. [2018] for Augsburg, Germany, or Kircsi and Szegedi [2003] for Szeged, Hungary). These studies are often using special measuring campaign data with high density of observations points but usually with short time period (few years), i.e., not suitable for capturing climate trend of UHI behavior. For Prague, such study was first done in 2005 (Beranova and Huth [2005])) using data from the 1961–1990 period, based on the Bradka synoptic catalog. This catalog distinguishes cyclonic/anticyclonic and directional characteristics (Bradka et al. [1961]). Beranova and Huth [2005] suggested that the North to North-East and South to South-West synoptic flows increase the Prague's heat island. However, it has to be mentioned that subjectivity of Bradka synoptic catalog has to be taken into account.

Therefore, in our research, an objective classification scheme of synoptic (weather) types was used for this purpose, the GrossWetterTypen (GWT) classification scheme of atmospheric circulation based on threshold criteria, like degrees of zonality, meridionality and vorticity of the large scale of MSLP field. This analysis deals with a period of 35 years between 1981 and 2016, i.e. a period greatly influenced by the developing climate change. Details can be found in Appendix A. Based on results of our research, the following points/main features of the UHI of Prague during last 60 years can be found:

1. UHI of Prague is a very pronounced and quite robust all-year-round feature of Prague's climate.

2. The UHI intensity varies between 2 °C and 2.5 °C based on daily minimum temperatures, with the highest values reached in August.

3. The maximum values of UHI intensity can exceed 4 °C (over 6 % of days, based on minimum temperatures).

4. The UHI intensity derived from mean and maximum temperatures is generally smaller (especially for the maximum temperatures) than minimum values.

5. City enlargement, traffic increase and changing of green spaces into buit-up areas have long-lasting magnified the UHI intensity in Prague, with a linear trend of around 0.13 °C / decade for daily minimum temperature.

6. UHI of Prague develops particularly under anticyclonic synoptic types, when south- to southwesterly wind prevail supporting warm air advection.

7. Fewer days of snow cover in the city center during the winter months have contributed to the increasing UHI intensity in winter season.

Although the results about UHI mentioned above are mainly connected with Prague, I also cooperated with colleagues from other countries in Europe, especially during the "UHI" project (Development and application of mitigation and adaptation strategies and measures for counteracting the global Urban Heat Islands phenomenon, 2011-2014), and particularly with urban researchers in Slovakia and Romania. Based on this cooperation, some interesting papers and conference proceedings were produced, dealing with Prague and Bratislava's similarities, and, especially, Bucharest. Despite Bucharest's distance from Prague, some similarities can be found in their physical-geographical background. The similar orographic features (with depression-like structures) partly affecting the synoptic scale circulation make them an interesting pair for comparison from an urban climate research point of view. Finally, both cities have experienced significant changes during the economic and political transition after 1990, which influenced their structure, industry, and transport characteristics.

2. Remote sensing approach

Regardless of its size, every settlement influences the meteorological elements. These influences have been traditionally studied with data from meteorological stations situated in the city and outside of the urban areas to describe the differences between them. Although there can be some difficulties when searching for the representative stations characterizing both areas (see Chapter 1), we usually can find suitable stations for larger (especially capital) cities describing either rural or urban areas. But when attempting to describe spatial features of urban climate and/or urban heat island, we are usually facing a lack of observing stations. Sometimes detailed information can be obtained by unique measuring campaigns (e.g., special rides with instruments investigating the urban environment or engaging a large number of measuring points), but these are usually time-limited and quite expensive. If a broader and more complex view of urban climate is required, remote sensing methods and its data can be used. These data were firstly available in the last decades of the 20th century as the satellite capabilities had developed and the spatial resolution of data provided increased. Further development occurred during the first two decades of the 21st century. Together with extending the length of data records, applicability in climate research has become more and more available.

For the European region, many climate data applicable for climate analyses can be obtained from the Satellite Application Facility on Climate Monitoring (CMSAF); details can be found at the webpage cmsaf.eu. CMSAF is one of eight Satellite Application Facility (SAF) of the EUMETSAT (European Organisation for the Exploitation of Meteorological Satellites). CMSAF provides both operational products and long-term datasets. We have been widely working with these data, and bringing them more into climatological community in the Czech Republic. A general overview and discussion of possibilities of using CMSAF data in the Czech Republic was given in the paper (Zak et al. [2015]). It can be found in Appendix B of this thesis. Based on these experiences, Prague's UHI has been studied from the remote sensing point of view.

Generally, when studying urban climate or UHI from a remote sensing perspective, we have to deal with another approach compared to surface observations. One aspect deals with the limited horizontal resolution, the second one with time resolution, and of course, different parameters are usually available compared to the meteorological station measurements. Horizontal resolution differs according to which type of sensor and satellite is used – in the best case, the resolution in central Europe varies between tens of meters to few kilometers with higher resolution available from polar-orbiting satellites compared to geostationary satellites. The temporal resolution is much higher for data coming from geostationary satellites (usually 15 minutes to 1 hour), while we usually have just a few observations from polar-orbiting satellites per day. This discrepancy between temporal and spatial resolution influences our decision of which data to use. If we focus more on detailed evolution throughout the day then geostationary data would be better for the analysis. If the spatial features are more important polar-orbiting data would be preferred.

Due to its measurement method, satellite data provide different pictures of

surface or close-to-surface climate compared to meteorological stations. For urban climate, traditionally, land surface temperature (LST) is the most used parameter. LST is the primary parameter when studying the physical processes of surface energy and water balance both on local and global scale (e.g. Li et al. [2013]). Knowledge of the LST provides information on the surface equilibrium state's temporal and spatial variations and is of a great importance in many urban climate applications. Therefore, LST has become quite popular among urban researchers (see e.g., Yang et al. [2020]) worldwide some years ago.

LST provides information about the thermodynamic temperature of the skin layer of a given surface. It tells us the how cold or hot the Earth's surface would be to the touch. It is a kinetic quantity without wavelength dependence. For ground-based, airborne, and spaceborne remote sensing instruments, LST is the aggregated radiometric surface temperature, i.e., based on a measure of radiance (Norman and Becker [1995]) ensemble of components within the sensor field of view. LST can be described as aggregated radiometric surface temperature obtained from combination of measurement of satellite-remote sensing instruments, airborne and ground based radiometric measurements.

The LST data can be obtained by mechanism described by Guillevic et al. [2018] as follows: *under clear sky conditions, the top of atmosphere radiance measured by a spaceborne sensor ($L_{sat,\lambda}$) includes contributions from the surface emission, the atmospheric upwelling radiance ($L_{\uparrow sky,\lambda}$) and atmospheric downwelling radiance ($L_{\downarrow sky,\lambda}$) reflected by the Earth's surface and attenuated by the atmosphere. Retrieval algorithms rely on one or more top-of-atmosphere spectral measurements to account for atmospheric effects and estimate LST:*

$$L_{sat,\lambda} = [\epsilon_\lambda B_\lambda(LST) + (1 - \epsilon_\lambda L_{\downarrow sky,\lambda})]\tau_\lambda + L_{\uparrow sky,\lambda}, \tag{2.1}$$

where ϵ_λ is the spectral emissivity at wavelength λ or representative of a specific (relatively narrow) domain [λ1, λ2] centred on wavelength λ, $B_\lambda(T)$ is the Planck function describing the radiance of a black body at temperature T, and τ_λ is the atmospheric transmittance.

LST product can be obtained from different instruments, e.g., sensor of Moderate Resolution Imaging Spectroradiometer (MODIS) aboard Aqua and Terra satellites or the Spinning Enhanced Visible Infrared Imager (SEVIRI) flying aboard METEOSAT satellites. These two primary sources were used in our work and analyses.

MODIS LST product from NASA is based on split-window approach and have a spatial resolution of 927 m at nadir. When the scan angle increases up to 65 degrees, the spatial resolution of the sensor degrades to about 6 km. Two bands - 31 (T31) centered on 11.03 μm and 32 (T32) centered on 12.03 μm - of brightness temperatures from MODIS are used to derive LST value by the generalized split-window algorithm (Wan and Dozier [1996]):

$$LST = b_0 + (b_1 + b_2\frac{1-\epsilon}{\epsilon} + b_3\frac{\triangle\epsilon}{\epsilon^2})\frac{T_{31}+T_{32}}{2} + (b_4 + b_5\frac{1-\epsilon}{\epsilon} + b_6\frac{\triangle\epsilon}{\epsilon^2})\frac{T_{31}+T_{32}}{2} \tag{2.2}$$

where ϵ and $\triangle\epsilon$ are the mean and the difference of the emissivity values in bands 31 and 32. The coefficients b_k (k = 0 to 6) are influenced by surface air temperature (Tair), viewing zenith angle and water vapor content. They

differs for day and nighttime (details can be found in Wan and Dozier [1996]). The spectral emissivity values in bands 31 and 32 is obtained from combination of senescent and green components (Snyder et al. [1997]). Satellites overpass central Europe twice during daytime and twice during nighttime.

CMSAF provide wide range of products from radiation over cloudiness to humidity and surface features, one of them being LST, too, although this variable can be obtained from the Satellite Applications Facility on Land Surface Analysis (LSA SAF), as well. The values are available every 15 minutes and the spatial resolution is 3 km (in nadir). The source for the LST computation in this SAF is Meteosat Second Generation (MSG), that fully covers central Europe. The retrieval algorithm details can be found in the corresponding Algorithm Theoretical Basis Document (Trigo et al. [2008]).

Based on LST remote sensing data, we can detect the so-called surface urban heat island (SUHI). SUHIs are observed using the remotely received spatial patterns of upwelling thermal radiance (Voogt and Oke [2003]).

SUHI can be characterized either by exceedance level or by comparing to prevalent meteorological conditions. Such information can help to identify the hot spots and/or the warmest areas throughout the city and allow for subsequent analysis of their causes. This can eventually lead up to urban planning changes in these overheat-prone areas in order to mitigate the adverse effect on urban inhabitants (see Chapter 3). When using real-time data, hot spots identification can improve heat warning issuing in the cities.

In case of Prague, before 2010s only limited usage of satellite data for UHI analysis can be found. During our research, firstly MODIS data have been used for identifying the SUHI in Prague – the main question was to find the possible limits of UHI. The extents of the UHIs were evaluated based on cross-profiles: the changing points along each profile were identified based on the Rodionov test (Rodionov [2004]) and correlated with land cover (Fig. 2.1).

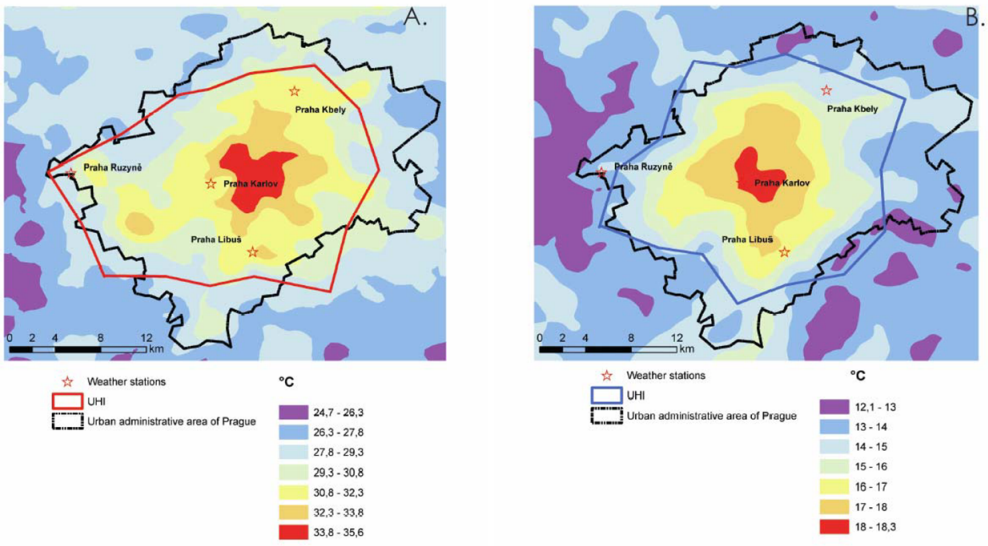

Figure 2.1: Day (A) and night (B) LST for area of Prague derived from only July MODIS images (2000-2006) with limits of UHI indicated (taken from Cheval et al. [2007]).

In order to find a long-term and seasonal characteristics uf SUHI, MODIS data were employed for 18 years long period in 2018 (during solving URBI PRAGENSI project, see Chapter 3). Based on satellite analysis of SUHI (Figs. 2.2 and 2.3), the following features can be found for Prague:

- the warmest part of the city (based on SUHI) is situated in the historical city centre (close to Vltava river) with relatively higher differences during night
- during daytime the warmest region is shifted south-eastward in the densely built-up area with only limited vegetation (see Land use map Fig. 2.4)
- the average intensity of SUHI is 5 to 6 °C for daytime, while being 4 to 5 °C for night-time
- the highest intensity of SUHI for daytime occurs in June (8 to 10 °C), for night-time in July (6 to 7 °C)
- throughout the year, the lowest intensity of SUHI for daytime can be found in November (around 2 °C) and for night-time in December (2 to 3 °C)

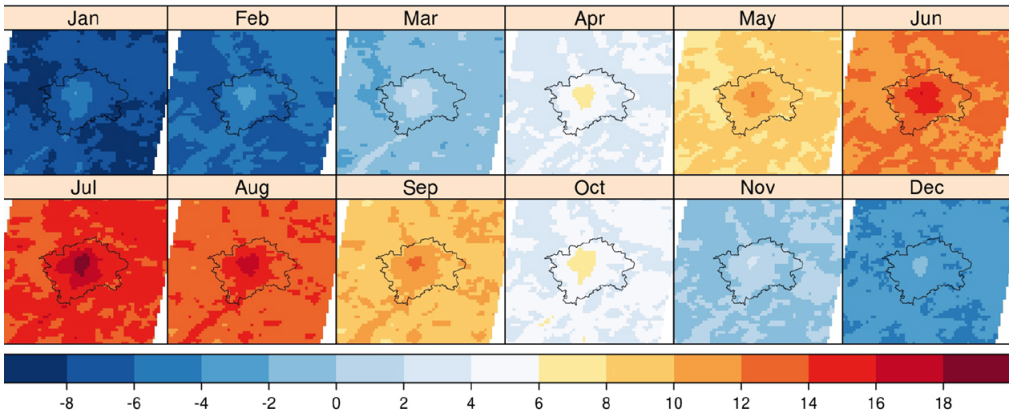

Figure 2.2: Monthly mean of LST based on nighttime MODIS images, period 2000 to 2017 (taken from Zak et al. [2019a]).

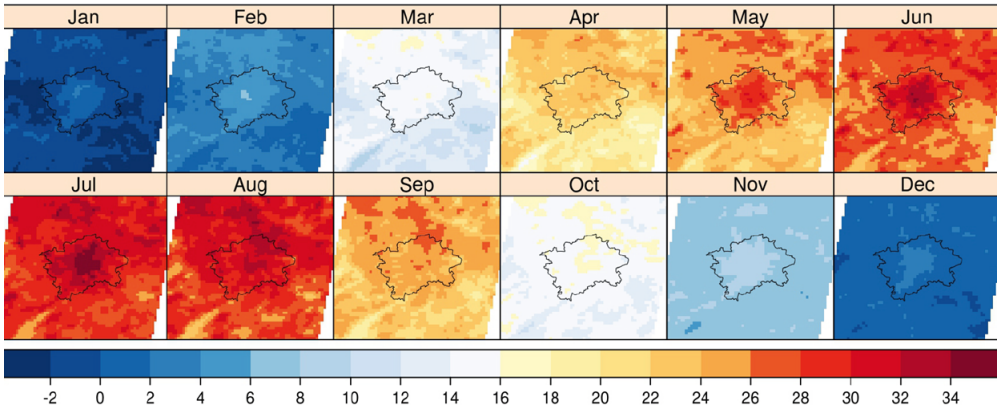

Figure 2.3: Monthly mean of LST based on daytime MODIS images, period 2000 to 2017 (taken from Zak et al. [2019a]).

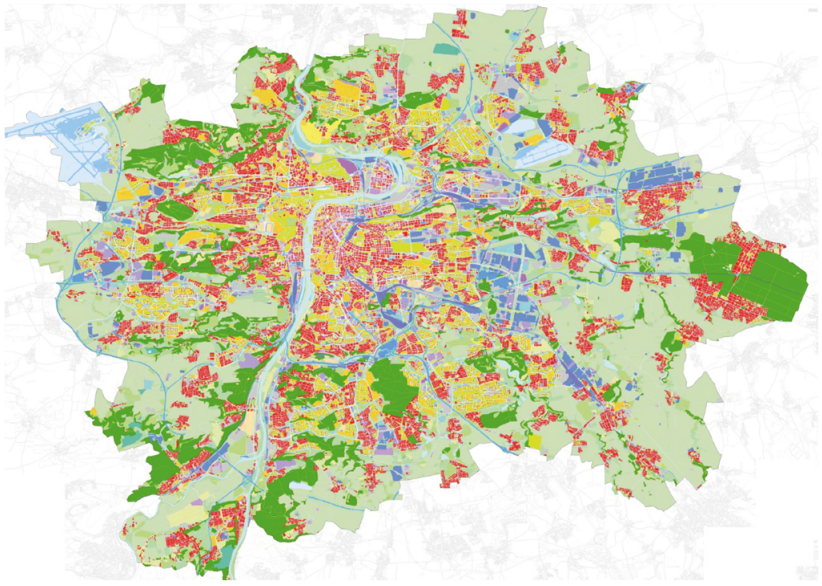

Figure 2.4: Land use map of Prague (blue - traffic infrastructure, red - housing, orange - public services, violet - industrial buildings, green - trees and green infrastructure, dark green - dumps, mining (source: http://app.iprpraha.cz).

3. Thermal comfort in cities and mitigation of the urban heat island effects

Urban Heat Island (UHI) is supposed to become on the main problems during this century due to increasing rate of urbanization of the human civilization (Rizwan et al. [2008]). UHI intensity for many cities around the world (including cities in central Europe such as Prague) has generally been increasing in the last decades. The main reason is the increasing density of built-up areas and changing brownfields and green spaces into areas with high-density buildings (usually having more floors, too). Also, the artificial sources of heat (air-condition, heating, transportation, industry) have been gradually contributing to this UHI intensity increase. This UHI intensification leads to urban overheating, generally negatively affecting the urban inhabitants. This overheating is causing substantial increase in energy demand for air-conditioning purposes. As shown by Santamouris et al. [2015]), the corresponding rise of the peak electricity load varies between 0.45% and 4.6% for each degree of temperature increase. The overheating also leads to the increase of harmful pollutants concentration, e.g., near-surface ozone.

Rising urban temperatures are causing increased thermal discomfort levels and generally influencing the health of the urban inhabitants. Heat exposure can have many negative effects. Firstly, it reduces occupational performance, it can worse minor illnesses, increase the risk of hospitalization, and eventually can increase risk of death. These health risks are probably to increase as the result of climate change and growing degree of urbanization in the future throughout many countries (Heaviside et al. [2017]). It takes its toll on the animal populations within cities, too. Some animal populations are more likely to struggle to find food, water, and shelter in hotter cities. But there is the other side of the coin, where some animal species may find cities more attractive than the wilderness and turn into urban pests that carry disease and become a nuisance (Kaiser et al. [2016], Tryjanowski et al. [2013]). Generally, increasing UHI intensity has negative effects worsening the city's economy and influencing, e.g., tourism.

These adverse effects have led to efforts to reduce the UHI. Various measures can be implemented to achieve this reduction, but generally, the modification of urban structures, surfaces, and materials are the most important. These include especially highly reflective materials (with high albedo) applied to buildings (e.g., in the form of cool roofs) as well as to urban surfaces. Based on the paper of Macintyre and Heaviside [2019], the largest temperature drop caused by cool roofs can be achieved when this method is applied to extensive industrial and commercial buildings, when reduction of temperature maxima above these surfaces can reach up to around 3 °C during the hottest days when the sun is in the highest position. Another possibility to mitigate UHI is using green measures – like green roofs and facades, or perhaps incorporating blue infrastructure measures, like increasing of the extent of areas with cooling water bodies (they

need to be deep enough in order to maintain their function even during long heat waves). Sometimes the combination of blue and green features can be incorporated, or even some changes in the structure of blocks of buildings or city quarters. Many studies can be found dealing with this topic (e.g., Yuan et al. [2017], Ambrosini et al. [2014], Fikfak et al. [2020], Lai et al. [2019], Macintyre and Heaviside [2019]), usually focusing on aspects of the energy budget of the urban areas and concentrating on air temperature reduction. For this aim, various models having different spatial resolutions are used. If possible, their results together with local measurements are used for case studies evaluation the benefits of the proposed solution. But when health-related effects of urban conditions are investigated, not only air temperature should be used as the human body cannot perceive individual climatic parameters like an instrument.

One possible approach for the thermoregulatory response is to use the human energy balance equation (Thompson and Perry [1997]):

$$(M + W) + Q + R + C + E + S = 0 \tag{3.1}$$

where M represents the metabolic heat (internal energy production), W the physical work output, Q short-wave solar radiation income, R the long wave radiation, C the convective heat flow, E is latent heat flow (to evaporate water diffusing through the skin, for heating and humidifying inbreathed air and for evaporation of sweat), and S the storage heat flow for heating or cooling the body mass. The terms in this equation are positive when they result in energy gain for the body, and are negative for energy loss of the body. M is always positive, W and E (except of part for humidifying and heating the inbreathed air) are always negative.

To quantitatively describe the thermal effects of UHI the inhabitants really feel, we need to use thermal indices based on the human energy balance. These indices provide detailed information on the effect of complex thermal environment on humans (Hoppe [1999]). They are influenced by all climatic parameters. Some of these parameters are being partly interrelated (i.e., affecting each other).

Frequently used thermal indices (based on the human energy balance) are Predicted Mean Vote (PMV, Fanger [1972]), Physiologically Equivalent Temperature PET (Matzarakis et al. [1999]), Standard Effective Temperature SET* (Gagge et al. [1986]) or Outdoor Standard Effective Temperature Out_SET* (Spagnolo and de Dear [2003]), Perceived Temperature pT (Staiger et al. [2012]) and Universal Thermal Climate Index UTCI (Jendritzky et al. [2012]).

Computation of the thermal indices is quite demanding on meteorological data. Usually, it requires the following meteorological elements: air temperature, air humidity, wind speed, short and longwave radiation fluxes (or sunshine duration and/or cloudiness). It has to be mentioned, that these parameters can have a large spatial and temporal variability and thus influence the thermal indices values. Temperature and wind speed usually have the highest variability since they are greatly influenced by the obstacles in the complex urban areas. This has to be taken into account, and use high quality measurement for calculating these parameters. Representativeness of the measuring point/station should be deeply reflected in the following analysis of the computed indices.

In the Czech Republic, using of thermal indices was not widely popular until 2010s when during the so-called "UHI "Project ("Development and application of

mitigation and adaptation strategies and measures for counteracting the global Urban Heat Islands phenomenon"), these quantities have started to be used more often (see Zahradnicek et al. [2014]), including in our research. Especially UTCI and PET have become quite popular in the Czech Republic in the last decade, the second one later used in the modified version of mPET (modified Physiologically Equivalent Temperature, an improvement of PET using the multi-node model defining UTCI, see e.g., Chen et al. [2011] and Matzarakis et al. [2014]). PET can be described as *"the air temperature at which, in a typical indoor setting (without wind and solar radiation), the energy budget of the human body is balanced with the same core and skin temperature as under the complex outdoor conditions to be assessed"* (Hoppe [1999]). It has become one of the most commonly used indices in bioclimatology, because the computed values can be easily compared to those from other studies (Matzarakis et al. [2014]). Another important advantage of (m)PET is the use of °C as a unit, making the results easier to interpret to the wider public without deeper knowledge of human biometeorology.

During our research, the PET index was calculated using the numerical model RayMan developedat the Meteorological Institute of the Albert-Ludwigs University Freiburg (Matzarakis et al. [2007]). This model requires hourly input data of air temperature, air humidity, wind speed and radiation or cloudiness. Based on our computation, the first pictures of PET values throughout the year as well as during the heat waves were obtained for the city of Prague (and other cities in Czechia, too). It should be noted that values between 18 °C and 23 °C are described as comfortable thermal perception, 23 °C to 29 °C as slightly warm, 29 °C do 35 °C as warm, 35 °C to 41 °C as hot, and over 41 °C as very hot thermal perception.

It's not a surprise that the highest values (partly over 30 °C) in Prague occur during summer months, July and the first half of August (Fig. 3.1), quite similar to the annual course of air temperature, but PET values during the afternoon/evening hours are about 3 °C to 6 °C higher than the air temperature. When comparing PET values in the city center with those in the urban outskirts, an interesting picture can be found – the largest difference over 4 °C occurs just after sunset during the summer season. A bit lower difference between PET in the city center and PET in the suburbs is detected during afternoon, especially in the summer. The smallest difference was found shortly after the time of sunrise in the summer half-year with values than 1.5 °C and in some days and shorter periods nearly approaching 0 °C – this is caused by less sunshine in the city center due to building obstacles during morning hours and connected to the urban cold island that can shortly develop during these periods. For the rest of the year and parts of the day, the difference between PET in the city center and the city suburb is usually about 2 to 3 °C. PET values can be used for computation of characteristics similar to those used for air temperature, like summer and tropical days, including the number of hours with PET above given threshold. E.g., the number of PET tropical days in Prague's center is about 2.5x higher than according to regular air temperature. Another interesting picture can be obtained if we look at the hottest days. The PET values are 5 °C to 8 °C higher during these extremely hot days, i.e., with PET values over 40 °C, making them days with very hot thermal perception. This highlights the potential hazard of these heatwaves, especially for elderly people and children.

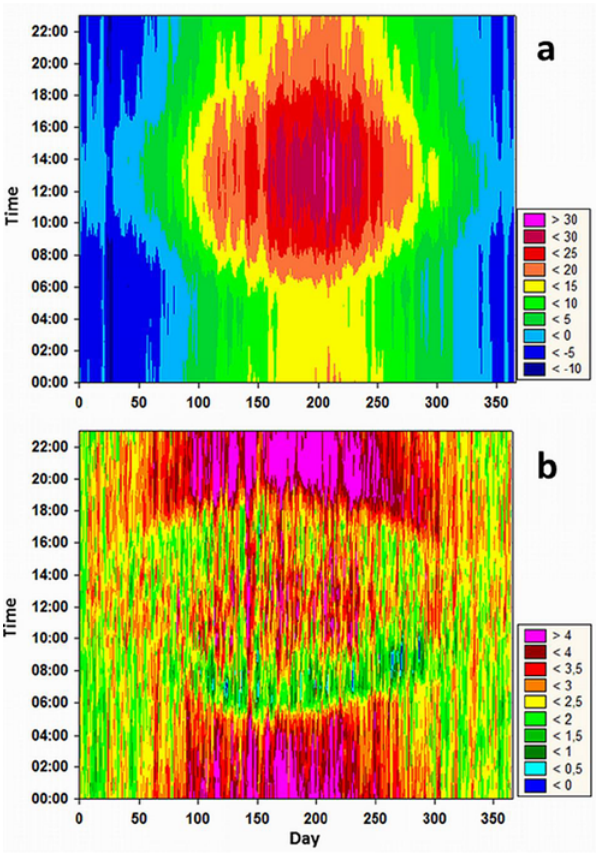

Figure 3.1: Example of the annual course of physiological equivalent temperature, PET (°C), at the Prague Karlov station (a) and difference between Karlov and Ruzyne station, period 2005-2013. 200th day is 19th July (taken from Zahradnicek et al. [2014]).

Compared to studies based only on air temperature, results using thermal indices ((m)PET or UTCI) produce different results. For example, using high reflective materials for the pavements or roads have an effect of greater shortwave reflection - this leads to increase of (m)PET values, although the air temperature is decrease since there is less energy stored in the surface. The green wall has different thermal characteristics, leading to lower (m)PET and, thus, more comfortable conditions. This is important not only from the thermal comfort point of view, but the aesthetic respect influences the use of the public space in cities by citizens and their choosing of places for spending time outdoors. Finally, easy understandable graphs and figures can be provided for better transfer of knowledge between researchers (climatologists) and end-users (urban planning, general public). The above-mentioned adverse effects of urban climate have gained more and more attention among urban planners and city stakeholders in the last decades, including the city of Prague. The era of changing climate leading to more intense heat waves, irregularities in precipitation regime, etc. contributes to the necessity of adaptation plans and/or cities' strategies. This planning is a complex matter where climatological inputs are very important and represent the first step. Therefore, cooperation between urban planners and climatologists is very desirable. To decide which adaptation measure is the best one, the climatological expertise and/or modeling approach is needed. This has become apparent to Prague's urban planners, too, especially during the solving of the "UHI" project, when the issues of of urban climate and urban heat island has gained large attention among the wider public. As a first step, the so-called pilot areas were selected to find the answer to the question "what happens when...".

For this reason, microclimatic simulations were performed for these pilot areas. Various types of simulations were used, from the quite simple one for a street corridor (Legerova) with heavy traffic using RayMan model, over a city quarter of typical brownfield (Bubny-Holesovice) using EVNI-met software, to green belt around the city using WRF (for meteorology) and CMAQ (for air quality) model. The results are described in Appendix C. Experiences gained during these simulations and the "UHI" project solving helped prepare the adaptation strategy of the city of Prague.

Experiences from the computations mentioned above were used and further improved during the implementation of another project, URBI-PRAGENSIS, solved between 2018 and 2020, where I have been involved, too. Some of the results of this project are discussed in Chapter 4.

4. Urban heat island modelling approaches

Adverse effects of urban climate, especially overheating due to exposure to extreme temperatures during heat waves can lead to thermal stress, hyperthermia, circulatory collapse or dehydration, and eventually even to death. The UHI phenomenon can be responsible for amplification of these dangers making mitigation strategies of great importance, as already mentioned in the previous chapter.

A wide variety of mitigation strategies can be found in urban planning to reduce UHI, as was mentioned in Chapter 4. These strategies when applied are good not only for reduction of thermal comfort in urban areas but can have quite complex influence on urban climatological conditions. And it is not always easy to evaluate the real response of these strategies. Therefore, numerical modelling of urban climate can be very helpful in answering the question what adaptation (or mitigation) strategies are the most suitable for the selected city or its part.

The urban climate models are diverse depending on the purposes of the study - we can e.g. explore the impact of the UHI on thermal comfort of citizens (on the scale of buildings), but also the effect of large-scale winds on urban ventilation (Mirzaei [2015]). Three levels/types of models can be distinguished: building scale models, micro-scale models and city-scale (that are actually mesoscale) models.

The building scale (or energy) models are mainly limited to an isolated building envelope and the influence of the buildings in the neighbourhood on its energy performance is neglected. They are constructed in order to investigate the impact of the future climate change scenario on the building envelope.

The micro-scale, or microclimate models are focused on interaction of a building with its surrounding environment in the surface layer. Urban canopy layer models (UCM) investigating the energy budget of an urban canopy layer belongs to this type of models, too (for details, see e.g. Mirzaei [2015])).

In the last decade, the urban boundary layer (UBL) have been increasingly studied by the mesoscale models with the urban canopy schemes coupled. Special impulse was provided after the widespread use of the mesoscale Advanced Research Weather Research and Forecasting (ARW-WRF) model (Liao et al. [2014]). UCM have a simplified urban geometry, like infinitely-long street canyons, and involves also 3-D urban surfaces (roofs, walls, roads). These models are, e.g., able to compute temperature profiles within the street canyon and include the important factor of an anthropogenic heat increasing the UHI intensity.

The influence of building surface material, orientation of buildings and street canyon configuration, vegetation including trees on inhabitants in the streets and on street ventilation can be investigated using UCM models. It has to be noted they have quite limited domain size due to high computational cost. City-scale models are very useful tool when investigating variation of UHI in a wider area of the whole city and its surroundings. These models are able to compute wide range of meteorological fields changes caused by urbanization, from temperature and moisture to cloudiness and radiation.

Very important question when modelling the UHI is how to parameterize the

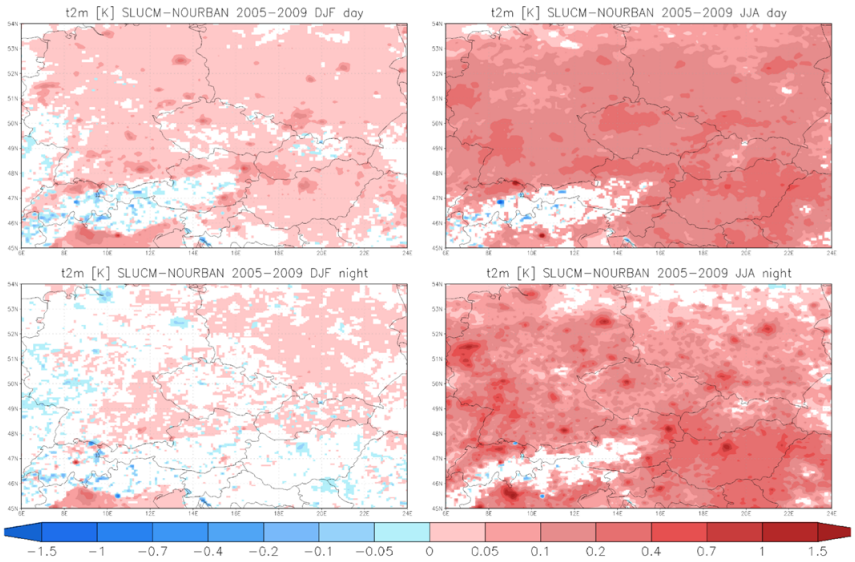

Figure 4.1: The impact of urbanized surfaces on the winter (left) and summer (right) near surface temperature for day (top) and night-time (bottom) conditions in K averaged over years 2005–2009 (reprint from Huszar et al. [2014]).

urban meteorological phenomena. This can be done simply by replacement of the surface parameters by an average value corresponding to the urban surface – so-called bulk parameterization (described, e.g. in Chen et al. [2011]). Another group of models have typically a single urban layer and an idealized street canyon (e.g. Single-Layer Urban Canopy Model - SLUCM; Kusaka et al. [2001]). The third type of models consider more layers of the urban environment with possibility of including different heights of the buildings and vertical structure of the urban canyon (e.g. Building Environment Parametrization - BEP; Martilli et al. [2002]).

It is important to mention that not only averaged values, but also the extremes and variability of meteorological parameters are crucial in assessing the urban impact including poorly observed or immeasurable parameters in the urban and suburban areas, like wind profile or boundary layer height. Generally, long-term simulations (the longer the better) are necessary if we want to evaluate the quality of computed variables against the measured parameters.

Modelling of UHI and/or urban climate specifics of Prague has started in the early 2010. An important stimulus appeared during solving the "UHI" project between 2011 and 2014 (see also Chapter 4). Regional climate model RegCM4.2 with coupled SLUCM was used in 2014 (Huszar et al. [2014]) of urbanization on conditions throughout the day and night in different seasons. The largest impacts were found during summer nights with up to 1.5 °C higher temperatures (Fig. 4.1) in the city centre than without considering urban surfaces, i.e. the results consistent with the values from the station observations. Another interesting findings derived from the simulations include the so called urban-breeze circulation (wind speed increase during nocturnal hours) (Fig 4.2), connected with convergent motions towards the city centre. This situation forms under the presence of thermally induced surface pressure gradient (Hidalgo et al. [2010]), or height increase of planetary boundary layer over most of time.

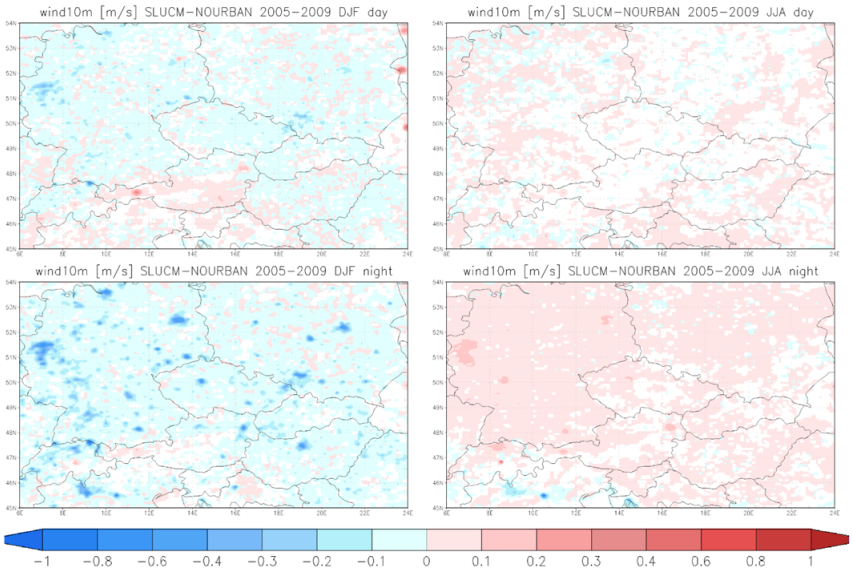

Figure 4.2: Same as 4.1 but for the wind velocity at 10 m in m.s-1 (reprint from Huszar et al. [2014]).

The question of different UHI modeling approaches was widely solved and discussed in the paper Karlicky et al. [2018], and the details can be found in Appendix D. Based on our results, all urban schemes captured the main features of urban meteorological conditions, not only UHI. No real difference between various models was discovered, and the anthropogenic heat influence on UHI was satisfactorily represented. Greater variance among different model approaches was found to impact the urban environment on the planetary boundary layer height and the surface wind speed. The investigation of pollutant dispersion modeling has shown slightly improving dispersion in the urban areas due to wind cleansing effect and convection and turbulence dispersion effect.

Later, the urban canopy meteorological forcing was studied (Huszar et al. [2020]), where the effect of the numerical model's sensitivity to grid resolution was investigated. A number of model simulations was carried out to answer the question what is the urban canopy meteorological forcing - this was realized by considering of the urban canopies or of the rural ones. These simulations were done primarily for Prague, but as can be seen from Fig. 4.3, the UHI of Berlin is also very well represented. The expected, well-pronounced effect on temperature (increase up to 2 °C, see Fig. 4.3) and wind (decreases by up to 2 m.s^1) was found, including similarities in the diurnal cycle of the urban canopy temperatures (with maximum warming over urban areas of Prague around 2.4 °C, see Fig. 4.4).

The question of impact of the urban land surface on extreme values was investigated in the paper by Huszar et al. [2020]). The results can be found in Tab. 4.1. Larger influence was found on the lowest temperatures compared to the average ones during winter (larger release of anthropogenic heat during cold days). Summer days with low temperatures and limited sunshine are affected less (radiation is trapped only limitary). In contrast, hot summer days with plenty of sunshine behave oppositely (much larger heat accumulation due to multiple reflections and trapping in street canyons). These results are similar to those shown by Zha et al. [2019]), who found that events with high and extreme temperatures

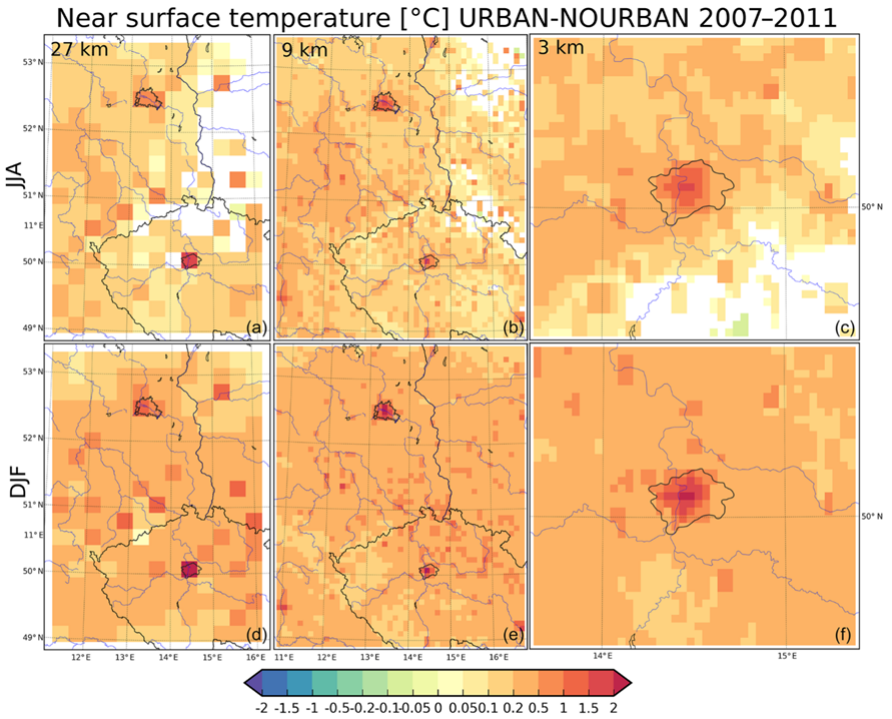

Figure 4.3: Impact of urban surfaces on near-surface temperature in °C for JJA (a, b, c) and DJF (d, e, f) for the three resolutions (27, 9 and 3km). Shaded areas represent statistically significant changes over the 98% threshold using a two-tailed t test. The geographic locations of Berlin and Prague are indicated by their administrative boundaries. (reprint from Huszar et al. [2020]).

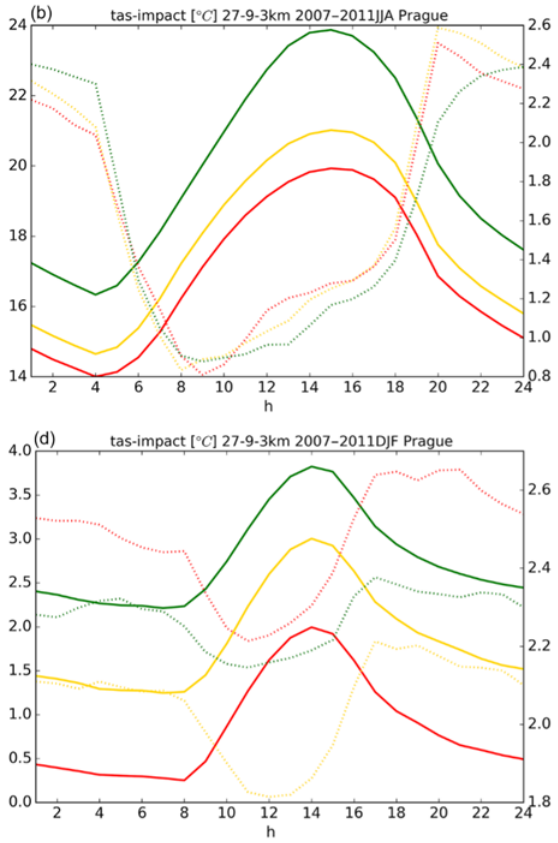

Figure 4.4: Impact of urban surfaces on near-surface temperature diurnal cycle in °C for JJA (b) and DJF (d) for the three resolutions (27km – red, 9km – orange and 3km – dark green). Solid lines are the absolute values (left-hand y axis) from the URBAN model experiment; dashed lines represent the urban impact (right-hand y axis). (reprint from Huszar et al. [2020]).

Prague	DJF			JJA		
	mean	5 %	95 %	mean	5 %	95 %
Δtas (°C)	2.4/1.3*	5.0/1.9	1.2/1.1	2.2/2.2	0.6/1.9	3.1/2.9
ΔPBLH (m)	384/128	294/45	450/248	480/265	248/195	491/353
Δwind10m ($m s^{-1}$)	−1.1/ − 0.5	−0.34/ − 0.26	−2.57/ − 1.6	−0.64/ − 0.15	−0.25/ − 0.29	−1.45/ − 0.35
Berlin						
Δtas (°C)	1.44/1.46	1.6/1.6	0.5/1.3	2.2/2.2	0.6/1.9	3.1/2.9
ΔPBLH (m)	238/170	142/70	227/279	307/337	162/279	280/433
Δwind10m ($m s^{-1}$)	−0.80/ − 0.74	−0.38/ − 0.28	−1.86/ − 2.1	−0.46/ − 0.32	−0.27/ − 0.30	−0.80/ − 0.58
Munich						
Δtas (°C)	1.33/1.82	2.89/2.65	0.59/2.19	1.12/2.2	0.53/1.96	1.76/2.83
ΔPBLH (m)	132/106	65/29	144/157	244/270	122/201	362/367
Δwind10m ($m s^{-1}$)	−0.46/ − 0.26	−0.25/ − 0.21	−0.77/ − 1.01	−0.32/ − 0.11	−0.21/ − 0.33	−0.52/ − 0.36
Budapest						
Δtas (°C)	1.13/1.37	2.60/1.02	0.54/1.74	1.2/2.4	0.71/2.16	1.40/2.97
ΔPBLH (m)	132/122	106/67	268/248	265/336	132/225	236/509
Δwind10m ($m s^{-1}$)	−0.91/ − 0.17	−0.33/ − 0.24	−1.92/ − 1.00	−0.59/ − 0.20	−0.39/ − 0.32	−0.83/ − 0.69

Table 4.1: Mean and 5% and 95% quantiles of the urban canopy impact for models RegCM and WRF on near-surface temperature (tas), the height of the boundary layer (PBLH) and 10m wind speed (wind10m) averaged over DJF and JJA 2015–2016 for centers of four different cities. For Prague, values are taken from the 1km simulations and 9km for the rest. (reprint from Huszar et al. [2020]).

(in terms of the number of summer days, i.e. days with maximum temperature over 25 °C) are becoming more often with increasing urbanization.

For the wind speed changes, strong winds are the modified in a most manner (almost twice to average wind speed). This is caused by the additional drag (due to urban surfaces) that is slowing the large-wind speed relatively more compared to the slow winds.

Relatively large difference in the impact on the average and extreme (low/high percentiles) values have been identified between cities. These differences can by explained by their different sizes, fractional urban land cover and population (e.g. Berlin has almost twice the population of Munich and is twice as large). Another reason can be connected to different climate in which the urban canopy meteorology forcing acts.

5. Conclusion

Throughout this text, the individual pieces of analysis have demonstrated a few examples of our contribution to the urban climate knowledge, focusing on Prague and especially (but not limited) to its urban heat island. The results and methods used are quite wide, and it is not easy to summarize them in a simple conclusion. But there are, of course, some points worth highlighting. Finally, some information about the related research's ongoing works with our participation is given in this section.

First, our results have brought more details about knowledge of the UHI of Prague. Based on the careful analyses, more information about the intensity has been gained and the UHI's behavior under various synoptic conditions. Of course, it is no surprise that the warming is the strongest in the city center and indirectly points out the UHI amplification. The reoccurrence of extremely hot days and especially nights is growing statistically significantly in the city center and faster than at suburban stations. Due to the presence and increasing intensity of the UHI, Prague's center has become the warmest place in the Czech Republic since the '1980s. We can conclude that Prague's center is about 1.0-1.5 °C warmer (based on daily means of temperature) thanks to the existence of UHI, but for minimum temperatures, the UHI intensity exceeds 2 °C. From a synoptic perspective, the UHI of Prague develops especially under anticyclonic synoptic types with south- to southwesterly flow. The UHI greatly vanishes when the wind speed exceeds 6 to 8 metres per second.

The study and analysis of UHI traditionally based on surface stations measurement can generally lead to results that are strongly influenced by the stations localization and exposure. For Prague this is not a big issue since the location of central stations is virtually exemplary in the sense of their proximity to the geometric centre of Prague. But the exposure should be taken into account where needed for certain analyses - especially for precipitation and snow. This influences the study of drought occurrence in Prague, where new interesting results have been found in Kveton and Zak [2021]). With method exploring the continuous days with daily precipitation totals not exceeding given threshold and continuous days with cumulative precipitation average not exceeding given threshold. The long-term analysis showed a small increase in drought duration since 2002.

Another picture of UHI (and other urban climate features) can be obtained by satellite measurement. Generally, more information about size and shape and even UHI magnitude can be obtained when using satellite data. But in this case, we should rather talk about Surface Urban Heat Island (SUHI) since we are usually working with land surface temperature (LST) data. MODIS LST data have been used for the first detailed analysis of Prague's SUHI, already in the '00s of 21st century, showing the first image of its shape. CM SAF LST data used in thesis Dolezalova [2020] studying the SUHI of Prague has confirmed the previous results of lower daytime SUHI intensity in winter compared to summer (4-5 °C vs. 8-10 °C). When using satellite data, some issues have to be taken into account. Certainly, limited spatial resolution (and for polar-orbiting satellite temporal resolution, too), as well as confinement to cases without cloudiness, can influence the obtained results. The second point is especially important in

winter season, when generally larger cloudiness is observed in central Europe, and especially the low stratiform clouds are often occurring. Another important issue is the presence of snow cover in winter months. It greatly influences the city center's albedo for such days, making the SUHI less expressed compared to UHI based on station measurement (Dolezalova [2020]). However, the UHI can be manifested thanks to important anthropogenic heat sources.

Urban climate and especially urban heat island can have adverse effects on urban inhabitants. It is therefore important to study possibilities of mitigation of these effects. Especially during prolonged heat waves increased risk of health complications occurs, mainly for elderly people and babies. Still, worse sleeping quality during warm nights can finally contribute to enhanced lassitude and decreased attention even for young people. The question of mitigating these adverse effects come to attention at the end of the last century. However, in the case of the Czech Republic, the urban planners and stakeholders become to deal with it not until the end of 00's of 21st century, when the importance of UHI becomes more apparent to the wider public. This activity has been partly supported by projects focused on UHI mitigation.

Although there was a large concern about the UHI of Prague (and perhaps other cities in the Czech Republic) in the scientific community, the question of thermal perception has become widely popular not before the last decade, partly due to studies of our team made during solving the European "UHI" project. Parameters like (m)PET and UTCI have started to be used to describe thermal comfort not only be climatologists but also by urban planners and stakeholders. Among the first works using these parameters were the pilot actions investigating the effects of diverse mitigating strategies for areas with deeply pronounced UHI effect, especially in the summer months. Since then, these quantities are now widely accepted and used to evaluate various mitigation and/or adaptation strategies in the city of Prague.

Last but not least, the modeling of urban influences gradually gains more and more attention. The first urban climate models were used during solving the MEGAPOLI (https://cordis.europa.eu/project/id/212520) project at the Department of Atmospheric Physics. By that time, more details the air quality issues were more prioritized to urban climate. But this has changed under increasing climate change impacts combined with the deepening UHI effects and when need of deepening our knowledge about Prague's climate arose.

Nowadays, UHI models can cover a wide spectrum of scales with respect to the study's aim or analysis. In this thesis, the modeling works have been focused on urban canopy layer models with limited domain size used to study the urban boundary layer's dynamic and thermal properties. These models are able to represent most features typical for the urban areas, like street canyons, walls, roofs, and roads, including sources of anthropogenic heat, increasing the UHI intensity. The representation of the "real weather" in the city and its surroundings is of great importance. Based on our results (mostly for Prague), the urban schemes could capture the typical urban weather modification features, especially the temperature (including the typical diurnal cycle). But not all parameters are simulated properly. For example, there can be found discrepancies between real and model-simulated wind speed and planetary boundary layer height, with the simulated values showing greater variance (although it is not easy to evaluate the

model values to the measured ones due to scarce station measurements).

Meteorological forcing of the urban canopy was underlined by (Huszar et al. [2020]), where model simulations were carried out either with rural or urban canopies. The models can be expected to become more and more powerful instruments when studying various effects of mitigation and adaptation strategies, but we are still lacking in the judgment of how correct they are when going into microclimate. Although there can be found several comparisons (e.g. Antoniou et al. [2019])) dealing with this matter in scientific literature, for Prague only limited measuring campaigns have been realized (some of them during URBI PRAGENSI project) focused mostly on small areas (typically with extent of hundreds of meters).

A bit more knowledge is expected to be gained during solving two-year project "Urban Heat Island in the Czech Republic" finishing by the end of this year (2021), which investigates Prague and other large cities in Czechia. As a part of the project solution, there are special measuring campaigns done by air-borne and car measurement – ways that have been implemented only a few times. In the case of car-rides for Prague, such an approach was applied only some decades ago.

Urban climate has become very important part of climatology in the Czech Republic since the end of the last century. Many projects and studies focused on this topic were solved during last two decades, mostly focused on urban heat island, although the issue of air quality is of a big importance, too. The question of UHI mitigation and adaptation to worsening conditions under the era of climate change is another topic being studied in the current and ongoing projects as well in student thesis at our Department of Atmospheric Physics.

Acknowledgement

The results presented here could not have been achieved without the support of a large number of people and organizations.

First, I would like to express my gratitude to all my collaborators named in the author lists and acknowledgments of individual papers related to the topics presented.

I am also deeply grateful to my co-workers at the Department of Atmospheric Physics of the Faculty of Mathematics and Physics, Charles University, for providing a pleasant and stimulating work environment and support during my professional career. I would like to express special thanks to my colleagues Petr Pisoft and Jiri Miksovsky for their valuable comments on this thesis, and to Pavel Zahradnicek for his help with data processing and inspiring cooperation.

Financial support was granted by various institutions: In particular, I would like to thank the Grant Agency of the Czech Republic (project 18-01625S), City Administration of Prague (project URBI PRAGENSI CZ.07.1.02/0.0/0.0/16_040/0000383 and Proof of Concept CZ.07.1.02/0.0/0.0/16_023/0000108), Ministry of Education of the Czech Republic (innovation project 23606419) and the European Commission (7th Framework Programme, project "UHI" 3CE292P3).

Finally, considering the nature of the climate research in general, and of time series-based studies in particular, our work would not have been possible without the effort of the many authors and providers of various datasets employed here and in the related contributions.

Bibliography

D Ambrosini, G Galli, B Mancini, I Nardi, and S Sfarra. Evaluating mitigation effects of urban heat islands in a historical small center with the envi-met® climate model. *Sustainability*, 6(10):7013–7029, 2014. doi: https://doi.org/10.3390/su6107013.

CI Anderson, WA Gough, and T Mohsin. Characterization of the urban heat island at Toronto: Revisiting the choice of rural sites using a measure of day-to-day variation. *Urban Climate*, 25:187–195, 2018. ISSN 2212-0955. doi: https://doi.org/10.1016/j.uclim.2018.07.002.

N Antoniou, H Montazeri, M Neophytou, and B Blocken. CFD simulation of urban microclimate: Validation using high-resolution field measurements. *Science of the Total Environment*, 695, 2019. ISSN 0048-9697. doi: https://doi.org/10.1016/j.scitotenv.2019.133743.

AJ Arnfield. Two decades of urban climate research: A review of turbulence, exchanges of energy and water, and the urban heat island. *International Journal of Climatology*, 23(1):1–26, 2003. ISSN 0899-8418. doi: https://doi.org/10.1002/joc.859.

C Beck, A Straub, S Breitner, J Cyrys, A Philipp, J Rathmann, A Schneider, K Wolf, and J Jacobeit. Air temperature characteristics of local climate zones in the Augsburg urban area (Bavaria, southern Germany) under varying synoptic conditions. *Urban Climate*, 25:152–166, 2018. ISSN 2212-0955. doi: https://doi.org/10.1016/j.uclim.2018.04.007.

R Beranova and R Huth. Long-term changes in the heat island of Prague under different synoptic conditions. *Theoretical and Applied Climatology*, 82(1-2):113–118, 2005. ISSN 0177-798X. doi: https://doi.org/10.1007/s00704-004-0115-y.

J Bradka, A Drevikovsky, Z Gregor, and J Kolesar. Weather on the Territory of Bohemia and Moravia in Typical Weather Situations (in Czech) . Hydrometeorological institute series of mean annual air temperatures of the czech republic in typical weather situations, Czech Hydrometeorological Institute, 1961.

F Chen, H Kusaka, R Bornstein, J Ching, CSB Grimmond, S Grossman-Clarke, T Loridan, KW Manning, A Martilli, SG Miao, D Sailor, FP Salamanca, H Taha, M Tewari, XM Wang, A A Wyszogrodzki, and CL Zhang. The integrated WRF/urban modelling system: development, evaluation, and applications to urban environmental problems. *International Journal of Climatology*, 31(2):273–288, 2011. ISSN 0899-8418. doi: https://doi.org/10.1002/joc.2158.

S Cheval, M Zak, A Dumitrescu, and V Kveton. MODIS-based investigations on the urban heat islands of Bucharest (Romania) and Prague (Czech Republic). 2007. Joint 2007 EUMETSAT Meteorological Satellite Conference and the 15th Satellite Meteorology Amsterodam Netherlands.

A Dolezalova. Study of Urban Heat Island with using of remote sensing investigations. Master's thesis, Charles University, Department of Atmospheric Physics, 2020. 104 pp.

K Dubec and V Orel. Gregor Mendel's scientific activity in meteorology. *Folia Mendeliana*, 15:215–242, 1980.

PO Fanger. Thermal comfort, analysis and application in environmental engineering, 1972.

A Fikfak, K Lavtizar, JP Grom, S Kosanovic, and M Zbasnik-Senegacnik. Study of Urban Greenery Models to Prevent Overheating of Parked Vehicles in P plus R Facilities in Ljubljana, Slovenia. *Sustainability*, 12(12), 2020. doi: https://doi.org/10.3390/su12125160.

D Founda and M Santamouris. Synergies between Urban Heat Island and Heat Waves in Athens (Greece), during an extremely hot summer (2012). *Scientific Reports*, 7, 2017. ISSN 2045-2322. doi: https://doi.org/10.1038/s41598-017-11407-6.

AP Gagge, AP Fobelets, and L Berglund. A standard predictive index of human response to the thermal environment. *Ashrae Transactions*, 92:709–731, 1986.

A Goncalves, G Ornellas, A C Ribeiro, F Maia, A Rocha, and M Feliciano. Urban Cold and Heat Island in the City of Braganca (Portugal). *Climate*, 6(3), 2018. ISSN 2225-1154. doi: https://doi.org/10.3390/cli6030070.

P Guillevic, F Göttsche, J Nickeson, G Hulley, D Ghent, Y Yu, I Trigo, S Hook, JA Sobrino, J Remedios, et al. Land surface temperature product validation best practice protocol Version 11. *Best Practice for Satellite-Derived Land Product Validation*, page 60, 2018. doi: https://doi.org/10.5067/doc/ceoswgcv/lpv/lst.001.

T Halenka, M Belda, P Huszar, J Karlicky, T Novakova, and M Zak. On the comparison of urban canopy effects parameterisation. *International Journal of Environment and Pollution*, 65(1-3):177–194, 2019. doi: https://doi.org/10.1504/IJEP.2019.101840.

C Heaviside, H Macintyre, and S Vardoulakis. The urban heat island: implications for health in a changing environment. *Current environmental health reports*, 4(3):296–305, 2017. doi: https://doi.org/10.1007/s40572-017-0150-3.

J Hidalgo, V Masson, and L Gimeno. Scaling the Daytime Urban Heat Island and Urban-Breeze Circulation. *Journal of Applied Meteorology and Climatology*, 49(5):889–901, 2010. ISSN 1558-8424. doi: https://doi.org/10.1175/2009jamc2195.1.

P Hoppe. The physiological equivalent temperature - a universal index for the biometeorological assessment of the thermal environment. *International Journal of Biometeorology*, 43(2):71–75, 1999. ISSN 0020-7128. doi: https://doi.org/10.1007/s004840050118.

L Howard. *The climate of London*, volume 1. Baldwin C, Printer, London, 1818.

P Huszar, T Halenka, M Belda, M Zak, K Sindelarova, and J Miksovsky. Regional climate model assessment of the urban land-surface forcing over central Europe. *Atmospheric Chemistry and Physics*, 14(22):12393–12413, 2014. ISSN 1680-7316. doi: https://doi.org/10.5194/acp-14-12393-2014.

P Huszar, J Karlicky, J Doubalova, K Sindelarova, T Novakova, M Belda, T Halenka, M Zak, and P Pisoft. Urban canopy meteorological forcing and its impact on ozone and PM25: role of vertical turbulent transport. *Atmospheric Chemistry and Physics*, 20(4):1977–2016, 2020. ISSN 1680-7316. doi: https://doi.org/10.5194/acp-20-1977-2020.

G Jendritzky, R de Dear, and G Havenith. UTCI-Why another thermal index? *International Journal of Biometeorology*, 56(3):421–428, 2012. ISSN 0020-7128. doi: https://doi.org/10.1007/s00484-011-0513-7.

A Kaiser, T Merckx, and H Van Dyck. The Urban Heat Island and its spatial scale dependent impact on survival and development in butterflies of different thermal sensitivity. *Ecology and Evolution*, 6(12):4129–4140, 2016. ISSN 2045-7758. doi: https://doi.org/10.1002/ece3.2166.

J Karlicky, P Huszar, T Halenka, M Belda, N Zak, P Pisoft, and J Miksovsky. Multi-model comparison of urban heat island modelling approaches. *Atmospheric Chemistry and Physics*, 18(14):10655–10674, 2018. doi: https://doi.org/10.5194/acp-18-10655-2018.

S Kato and Y Yamaguchi. Estimation of storage heat flux in an urban area using ASTER data. *Remote Sensing of Environment*, 110(1):1–17, 2007. doi: https://doi.org/10.1016/j.rse.2007.02.011.

A Kircsi and S Szegedi. The development of the urban heat island studied on temperature profiles in Debrecen. *Acta Climatologica et Chorologica Universitatis Szegediensis*, 36(37):63–69, 2003.

ES Krayenhoff and JA Voogt. A microscale three-dimensional urban energy balance model for studying surface temperatures. *Boundary-Layer Meteorology*, 123(3):433–461, 2007. ISSN 0006-8314. doi: https://doi.org/10.1007/s10546-006-9153-6.

H Kusaka, H Kondo, Y Kikegawa, and F Kimura. A simple single-layer urban canopy model for atmospheric models: Comparison with multi-layer and slab models. *Boundary-layer meteorology*, 101(3):329–358, 2001. doi: https://doi.org/10.1023/A:1019207923078.

V Kveton and M Zak. Drought periods occurrence at Prague-Klementinum station. *Meteorological Bulletin*, 2021. ISSN 0026-1173. accepted for publication.

D Y Lai, WY Liu, TT Gan, KX Liu, and QY Chen. A review of mitigating strategies to improve the thermal environment and thermal comfort in urban outdoor spaces. *Science of the Total Environment*, 661:337–353, 2019. ISSN 0048-9697. doi: https://doi.org/10.1016/j.scitotenv.2019.01.062.

Helmut E Landsberg. *The urban climate*. Academic press, 1981.

ZL Li, BH Tang, H Wu, HZ Ren, GJ Yan, ZM Wan, IF Trigo, and JA Sobrino. Satellite-derived land surface temperature: Current status and perspectives. *Remote Sensing of Environment*, 131:14–37, 2013. ISSN 0034-4257. doi: https://doi.org/10.1016/j.rse.2012.12.008.

JB Liao, TJ Wang, XM Wang, M Xie, ZQ Jiang, XX Huang, and JL Zhu. Impacts of different urban canopy schemes in WRF/Chem on regional climate and air quality in Yangtze River Delta, China. *Atmospheric Research*, 145:226–243, 2014. ISSN 0169-8095. doi: https://doi.org/10.1016/j.atmosres.2014.04.005.

H.L. Macintyre and C. Heaviside. Potential benefits of cool roofs in reducing heat-related mortality during heatwaves in a European city. *Environment International*, 127:430–441, 2019. ISSN 0160-4120. doi: https://doi.org/10.1016/j.envint.2019.02.065.

A Martilli, A Clappier, and MW Rotach. An urban surface exchange parameterisation for mesoscale models. *Boundary-Layer Meteorology*, 104(2):261–304, 2002. ISSN 0006-8314. doi: https://doi.org/10.1023/a:1016099921195.

A Matzarakis, H Mayer, and MG Iziomon. Applications of a universal thermal index: physiological equivalent temperature. *International Journal of Biometeorology*, 43(2):76–84, 1999. ISSN 0020-7128. doi: https://doi.org/10.1007/s004840050119.

A Matzarakis, F Rutz, and H Mayer. Modelling radiation fluxes in simple and complex environments - application of the RayMan model. *International Journal of Biometeorology*, 51(4):323–334, 2007. ISSN 0020-7128. doi: https://doi.org/10.1007/s00484-006-0061-8.

A Matzarakis, S Muthers, and F Rutz. Application and comparison of UTCI and PET in temperate climate conditions. *Finisterra*, 49(98), 2014.

PA Mirzaei. Recent challenges in modeling of urban heat island. *Sustainable Cities and Society*, 19:200–206, 2015. ISSN 2210-6707. doi: https://doi.org/10.1016/j.scs.2015.04.001.

PA Mirzaei and F Haghighat. Approaches to study Urban Heat Island - Abilities and limitations. *Building and Environment*, 45(10):2192–2201, 2010. ISSN 0360-1323. doi: https://doi.org/10.1016/j.buildenv.2010.04.001.

CJG Morris, I Simmonds, and N Plummer. Quantification of the influences of wind and cloud on the nocturnal urban heat island of a large city. *Journal of Applied Meteorology and Climatology*, 40(2):169–182, 2001. doi: https://doi.org/10.1175/1520-0450(2001)040⟨0169:QOTIOW⟩2.0.CO;2.

JM Norman and F Becker. Terminology In Thermal Infrared Remote-Sensing Of Natural Surfaces. *Agricultural and Forest Meteorology*, 77(3-4):153–166, 1995. ISSN 0168-1923. doi: https://doi.org/10.1016/0168-1923(95)02259-z.

Timothy R Oke. Review of urban climatology 1973-1976. 1979. Technical Note 169 Geneva: World Meteorological Organization.

TR Oke. The Energetic Basis Of The Urban Heat-Island. *Quarterly Journal of the Royal Meteorological Society*, 108(455):1–24, 1982. ISSN 0035-9009. doi: https://doi.org/10.1002/qj.49710845502.

TR Oke. The Urban Energy-Balance. *Progress in Physical Geography*, 12(4):471–508, 1988. ISSN 0309-1333. doi: https://doi.org/10.1177/030913338801200401.

TR Oke and GB Maxwell. Urban Heat Island Dynamics In Montreal And Vancouver. *Atmospheric Environment*, 9(2):191–200, 1975. ISSN 1352-2310. doi: https://doi.org/10.1016/0004-6981(75)90067-0.

M Polrolniczak, L Kolendowicz, A Majkowska, and B Czernecki. The influence of atmospheric circulation on the intensity of urban heat island and urban cold island in Poznan, Poland. *Theoretical and Applied Climatology*, 127(3-4):611–625, 2017. ISSN 0177-798X. doi: https://doi.org/10.1007/s00704-015-1654-0.

AM Rizwan, LYC Dennis, and L Chunho. A review on the generation, determination and mitigation of Urban Heat Island. *Journal of environmental sciences*, 20(1):120–128, 2008. doi: https://doi.org/10.1016/S1001-0742(08)60019-4.

SN Rodionov. A sequential algorithm for testing climate regime shifts. *Geophysical Research Letters*, 31(9), 2004. ISSN 0094-8276. doi: https://doi.org/10.1029/2004gl019448.

Y Sakakibara and E Matsui. Relation between heat island intensity and city size indices/urban canopy characteristics in settlements of Nagano basin, Japan. *Geographical review of Japan*, 78(12):812–824, 2005.

M Santamouris, C Cartalis, A Synnefa, and D Kolokotsa. On the impact of urban heat island and global warming on the power demand and electricity consumption of buildings-A review. *Energy and Buildings*, 98:119–124, 2015. ISSN 0378-7788. doi: https://doi.org/10.1016/j.enbuild.2014.09.052.

JS Scire, FR Robe, ME Fernau, and RJ Yamartino. A user's guide for the CALMET Meteorological Model. *Earth Tech, USA*, 37, 2000.

WC Snyder, ZM Wan, YL Zhang, and YZ Feng. Thermal infrared (3-14 mu m) bidirectional reflectance measurements of sands and soils. *Remote Sensing of Environment*, 60(1):101–109, 1997. ISSN 0034-4257. doi: https://doi.org/10.1016/s0034-4257(96)00166-6.

J Spagnolo and R de Dear. A field study of thermal comfort in outdoor and semi-outdoor environments in subtropical Sydney Australia. *Building and Environment*, 38(5):721–738, 2003. ISSN 0360-1323. doi: https://doi.org/10.1016/s0360-1323(02)00209-3.

H Staiger, G Laschewski, and A Gratz. The perceived temperature–a versatile index for the assessment of the human thermal environment. Part A: scientific basics. *International journal of biometeorology*, 56(1):165–176, 2012. doi: https://doi.org/10.1007/s00484-011-0409-6.

RD Thompson and A Perry. Applied Climatology, 1997.

IF Trigo, IT Monteiro, F Olesen, and E Kabsch. An assessment of remotely sensed land surface temperature. *Journal of Geophysical Research-Atmospheres*, 113 (D17), 2008. ISSN 2169-897X. doi: https://doi.org/10.1029/2008jd010035.

P Tryjanowski, T H Sparks, S Kuzniak, P Czechowski, and L Jerzak. Bird Migration Advances More Strongly in Urban Environments. *Plos One*, 8(5), 2013. ISSN 1932-6203. doi: https://doi.org/10.1371/journal.pone.0063482.

LWA van Hove, CMJ Jacobs, BG Heusinkveld, JA Elbers, BL van Driel, and AAM Holtslag. Temporal and spatial variability of urban heat island and thermal comfort within the Rotterdam agglomeration. *Building and Environment*, 83:91–103, 2015. ISSN 0360-1323. doi: https://doi.org/10.1016/j.buildenv.2014.08.029.

JA Voogt and TR Oke. Thermal remote sensing of urban climates. *Remote Sensing of Environment*, 86(3):370–384, 2003. ISSN 0034-4257. doi: https://doi.org/10.1016/s0034-4257(03)00079-8.

James Voogt. How researchers measure urban heat islands. In *United States Environmental Protection Agency (EPA), State and Local Climate and Energy Program, Heat Island Effect, Urban Heat Island Webcasts and Conference Calls*, 2007.

ZM Wan and J Dozier. A generalized split-window algorithm for retrieving land-surface temperature from space. *Ieee Transactions on Geoscience and Remote Sensing*, 34(4):892–905, 1996. ISSN 0196-2892. doi: https://doi.org/10.1109/36.508406.

HB Yang, CF Xi, XC Zhao, PL Mao, ZM Wang, Y Shi, T He, and ZH Li. Measuring the Urban Land Surface Temperature Variations Under Zhengzhou City Expansion Using Landsat-Like Data. *Remote Sensing*, 12(5), 2020. doi: https://doi.org/10.3390/rs12050801.

J H Yuan, K Emura, and C Farnham. Is urban albedo or urban green covering more effective for urbanmicro climate improvement?: A simulation for Osaka. *Sustainable Cities and Society*, 32:78–86, 2017. ISSN 2210-6707. doi: https://doi.org/10.1016/j.scs.2017.03.021.

P Zahradnicek, M Zak, and P Skalak. Physiological equivalent temperature as an indicator of the UHI effect with the city of Prague as an example. 2014. Mendel and Bioclimatology International Conference Brno Czech Republic.

M Zak and H Skachova. Study of Prague's UHI development with respect to wind field computed by CalmetIntegrator Programme. 2010. DACH 2010 Bonn Germany.

M Zak, J Miksovsky, and P Pisoft. CMSAF radiation data: New possibilities for climatological applications in the Czech Republic. *Remote Sensing*, 7(11): 14445–14457, 2015. ISSN 2072-4292. doi: https://doi.org/10.3390/rs71114445.

M Zak, P Zahradnicek, P Skalak, T Halenka, D Ales, V Fuka, M Kazmukova, O Zemanek, J Flegl, K Kiesel, R Jares, J Ressler, and P Huszar. *Pilot Actions in European Cities – Prague*, pages 373–400. Springer International Publishing, Cham, 2016. ISBN 978-3-319-10425-6. doi: https://doi.org/10.1007/978-3-319-10425-6_14.

M Zak, A Dumitrescu, M Belda, and T Halenka. Urban heat island in changing climate. 2019a. European Geosciences Union General Assembly 2019 Vienna Austria.

M Zak, Kveton, and P V, Zahradnicek. Urban heat island of Prague and it's effect on day to day temperature variation. 2019b. European Meteorological Society Annual Meeting 2019 Copenhagen Denmark.

M Zak, IA Nita, A Dumitrescu, and S Cheval. Influence of synoptic scale atmospheric circulation on the development of urban heat island in Prague and Bucharest. *Urban Climate*, 34:100681, 2020. ISSN 2212-0955. doi: https://doi.org/10.1016/j.uclim.2020.100681.

JL Zha, DM Zhao, J Wu, and PW Zhang. Numerical simulation of the effects of land use and cover change on the near-surface wind speed over Eastern China. *Climate Dynamics*, 53(3-4):1783–1803, 2019. ISSN 0930-7575. doi: https://doi.org/10.1007/s00382-019-04737-w.

DL Zhang, YX Shou, and RR Dickerson. Upstream urbanization exacerbates urban heat island effects. *Geophysical Research Letters*, 36, 2009. ISSN 0094-8276. doi: https://doi.org/10.1029/2009gl041082.

Appendix A

M Zak, IA Nita, A Dumitrescu, and S Cheval. Influence of synoptic scale atmospheric circulation on the development of urban heat island in Prague and Bucharest. *Urban Climate*, 34:100681, 2020. ISSN 2212-0955.
doi:https://doi.org/10.1016/j.uclim.2020.100681.

Urban Climate 34 (2020) 100681

Contents lists available at ScienceDirect

Urban Climate

journal homepage: www.elsevier.com/locate/uclim

Influence of synoptic scale atmospheric circulation on the development of urban heat island in Prague and Bucharest

Michal Zak[a,b,*], Ion-Andrei Nita[c,d], Alexandru Dumitrescu[f], Sorin Cheval[b,c,e]

[a] Department of Atmospheric Physics, Charles University, Prague, Czech Republic
[b] The Research Institute of the University of Bucharest, Bucharest, Romania
[c] National Meteorological Administration, Department of Research, Bucharest, Romania
[d] "Alexandru Ioan Cuza University" of Iasi, Faculty of Geography and Geology, Iasi, Romania
[e] "Henri Coandă" Air Force Academy, Brașov, Romania
[f] National Meteorological Administration, Department of Climatology, Bucharest, Romania

ARTICLE INFO

Keywords:
Urban climate
Urban heat island
Synoptic scale atmospheric circulation
Climate change
Trend analysis

ABSTRACT

This study has analysed the development of the urban heat island (UHI) under various synoptic scale atmospheric circulation for two large cities – Prague in central Europe and Bucharest in south-eastern Europe, including seasonal differences and long-term changes. At the best of our knowledge, it is the first comparison between two European cities from this perspective. Analysis was conducted on the base of minimum air temperature data from pairs of urban and peri-urban stations. The average UHI intensity is 2.3 °C for Prague and 1.8 °C for Bucharest, it exceeds 4 °C in 6–10% of cases, and the highest values occur in August in both cities. The annual course of monthly mean values of UHI intensities has higher amplitude in Bucharest (1.2 °C) than Prague (0.6 °C). Synoptic scale circulation is classified according to mean sea level pressure data from ECMWF Era-Interim reanalysis using cost733class software. The results show that UHI is more intense under anticyclonic situations with southern winds in the both cities. Over 1981–2016, we found that the UHI intensity followed statistically significant increasing trend, much larger trend for Bucharest than Prague (3.3 °C vs. 1.3 °C / 100 years).

1. Introduction

Urban heat island (UHI) is a phenomenon occurring at the crossroad between the metropolitan areas and regional climate, consisting of a significantly higher city temperature in respect to the surrounding peri-urban and rural neighbourhoods. The reasons for the UHI occurrence are relatively well understood (e.g. Landsberg, 1981; Oke, 1982; Arnfield, 2003), and the effect of meteorological parameters on UHI magnitude was the subject of considerable research (Sakakibara and Matsui, 2005, Park, 1986, Stewart, 2011; Hove et al., 2015.

Since the intensity of the UHI largely depends on the size and population of the cities, one can expect an increasing UHI intensity in the coming years due to the foreseen growing of population living in urban areas. The effect of the UHI will very likely increase the adverse effect of heat waves which are expected to become more frequent as the result of global warming Founda and Santamouris (2017). Consequently, its impact on different sectors e.g. health, transportation or building industry will be higher.

The development of the UHI is strongly influenced by synoptic circulation. The anticyclonic conditions are generally more

* Corresponding author.
E-mail address: michal.zak@mff.cuni.cz (M. Zak).

https://doi.org/10.1016/j.uclim.2020.100681
Received 11 January 2019; Received in revised form 24 May 2020; Accepted 31 July 2020
Available online 14 August 2020

favourable because of higher direct radiation due to lack of cloudiness and weak winds (Morris et al., 2001). However, even under anticyclonic conditions low cloudiness can develop and hinder the “radiation weather” in the city. Wind can be quite strong, destroying or barring the UHI development. Therefore, the influence of the anticyclonic conditions on UHI are different according to the geographic position of the anticyclone and prevailing wind direction (Morris and Simmonds, 2000). The lowest UHI magnitude does not necessarily occur under cyclonic conditions. Many papers focus on the optimal conditions for UHI development, such as clear sky, and weak wind, or describe its average features, while the number of studies dealing in depth with the relationship between the UHI magnitude and various synoptic conditions is considerable smaller (e.g. Beranova and Huth, 2005; Półrolniczak et al., 2017).

In the central and south-eastern Europe, the influence of the synoptic conditions on the UHI characteristics was studied for medium-size cities, e.g. Szeged (Unger, 1996) and Debrecen in Hungary (Szegedi and Kircsi, 2003), or Poznań in Poland (Półrolniczak et al., 2017), as well as for large cities e.g. Athens, Greece Mihalakakou et al., 2004), or Augsburg, Germany (Beck et al., 2018). These studies used data from measuring campaigns with the advantage of large spatial coverage, but at short time span (2 to 6 years), unsuitable for capturing climate trends or long- term behaviour of UHI. Beranova and Huth (2005) studied the UHI of Prague over 1961–1990 period, based on the Bradka synoptic catalogue,[1] which uses the cyclonic/anticyclonic and directional characteristics (Bradka et al., 1961). The results showed that the North to North-East and South to South-West synoptic flows amplify the Prague's heat island. However, the results may be biased because the use of the Bradka synoptic catalogue is limited to central Europe.

The main objective of this paper is to characterize the development of the UHI under various synoptic scale atmospheric circulation for two large cities – Prague, in Central Europe – and Bucharest – in South-Eastern Europe. The analysis includes seasonal differences and long-term changes. The comparison of two cities placed in different geographic conditions can enhance our understanding in UHI formation and may facilitate the transfer of the results to other areas.

2. Study areas

The selection of Prague and Bucharest is motivated by the similarities in their physical-geographical background. Both cities are situated in large depression-like structures (Bohemian Depression for Prague and Romanian Plain for Bucharest) surrounded by mountain barriers around at 100 to 200 km distance, which shapes the atmospheric circulation at synoptic scale (i.e. Krusne hory/Erzgebirge and Krkonose to the west to north, and Sumava to the south from Prague, and Carpathians, to the north to west and Balkan Mountains, to the south of Bucharest).

2.1. Prague

Prague is the most populated and the capital city of the Czech Republic settled along both sides of the Vltava river. The distribution of green infrastructure (i.e. parks and woods) is quite non-uniform, with generally more green areas situated in the southwestern part of the city.

The climate of Prague is mild and transitory between maritime and continental with thermal continentality according to Gorczyański 26–27% (Kveton and Zak, 2007), the multiannual thermal amplitude is 28.7 °C, with mean daily minimum temperature of −3.6 °C in January and mean daily maximum temperature of 25.1 °C in July (Table 1).

The territorial development of Prague has led to continuous spread of built up areas and change in land cover types from green/agricultural to built-up (e.g. flats, factories, commercial and transport areas) parallel with increase of the population (i.e. from one million at the end of the 1940s to approx. 1.3 million nowadays). Two periods of important changes of the land cover types may be delimited, namely the period 1960–1980 and the period after 1990, defined by the transformation of economy from state controlled economy to market economy, when almost 2% of „green “areas was converted into built-up categories (Environment Portal of Prague, 2020). Nowadays green areas (parks, gardens, woods, grass areas) represent approx. 25% of the city. The role of this green areas on the UHI is not very strong, since the larger regions of greenery are situated mostly in the outer parts of the city having only limited influence – mainly in reducing the size of the UHI of Prague (Huszár et al., 2014). The historical densely built-up centre is surrounded by scattered forms of houses usually having 4 to 8 floors, partly modern partly almost 100 years old. Further, large areas of blocks of flats built in the period 1960–1980 mixed with modern high-rise buildings (often office buildings) arise. Details on land use of Prague can be seen on Fig. 1.

2.2. Bucharest

Bucharest has about 2 million permanent residents, and it is situated in the south-eastern part of Romania, along the Dâmbovița River. The climate is characterized mostly by moderate continental features with a multiannual thermal amplitude of 48.4 °C, mean daily minimum temperature of −11.9 °C in January and mean daily maximum temperature of 36.5 °C in July (Table 1).

The city has a highly disruptive urban architectural structure as a result of different political regimes and planning strategies. Single- or two story-houses, often surrounded by small gardens are characteristics for the 19th century part of the city. Between the two world wars, taller buildings were erected, usually with 3–8 storeys, setting better the urban profile of the epoch. Abrupt changes occurred during the socialist period (1950–1989), and especially in the eighties, when built-up areas replaced many green areas, and the height profile of the city changed dramatically. Compact areas built after the devastating earthquake that hit Bucharest in 1977

[1] http://portal.chmi.cz/historicka-data/pocasi/typizace-povetrnostnich-situaci#

Table 1
Comparison of main geographic and meteorological characteristics of Prague and Bucharest.

	Prague	Bucharest
General characteristics		
Area	496 km^2	240 km^2
Population	1,300,000	2.104.967
Average altitude above sea level	235 m	72 m
Altitudinal range	180–395 m	54–90 m
Size of green areas	25%	12%
Meteorological characteristics		
Annual average temperature	8.9–10.8 °C	11.6 °C
July average temperature	20.8 °C	23.4 °C
January average temperature	0.9 °C	−0.7 °C
Annual average precipitation	500 mm	603.3 mm
The driest month	February (20 mm)	February (35.6. mm)
The wettest month	June (70 mm)	June (78 mm)

have 4 to 10 story-buildings and they are widespread over the city. After 1990, the building profile have gradually changed. The central part of the city became more compact, and the city extended over the marginal neighbourhood, sometimes at the expense of significant green areas, such Băneasa Forest, in the northern part of the city.

Currently, the urban area of Bucharest includes 7 urban lakes covering 46.9 ha, while other 9 "outer", can be found in the neighbouring rural areas, comprising 1044.9 ha. Cheval and Dumitrescu (2015) linked the formation of the Bucharest summer surface UHI to the land cover (Fig. 2) and emphasized the role the urban blue infrastructure in alleviating the UHI impact. For example, In July, the daytime land surface temperature is with 2–3 °C lower over inland waters than over urban fabric.

3. Data and methods

Traditionally, the UHI intensity is calculated as a difference between urban and rural air temperatures, and it depends on factors such as the size of the city and its population, topography, climate zone and meteorological conditions (Oke et al., 1991).

The UHI intensity for the two cities was computed based on pairs of stations. For Prague, we used the weather stations Klementinum, situated in the historical centre (191 m a.s.l., 50°05′1"N, 14°24' E), with the highest annual average temperature in the Czech Republic (10.2 °C for period 1961-2000), and Kbely, situated at the military airport (284 m a.s.l., 50°7'25"N, 14°32′E) as a rural station. Kbely is still within the Prague metropolitan area, but due to its peripheral location with flat, open fields enclosed by green and agricultural terrain, it is treated as a reference station for UHI analysis. For Bucharest, the weather stations București-Filaret (82 m above sea level) in the city centre (44° 24′ 44" N, 26° 05' E), and București-Băneasa (90 m a.s.l.) in the northern outskirts of the city (44°30' 39.95" N, 26° 05′ E) were used. București-Filaret station is placed in an urban park, and Băneasa is situated in an area with intense changes, such shifting from green to built-up spaces, which occurred after 2000. The distance between the rural and urban stations is about 10 km both for Prague and Bucharest (Figs. 1 and 2).

This study focuses on the daily minimum temperatures, as UHI is usually more intense at night-time (Martinez et al., 1991; Unger, 1996; Montavez et al., 2000; Sfîcă et al., 2017; Karlický et al., 2018), and the GrossWetterTypen (GWT) classification scheme of atmospheric circulation based on threshold criteria (Beck, 2000; Beck et al., 2007). This classification is based on daily mean sea level pressure (MSLP) at 12:00 UTC data from ECMWF Era-Interim reanalysis (Dee et al., 2011), using cost733class software (Philipp et al., 2014). The GWT classification characterizes the circulation patterns in three terms of varying degrees of zonality, meridionality and vorticity of the large scale MSLP field. The first one is based on MSLP values increasing from North to South; the second denotes the MSLP increasing from West to East, while the third type denoted the cyclone pattern with pressure values increasing from the baric centre to the outer isobars. Based on the correlation between each input field (i.e. MSLP) and the predefined types, a day is automatically assigned to a class However, the term "objective" is arguable, since the decision for thresholds and criteria still involves subjective decisions. The reproducibility and the fast processing are still important advantages of the GWT classification scheme.

In order to clearly separate the atmospheric circulations types (CT), we have used 18 types, divided in 8 cyclonic, 8 anticyclonic, and 2 types for centre low and centre high situations, as derived from the surface pressure field. The description of all types can be found in Table 2. The overview of the CTs, based on centroids showing the MSLP spatial distribution (Fig. 3), and the frequency and average persistency of each CT (Table 3) show the average synoptic context of the analysed cities.

Fig. 4 illustrates the mean deviation of daily minimum temperatures for all CTs against the multiannual mean, as derived from ECA&D dataset (Haylock et al., 2008). For both cities, the highest positive deviations occur under Ec, SEc and NWa. The largest negative values usually occur under NEa, SWc and Sa types, for Bucharest also during type Ea. In order to increase the sample size for further analyses, the circulation types were divided in two larger groups according to their (anti)cyclonic patterns. Further, these two groups were divided by their mean advection trajectory towards the centre of the domain assessed by the U and V 10 m-wind components retrieved from ERA Interim (Dee et al., 2011). At the end, four circulation classes resulted, as follows: (1) southerly cyclonic, (2) southerly anticyclonic, (3) northerly cyclonic, and (4) northerly anticyclonic (Fig. 2). We preferred to group the circulations into four groups (cyclonic/anticyclonic; northerly and southerly) since this would be easier to interpret the results in the terms of airflow directions.

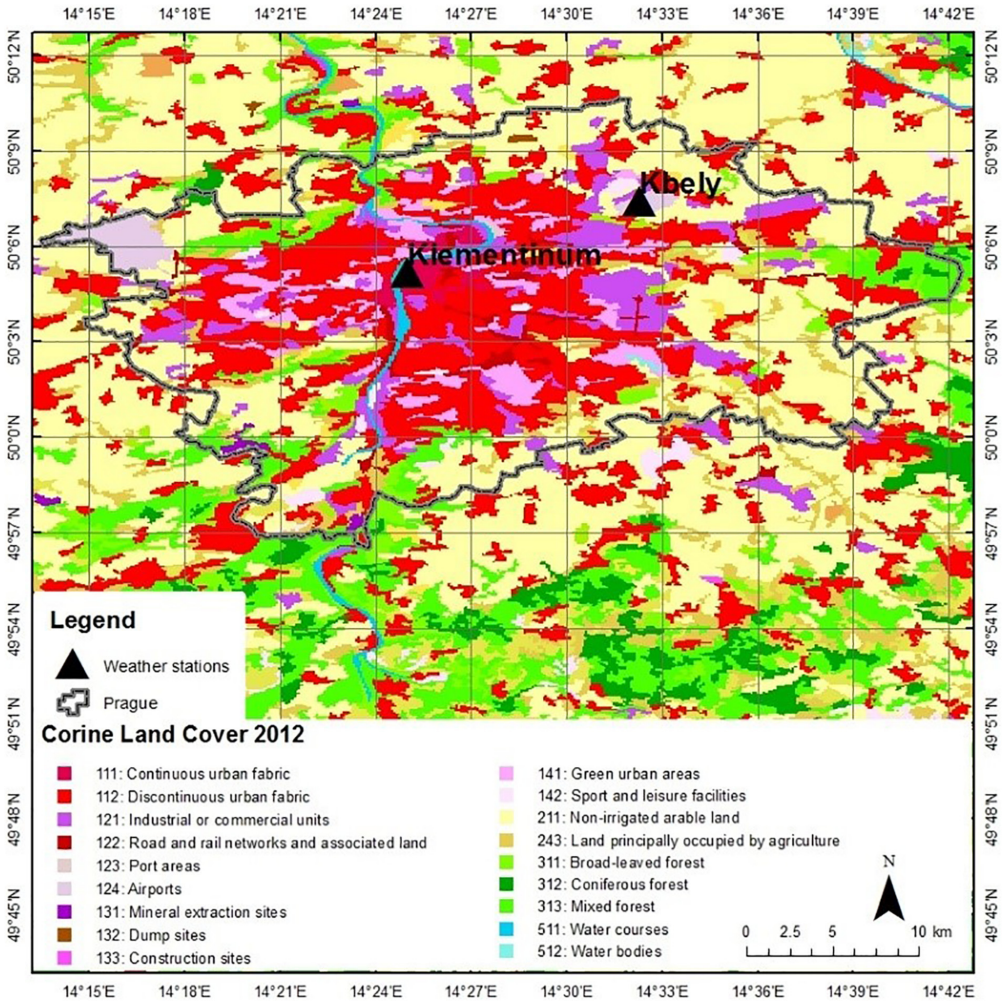

Fig. 1. Land cover map of Prague and weather stations used for this study (source: European Environment Agency - https://land.copernicus.eu/pan-european/corine-land-cover/clc-2012).

In this manner, a western or an eastern circulation type was also grouped into a northern/southern type depending on the predominant mean wind direction for that type. For example, if a circulation had a northwest wind direction, it was labelled as being a northerly (cyclonic or anticyclonic) type. Also, if the airflow had a clear west/east direction, we considered the location of the pressure system imprinting the wind direction. For example, if a high-pressure system was located in the southwestern Europe and the wind direction for Prague (or Bucharest) was predominantly from the west, the circulation was labelled as south anticyclonic. The GWT catalogue provides the CTs for the period 1981–2016.

4. Annual and seasonal regime of the UHI intensity in Prague and Bucharest

Downtown areas are warmer than the outskirts, both for Prague (99% of the total number of nights) and Bucharest (87%), outlining a very clear night-time UHI (Table 3). The differences between the urban and rural areas are mostly less than 2.5 °C, but under convenient circumstances, they can raise up to 8 °C. The situations with night-time UHI intensity higher than 1 °C is 92% for Prague and 59% for Bucharest, while situations with UHI intensity over 3 °C occur in 22% for Prague, and 25% for Bucharest. The

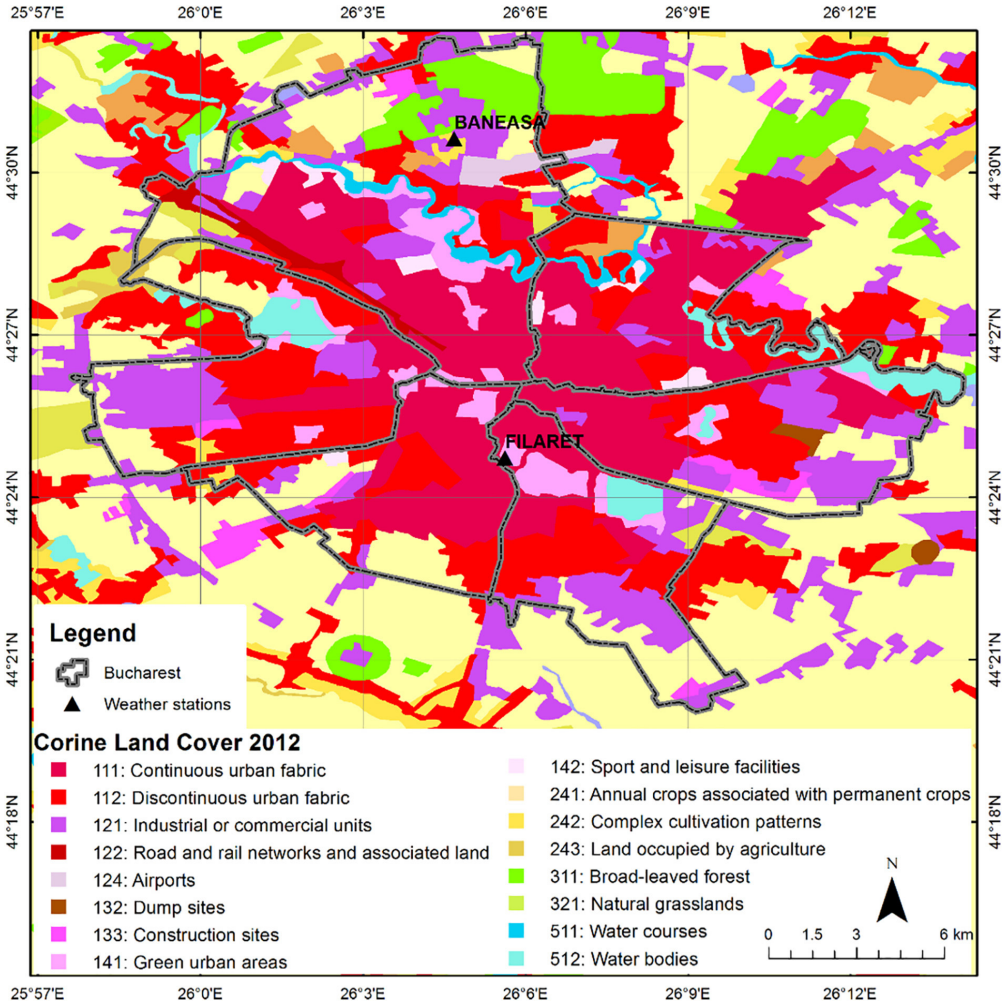

Fig. 2. Land cover map of Bucharest and weather stations used for this study (source: European Environment Agency - https://land.copernicus.eu/pan-european/corine-land-cover/clc-2012).

situations with UHI intensity over 4 °C can be called as an "extreme" UHI. For these situations, an overview is given in Table 4. The relation between cyclonic or anticyclonic weather types and "extreme" UHIs shows that, generally, very strong nocturnal UHIs are more often in Bucharest than in Prague (i.e. 10%, respectively 6%), and they occur more frequently under anticyclonic weather conditions for all seasons in both locations. There are clear seasonal differences between Bucharest and Prague in respect of "extreme" night-time UHI situations. In Bucharest they occur most often in spring and summer, and rarely in winter, while for Prague the highest frequency of the very intense nocturnal UHIs is in winter and spring, while in summer they happen less often.

The UHI is a dynamic phenomenon, with relatively high seasonal variability. The highest monthly average of UHI intensity occurs in August for both cities, while the lowest values can be found for Prague during November and December, and for Bucharest during December and January (see Fig. 5). The larger UHI intensity occurs in Prague (annual average 2.3 °C) than for Bucharest (1.8 °C), but the annual amplitude of the monthly UHI intensity is almost double in Bucharest compared to Prague (i.e. 1.2 °C vs 0.6 °C). This can be caused by the geographical configuration of the compared cities. Bucharest is placed over a relatively flat area, with less than 100 m altitudinal range, while Prague is cut by the Vltava river, with more than 100 m altitudinal amplitude. The historical downtown Prague is very densely built up leading to less intense cooling during winter nights compared to the rate of cooling at

Table 2
Synoptic scale weather circulation types and groups, their persistency and frequency.

Code	Circulation Type	Description	(Anti)cyclonic group	Groups	Persistence	Frequency
1	Nc	Northern cyclonic	Cyclonic	Southerly Cyclonic	1.1	337
2	NWc	Northwest cyclonic	Cyclonic	Southerly Cyclonic	1.2	461
3	NEc	Northeast cyclonic	Cyclonic	–	1.0	220
4	Ec	East cyclonic	Cyclonic	Notherly Cyclonic	1.2	297
5	SEc	Southeast cyclonic	Cyclonic	Notherly Cyclonic	1.4	508
6	Sc	South cyclonic	Cyclonic	Notherly Cyclonic	1.5	581
7	SWc	Southwest cyclonic	Cyclonic	–	1.4	491
8	Wc	West cyclonic	Cyclonic	Southerly Cyclonic	1.3	460
9	Sa	South anticyclonic	Anticyclonic	–	1.5	1359
10	SEa	Southeast anticyclonic	Anticyclonic	Southerly Anticyclonic	1.4	1032
11	SWa	Southwest anticyclonic	Anticyclonic	–	1.4	1156
12	Wa	West anticyclonic	Anticyclonic	Northerly Anticyclonic	1.4	1061
13	NWa	Northwest anticyclonic	Anticyclonic	Northerly Anticyclonic	1.6	1086
14	Na	North anticyclonic	Anticyclonic	–	1.6	994
15	NEa	Northeast anticyclonic	Anticyclonic	–	1.5	706
16	Ea	East anticyclonic	Anticyclonic	Southerly Anticyclonic	1.4	656
17	L	Central Low	Cyclonic	Southerly Cyclonic	1.2	335
18	H	Central High	Anticyclonic	Northerly Anticyclonic	1.4	1409

București-Filaret, the urban station used for Bucharest, placed in a park. This is consistent with the demonstrated different behaviour of urban compact areas, such as Klementinum station in Prague, and less built-up areas, such as urban parks or smaller buildings, such as București-Filaret (Cheval and Dumitrescu, 2017). The climate continentality is more pronounced in Bucharest than in Prague (Cheval et al., 2017) triggering a higher temperature variability during the year, and the UHI follows the same pattern.

5. UHI intensity in Prague and Bucharest under various synoptic circulation types

The average annual intensity of the nocturnal UHI was computed for all individual circulation types for both cities (Fig. 6). As expected, the UHI is stronger developed under weather types characterized by high radiation, low wind, and minimum cloudiness. For Prague, the highest intensity of UHI is observed under H type (2.8 °C) following by NEa type (2.7 °C), with prevailing south- to south-westerly wind, i.e. warm air with anticyclone conditions. For Bucharest, the situation is slightly different; the largest UHI occurs for the L circulation type (2.2 °C) that has actually only small frequency, followed by Ea type (2.1 °C). While this is quite reasonably for Ea (southerly wind component, more or less anticyclonic circulation, i.e. suitable conditions for UHI development), large UHI intensities for cyclonic low (L) are less expected, since this weather pattern consists of a low- pressure system upon Central Europe extended over the western Romania as well (i.e. less suitable for UHI development). The lowest intensity of UHI can be observed under Nc type for Prague (around 1.8 °C) connected with higher pressure gradient over Czech Republic and wind from North Atlantic bringing more cloudiness. For Bucharest, the UHI is less developed under SWc circulation type (1.1 °C), reflecting the cyclogenesis conditions in the northern Adriatic Sea. This weather pattern is accompanied by cyclonic trajectories and it is responsible for rainy weather over the Balkan Peninsula and Romania.

The annual regime of the UHI was investigated based on the directional groups of CT (see Table 5) to have the similar circulation types in homogenous groups. The maximum UHI can be found for winter season in Prague except for SA group where a bit larger value is observed in spring (although differences between seasons are not too large, usually smaller than 0.3 °C, see Fig. 7). For Bucharest different results can be found with largest intensities occurring during summer (Fig. 8). There are larger differences among seasons for individual groups and seasons compared to Prague, as well. During the summer, the Azores High western ridge is extended towards the eastern Mediterranean delivering southerly air advection for southern Europe. As a consequence of air stability associated to high pressure systems, the summer cloudiness is lower than in the other seasons, leading implicitly to greater direct radiation values.

The lowest UHI intensity for Prague occurs in summer, but not for all directional groups, i.e.NC is smallest in autumn, while for Bucharest, for all directional groups, the lowest intensity happens in winter (Fig. 8).

6. Decadal variability of the UHI

Due to various factors like population increase, enlargement of built up areas and associated development of transport, energy consumption or industrial activities, the UHI can often increase along time. The statistical significance of the linear trends of the UHI intensity variability over 1981–2016 was tested with AnClim software (Stepanek, 2008) at 95% confidence level by the Mann-Kendall test. Increasing trends of UHI intensity are revealed for both studied cities, at a higher rate for Bucharest (Table 6). The trends differ for different seasons and directional groups. The highest increase in Prague occurs during winter season, especially for SA and SC groups, very likely in connection with more often snowless situations occurring in the city centre of under warming climate and more intense UHI development. It is worthy to be noted that trends for NC group are not statistically significant in Prague. For Bucharest, the largest increase can be found during spring, especially for SC group, and for summer days within SA group (above 4 °C

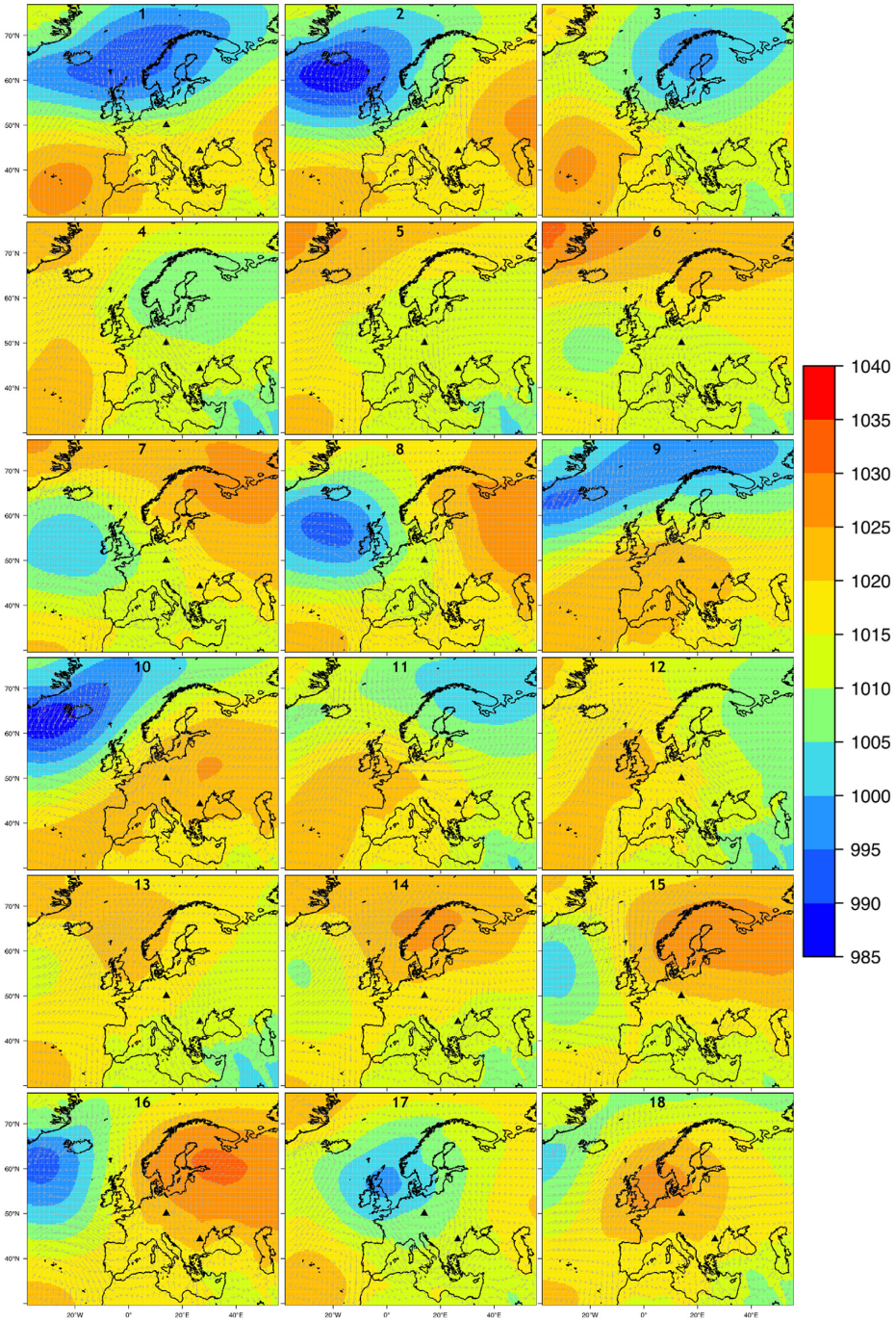

Fig. 3. Weather types based on CT classification scheme (using GWT classification (Beck, 2000).

Table 3
Percent of days with given UHI intensity for Prague and Bucharest.

UHI intensity	0–0.5 °C	0.5–1.0 °C	1.0–1.5 °C	1.5–2.0 °C	2.0–2.5 °C	2.5–3.0 °C	3.0–3.5 °C	3.5–4.0 °C	over 4 °C
Bucharest	14.5%	12.9%	9.6%	9.7%	8.8%	8.6%	7.9%	6.9%	10.4%
Prague	1.8%	5.3%	14.6%	22.4%	18.5%	14.2%	10%	6.3%	6.3%

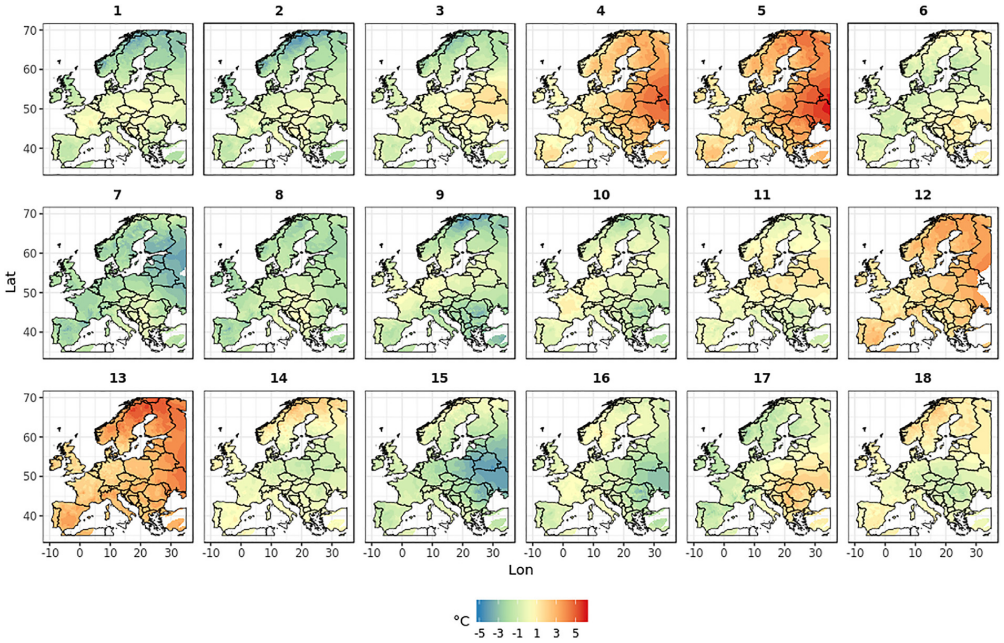

Fig. 4. Mean deviation of daily minimum temperatures for all CTs against the multiannual mean.

Table 4
Number of cases and relative frequencies of the "extreme" UHI occurrence with the intensity over 4 °C in groups of types.

Season	(Anti)cyclonic group	all cases	cases with UHI intensity over 4 °C			
			Prague		Bucharest	
			number of cases	percent of all cases	number of cases	percent of all cases
Spring	anticyclonic	1572	128	8.1	199	12.7
Spring	cyclonic	1740	113	6.5	223	12.8
Spring	all	3312	241	7.3	422	12.7
Summer	anticyclonic	2045	83	4.1	223	10.9
Summer	cyclonic	1267	52	4.1	150	11.8
Summer	all	3312	135	4.1	373	11.3
Autumn	anticyclonic	1825	111	6.1	198	10.8
Autumn	cyclonic	1451	68	4.7	124	8.5
Autumn	all	3276	179	5.5	322	9.8
Winter	anticyclonic	1783	153	8.6	152	8.5
Winter	cyclonic	1466	122	8.3	94	6.4
Winter	all	3249	275	8.5	246	7.6
Year	anticyclonic	7235	475	6.6	772	10.7
Year	cyclonic	5924	355	6.0	591	10.0
Year	all	13,159	830	6.3	1363	10.4

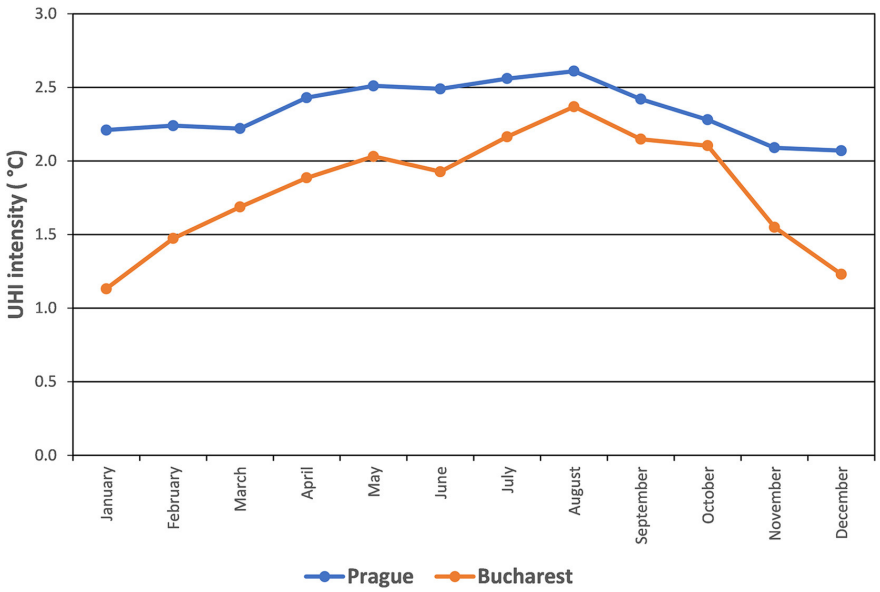

Fig. 5. Annual regime of the mean monthly UHI intensity in Bucharest and Prague.

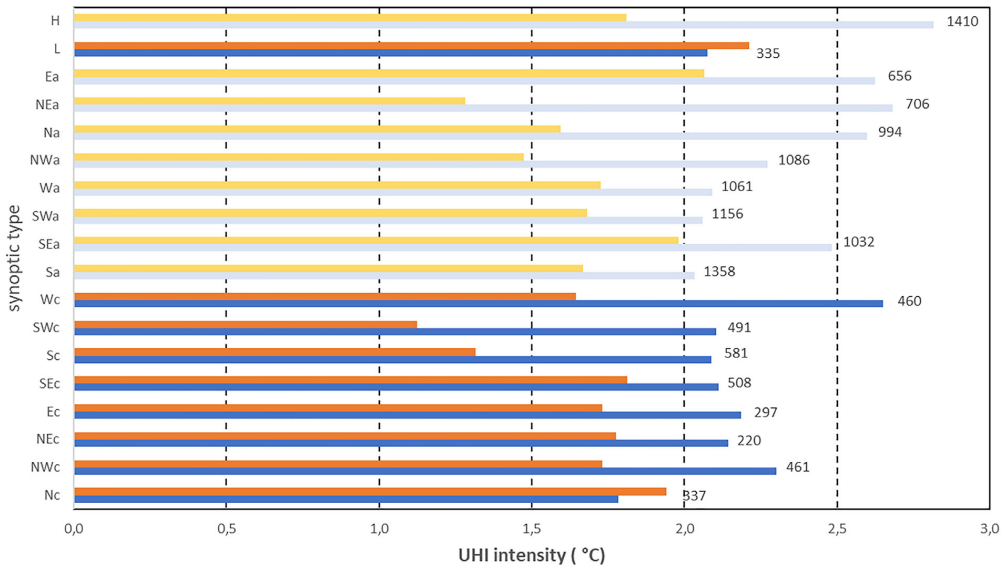

Fig. 6. Average annual intensity of the UHI for different circulation types in Prague (blue) and Bucharest (red-orange). Cyclonic circulation types are marked in dark colours, anticyclonic types are marked in light colour, and figures mean the total number of days for each CT. (For interpretation of the references to colour in this figure legend, the reader is referred to the web version of this article.)

Table 5
Directional groups and corresponding circulation types.

Directional group	Types
NC	Ec, SEc, Sc
SC	Nc, NWc, Wc, L
NA	Wa, NWa, H
SA	SEa, Ea

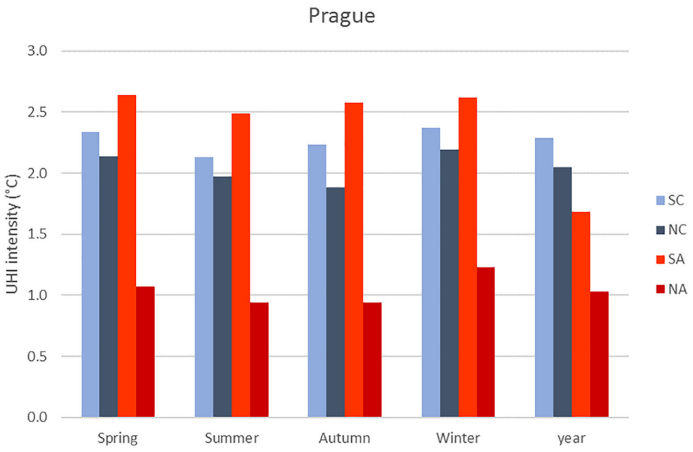

Fig. 7. Average seasonal and annual values of the urban heat island intensity in the directional groups for Prague.

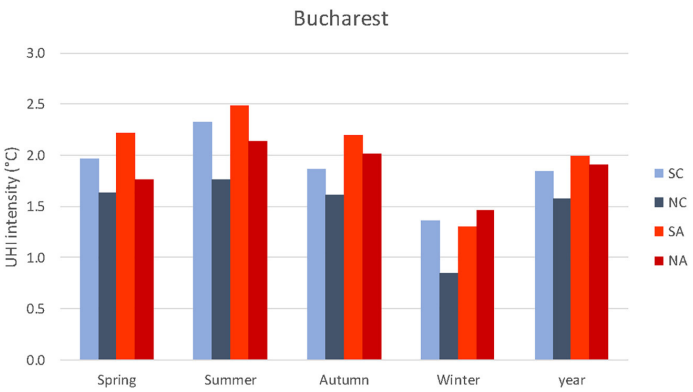

Fig. 8. Average seasonal and annual values of the urban heat island intensity by directional groups for Bucharest.

/ 100 years). Explained variance is generally smaller in Prague compared to Bucharest with higher values for winter and spring, while in Bucharest the highest explained variance is in spring and summer. Figs. 9 and 10 show the variability and trend lines at annual scale (left panels), the seasons with highest trend (middle panels), and the highest trend for given group and season (right panels).

7. Discussion

The urban heat island is a very important climate feature of both studied cities, Prague and Bucharest, especially under era of climate change leading to larger heat stress during warm and heat periods, and more frequently occurrence of tropical days and length of periods with continuous tropical days. The number of warm and/or tropical nights is expected to increase in the next decades (IPCC, 2013) and the question of UHI mitigation needs to be carefully considered by urban planners and architects.

Table 6
Long-term changes in the UHI intensity: linear trend (°C/100 years) and determination coefficient R^2 (explained variance). Statistically significant trends are emphasized in bold.

Group	season	count	Prague		Bucharest	
			trend (°C/100 years)	explained variance	trend (°C/100 years)	explained variance
NA	spring	673	**1.7**	0.17	**3.8**	0.36
	summer	1413	*0.4*	0.02	**3.9**	0.46
	autumn	759	*1.2*	0.11	**2.6**	0.18
	winter	712	*1.2*	0.08	**3.5**	0.27
	year	3557	**1**	0.14	**3.4**	0.54
NC	spring	501	*1.2*	0.1	**2.9**	0.16
	summer	462	*0.8*	0.03	**3.6**	0.27
	autumn	214	*0.9*	0.04	*0.2*	0
	winter	209	*1.1*	0.06	*2.3*	0.08
	year	1386	*0.9*	0.1	**3.2**	0.42
SA	spring	363	**2.1**	0.17	**3.8**	0.32
	summer	230	*-2*	0.03	**4.6**	0.3
	autumn	645	*0.9*	0.05	**2.2**	0.13
	winter	450	**3.4**	0.26	**3.1**	0.11
	year	1688	**1.5**	0.19	**3**	0.4
SC	spring	594	**2.2**	0.22	**4.5**	0.38
	summer	238	*1*	0.05	**3.6**	0.2
	autumn	357	***2.4***	0.32	***3.5***	0.21
	winter	404	**2.4**	0.22	**2.8**	0.2
	year	1593	**2.1**	0.36	**3.3**	0.43
All	spring	3312	**1.5**	0.21	**4.2**	0.53
	summer	3312	*0.8*	0.06	**4**	0.5
	autumn	3276	**1.1**	0.12	**2.1**	0.22
	winter	3249	**1.7**	0.23	**2.9**	0.33
	year	13,149	**1.3**	0.23	**3.3**	0.55

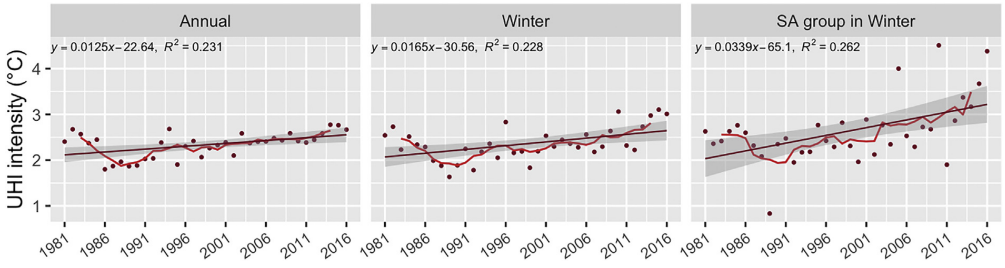

Fig. 9. Variability and linear trendline of the UHI average annual intensity for all situations (left), in winter (middle) and SA group in winter (right) for Prague. Regression line and 5 years running mean are interspersed with a graph. The grey shaded area represents the upper and the lower bounds for the confidence interval (set at 95%) from the linear prediction model line.

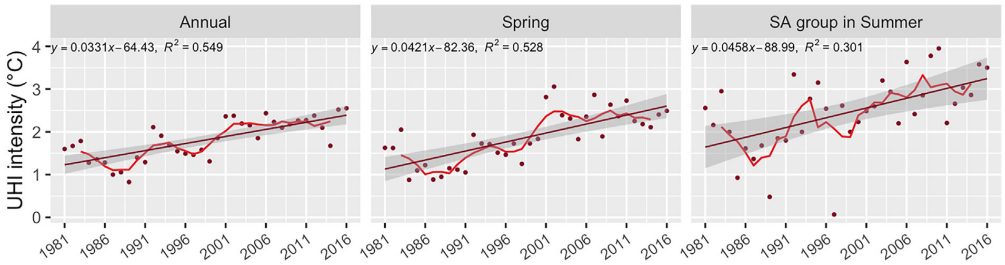

Fig. 10. Variability and linear trendline of the UHI average annual intensity for all situations (left), in spring (middle) and SA group in summer (right) for Bucharest. Regression line and 5 years running mean are interspersed with a graph. The grey shaded area represents the upper and the lower bounds for the confidence interval (set at 95%) from the linear prediction model line.

This study focuses on the connection between UHI development and various synoptic scale circulation patterns during period of 1981–2016. Based on the weather classification provided by the COST 733 Action, we delimited 18 circulation types, half of them cyclonic, and half of them anticyclonic. The classification holds objectivity and it is replicable, which is an important reason for using it. It has to be mentioned that the usage of thresholds and criteria partly involves expert-based decisions. The size of the area containing Bucharest and Prague fits the synoptic analysis, but the position of various pressure system centres can lead to different weather conditions in both cities and influence the UHI development.

The local geography and urban characteristics trigger differences in the UHI intensity and behaviour. With lower population, but more extended spatially, Prague's nocturnal UHI is more intense than the Bucharest one in terms of monthly average. The location of the urban stations is also important in the differentiation, since Prague-Klementinum is placed in a compact built-up area, while București-Filaret is situated in an urban park.

City enlargement, traffic increase and conversion of green areas into built up zones have constantly augmented the UHI intensity in both cities during the last decades. The more than doubled increase for Bucharest compared to Prague can be connected to larger changes in the land-use in this city. For Bucharest, one explanation regarding its positive trends in UHI intensity is the aggressive urbanisation that started in late 1970s by the communist regime and has continued during the recent decades. The patterns of increase are quite similar for both cities (see Figs. 9 and 10), which emphasizes that in this respect the role of the general atmospheric circulation is more important than local land cover changes or different geographic conditions (central Europe/ South-Eastern Europe). A thorough analysis shows that an accumulation of more cyclonic and/or abnormal warm situations would lead to lower UHI intensity. These interesting feature can be observed for both cities in the last pentad of the 1980s, also reflected in the annual means of the UHI intensity (Fig. 10). As regards the temporal variability of the UHI, the increasing trends are more often statistically significant for Bucharest (with more continental climate) compared to Prague.

8. Conclusions

This study has analysed the influence of synoptic scale atmospheric circulation on the UHI intensity for Prague and Bucharest, as well as temporal variability of UHI. At the best of our knowledge, it is the first comparison between two European cities from this perspective. The comparison shows differences and similarities, as described below, and demonstrated the utility of the European circulation types provided by the COST 733 Action.

The UHI phenomenon is common for both cities, at different intensities. For Prague, the average UHI intensity computed from daily minimum air temperatures is 2.3 °C, while for Bucharest is 1.8 °C. The maximum values of the mean UHI intensity can exceed 4 °C (e.g. in Bucharest it occurs in 10% of all cases). The annual course of monthly mean values of UHI intensities has higher amplitude for Bucharest (1.2 °C) than for Prague (0.6 °C). This difference can be caused by higher anthropogenic heat production in downtown Prague during the winter months caused by higher heating in older buildings with less efficient isolation than in downtown Bucharest triggering the intense UHI development. The highest monthly average of UHI intensity occurs in August for both cities when built areas still accumulate radiant heat during daytime in the summer months (JJA) and releasing it slowly during night, while the rural neighbourhood starts cooling more rapidly during longer nights in August.

Different synoptic circulation types influence the UHI development and intensity in the two cities. The UHI of Prague develops especially under H and NEa types, i.e. south- to southwesterly winds, typically under the influence of anticyclone with warm air advection. For Bucharest, the largest intensity of UHI occurs especially under Ea type, i.e. situation with southerly wind component having more or less anticyclonic circulation. The lowest intensity of UHI is observed under Nc type for Prague and SWc for Bucharest. The statistically significant increasing trend of the UHI intensity has been proved for both cities with much larger trend found for Bucharest (3.3 °C vs. 1.3 °C for Prague per 100 years). The changes in the central parts of the two cities were quite different in the last decades, being more dramatic in Bucharest and less pronounced in Prague. This increase differs at seasonal level. In Prague, larger significant increase can be observed during winter, especially for SA and SC directional group, while for Bucharest the largest increase can be found during spring season (especially for SC directional group) and in summer (mainly for SA group). It can be concluded that for both cities the UHI is more intense under anticyclonic situations with southern winds. Such cases are connected with a weakening of atmospheric pressure horizontal gradient leading to weak winds preventing mixing of air in the city and its surroundings and to greater direct radiation values supporting UHI development.

For Prague, the further increase of the UHI intensity is expected since the density of built up areas is increasing and its metropolitan plan prefers the redevelopment of brown fields, usually meaning new more floors buildings. There are plans in mitigating the UHI effects mostly in microclimate scale like adjustment of street canyons, using of green roofs etc., but these measures are probably not so widespread to exceed the UHI increasing trend in the first half of this century.

Similarly, the urban expansion is an ongoing process in Bucharest, together with population increase, business and transport intensification. At the same time, adaptation and mitigation measures are still isolated and far from being efficient. UHI impact is likely to increase unless the urban development is rapidly shaped according to the real needs.

Both Prague and Bucharest will be at least 1 °C warmer by the middle of the century (Cheval et al., 2017)

Considering the comparative approach adopted for this study, including the application of a common methodology for two cities with distinct geographical settings, the use of this concept can be easily performed in other urban areas of similar sizes and complexity.

Declaration of Competing Interest

None

Acknowledgment

We acknowledge the *E*-OBS dataset from the EU-FP6 project UERRA (http://www.uerra.eu) and the Copernicus Climate Change Service, and the data providers in the ECA&D project (https://www.ecad.eu). We thank Assoc. Prof. Lucian Sfică (University "Alexandru Ioan Cuza"of Iași, Romania) for his valuable comments on the manuscript.

References

Arnfield, A.J., 2003. Two decades of urban climate research: a review of turbulence, exchanges of energy and water, and the urban Heat Island. Int. J. Climatol. 23, 1–26. https://doi.org/10.1002/joc.859.
Beck, C., 2000. ZirkulationsdynamischeVariabilitätimBereichNordatlantik-Europa seit 1780 (variability of circulation dynamics in the North-Atlantic–European region). Würzburger Geographische Arbeiten 95 (in German).
Beck, C., et al., 2018. Air temperature characteristics of local climate zones in the Augsburg urban area (Bavaria, southern Germany) under varying synoptic conditions. Urban Clim. 25, 152–166.
Beck, C., Jones, P.D., Jacobeit, J., 2007. Frequency and within-type variations of large-scale circulation types and their effects on low-frequency climate variability in central europe since 1780. Int. J. Climatol. 27 (4), 473–491. https://doi.org/10.1002/joc.1410.
Beranova, R., Huth, R., 2005. Long-term changes in the heat island of Prague under different synoptic conditions. Theor. Appl. Climatol. 82, 113–118.
Bradka, J., Drevikovsky, A., Gregor, Z., Kolesar, J., 1961. Weather on the Territory of Bohemia and Moravia in Typical Weather Situations (in Czech) Hydrometeorological Institute Series of Mean Annual Air Temperatures of the Czech Republic in Typical Weather Situations (in Czech). Hydrometeorological Institute, Prague 32 pp.
Cheval, S., Dumitrescu, A., 2015. The summer surface urban heat island of Bucharest (Romania) retrieved from MODIS images. Theor. Appl. Climatol. 121 (3), 631–640. https://doi.org/10.1007/s00704-014-1250-8.
Cheval, S., Dumitrescu, A., 2017. Rapid daily and sub-daily temperature variations in an urban environment. Clim. Res. 73, 233–246. https://doi.org/10.3354/cr01481.
Cheval, S., Dumitrescu, A., Birsan, M.-V., 2017. Variability of the aridity in the South-Eastern Europe over 1961–2050. Catena 151, 74–86. https://doi.org/10.1016/j.catena.2016.11.029.
Dee, Dick P., et al., 2011. The ERA-interim reanalysis: configuration and performance of the data assimilation system. Q. J. R. Meteorol. Soc. 656, 553–597.
Environment portal of Prague, 2020. http://portalzp.praha.eu/jnp/en/environment/for_experts_and_partner_cities/eia_in_prague/index.xhtml.
Founda, D., Santamouris, M., 2017. Synergies between Urban Heat Island and Heat Waves in Athens (Greece), during an extremely hot summer 2012. Sci Rep. 7 (1), 10973. https://doi.org/10.1038/s41598-017-11407-6Haylock.
Haylock, M.R., Hofstra, N., Klein Tank, A.M.G., Klok, E.J., Jones, P.D., New, M., 2008. A European daily high-resolution gridded dataset of surface temperature and precipitation. J. Geophys. Res (Atmospheres) 113 12 pp.
Hove, L.W.A., et al., 2015. Temporal and spatial variability of urban heat island and thermal comfort within the Rotterdam agglomeration. Build. Environ. 83, 91–103.
Huszár, P., Halenka, T., Belda, M., Zak, M., Sindelarova, K., Miksovsky, J., 2014. Regional climate model assessment of the urban land-surface forcing over Central Europe. Atmos. Chem. Phys. 14, 12393–12413. https://doi.org/10.5194/acp-14-12393-2014.
IPCC, 2013. Climate Change 2013: The Physical Science Basis. In: Stocker, T.F., Qin, D., Plattner, G.-K., Tignor, M., Allen, S.K., Boschung, J. ... Midgley, P.M. (Eds.), Contribution of Working Group I to the Fifth Assessment Report of the Intergovernmental Panel on Climate Change. Cambridge University Press Cambridge, United Kingdom and New York, NY, USA. 1535 pp.
Karlický, J., Huszár, P., Halenka, T., Belda, M., Žák, M., Pišoft, P., Mikšovský, J., 2018. Multi-model comparison of urban heat island modelling approaches. Atmos. Chem. Phys. 18, 10655–10674. https://doi.org/10.5194/acp-18-10655-2018.
Kveton, V., Zak, M., 2007. New climate atlas of Czechia. Stud. Geophys. Geod. 51, 345–349. https://doi.org/10.1007/s11200-007-0019-2.
Landsberg, H.E., 1981. Urban Climate. Academic Press 275 pp.
Martinez, A., Yagüe, C., Zurita, E., 1991. Statistical analysis of the Madrid urban heat island, *Atmospheric Environment. Part B*. Urban Atmosphere 25, 327–332.
Mihalakakou, G., Santamouris, M., Papanikolaou, N., Cartalis, C., Tsangrassoulis, A., 2004. Simulation of the urban heat island phenomenon in Mediterranean climates. Pure Appl. Geophys. 161, 429–451. https://doi.org/10.1007/s00024-003-2447-4.
Montavez, J.P., Jimenes, J.I., Sarsa, A., 2000. A Monte Carlo model of the nocturnal surface temperatures in urban canyons. Bound-Lay. Meteorol. 96, 433–452.
Morris, C.J.G., Simmonds, I., 2000. Associations between varying magnitudes of the urban heat island and the synoptic climatology in Melbourne Australia. Int. J. Climatol. 20, 1931–1954.
Morris, C.J.G., Simmonds, I., Plummer, N., 2001. Quantification of the influences of wind and cloud on the nocturnal urban heat island of a large city. J. Appl. Meteorol. 40, 169–182. https://doi.org/10.1175/1520-04500402.0.CO.
Oke, T.R., 1982. The energetic basis of the urban heat island. Q. J. R. Meteorol. Soc. 108, 1–24.
Oke, T.R., Johnson, D.G., Steyn, D.G., Watson, I.D., 1991. Simulation of surface urban heat islands under 'ideal' conditions at night —part 2: diagnosis of causation. Bound-Layer Meteor. 56, 339–358.
Park, H.-S., 1986. Features of the urban heat island in Seoul and its surrounding cities. Atmos. Environ. 20, 1859–1866.
Philipp, A., Beck, C., Huth, R., Jacobeit, J., 2014. Development and comparison of circulation type classifications using the COST 733 dataset and software. Int. J. Climatol. https://doi.org/10.1002/joc.3920. 20 pp.
Półrolniczak, M., Kolendowicz, L., Majkowska, A., et al., 2017. The influence of atmospheric circulation on the intensity of urban heat island and urban cold island in Poznań, Poland. Theor. Appl. Climatol. 27, 611–625. https://doi.org/10.1007/s00704-015-1654-0.
Sakakibara, Y., Matsui, E., 2005. Relation between heat island intensity and city size indices/urban canopy characteristics in settlements of Nagaro Basin, Japan. Geogr. Rev. Japan 78, 812–824.
Sfică, L., Ichim, P., Apostol, L., Ursu, A., 2017. The extent and intensity of the urban Heat Island in Iași city, Romania. Theor. Appl. Climatol. 134, 777–791. https://doi.org/10.1007/s00704-017-2305-4.
Stepanek, P., 2008. AnClim - Software for Time Series Analysis. Department of Geography Faculty of Natural Sciences, MU, Brno.
Stewart, I.D., 2011. A systematic review and scientific critique of methodology in modern urban heat island literature. Int. J. Climatol. 31 (2), 200–217. https://doi.org/10.1002/joc.2141.
Szegedi, S., Kircsi, A., 2003. The development of the urban heat island studied on temperature profiles in Debrecen. Acta Climatol. Chorologica Univ. Szegediensis 36-37, 63–69.
Unger, J., 1996. Heat island intensity with different meteorological conditions in a medium-sized town: Szeged, Hungary. Theor. Appl. Climatol. 54, 147–151.

Appendix B

M Zak, J Miksovsky, and P Pisoft. CMSAF radiation data: New possibilities for climatological applications in the Czech Republic. *Remote Sensing*, 7(11):14445–14457, 2015. ISSN 2072-4292.
doi: https://doi.org/10.3390/rs71114445.

Remote Sens. **2015**, *7*, 14445-14457; doi:10.3390/rs71114445

OPEN ACCESS

remote sensing

ISSN 2072-4292

www.mdpi.com/journal/remotesensing

Article

CMSAF Radiation Data: New Possibilities for Climatological Applications in the Czech Republic

Michal Žák [1,2,*], Jiří Mikšovský [1] and Petr Pišoft [1]

[1] Department of Atmospheric Physics, Faculty of Mathematics and Physics, Charles University, V Holešovičkách 2, 1800 00 Praha 8, Czech Republic; E-Mails: jiri.miksovsky@mff.cuni.cz (J.M.), petr.pisoft@mff.cuni.cz (P.P.)

[2] Czech Hydrometeorological Institute, Na Sabatce 17, 143 06 Praha 4, Czech Republic

* Author to whom correspondence should be addressed; E-Mail: michal.zak@chmi.cz; Tel.: +420-777-934-479.

Academic Editors: Richard Müller and Prasad S. Thenkabail

Received: 6 August 2015 / Accepted: 22 October 2015 / Published: 30 October 2015

Abstract: Satellite Application Facility on Climate Monitoring (CMSAF) data have been studied in the Czech Republic for approximately 10 years. Initially, validation studies were conducted, particularly regarding the incoming solar radiation product and cloudiness data. The main focus of these studies was the surface incoming shortwave (SIS) radiation data. This paper first briefly describes the validation of CMSAF SIS data for the period of 1989–2009. The main focus is on the use and possible applications of CMSAF data. It is shown that maps of SIS radiation in combination with surface data may be useful for solar power plant operators as well as for assessing the climate variability in the Czech Republic during different years and seasons. This demonstrates that the CMSAF data can improve our understanding of local climate, especially in regions lacking traditional surface observations and/or in border regions with a scarcity of stations in the neighboring countryside. Furthermore, data from the recently released SARAH (Surface Solar Radiation Data Set-Heliosat) dataset (1983–2013) are also briefly described and their use for trend computing is demonstrated. Finally, an outlook is given in terms of further possibilities for using CMSAF data in the Czech Republic.

Keywords: CMSAF; surface incoming shortwave radiation; weather test reference year

1. Introduction

Traditional observations of meteorological elements provide high-quality data but fairly low spatial representativeness, especially for high variability variables. Although the density of the measuring grid could be increased, the cost would exceed the means of the national meteorological services. For some elements, it is possible to replace or complement them with data measured by meteorological satellites. Currently, there is a multitude of products available originating from these measurements, and sometimes it is difficult to determine the parameter best suited to user needs. One option for the European region is provided by METEOSAT through its Satellite Application Facilities [1], which include the Satellite Application Facility on Climate Monitoring (CMSAF), focusing on climate data [2]. CMSAF provides both operational products and long-term datasets.

The operational products have documented non-relevant limitations, which largely satisfy the applicable requirements and/or are deemed sufficiently mature by the relevant Steering Group to be distributed to users [3]. With near real-time availability, they are distributed in a timely manner (within eight weeks) to support operational climate-monitoring applications (e.g., national meteorological and hydrological services). Due to the inhomogeneity caused by the timeliness requirement, these products may not be suitable for monitoring the inter-annual variability and trends with a high confidence. Bias errors due to the shift of equator overpass times, orbit height decay, and instrument errors can cause inter-satellite biases to remain uncorrected for the operational monitoring product. However, the characterization of significant anomalies on the monthly scale is possible.

The datasets, similarly to the operational products, largely satisfy the applicable requirements with documented characteristics, validations, results, and limitations, and they are also deemed sufficiently mature for target applications by the relevant Steering Group. They are retroactively produced and based on carefully inter-sensor calibrated radiances. Their aim is the provision of homogenous sets of high-quality data for the investigation of climate variability and long-term changes of the mean climate state (by minimizing the errors of operational products).

One group of products addresses solar radiation. The solar surface radiation represents one of the basic climate elements. It plays an important role in the global energy cycle, is crucial for many human activities, such as agriculture and solar energy, and, of course, is a factor in many climate processes. The accurate measurement of solar radiation is critical in many fields of (and not limited to) applied climatology, from climate monitoring to solar energy and land surface studies. In the territory of the Czech Republic, the surface incoming shortwave radiation is measured by the Czech Hydrometeorological Institute (CHMI) radiation network. This network was established in 1984, providing 30 years of continuous measurement. The network is composed of just 11 stations (although eight new stations have been added since 2002). Although these traditional man-operated observations usually provide high-quality data, the density of the radiation stations is not high enough to thoroughly cover the area of the Czech Republic (Figure 1). Solar radiation products from CMSAF provide a more complex view of the solar parameter fields, and they are definitively less expensive, with comparable quality to the surface instrumental measurements. This is why products and datasets from CMSAF started to be used in the CHMI. The main focus has been on the surface incoming shortwave radiation, the SIS product (also known as the global irradiance). This climatological element is crucial for various fields of applied climatology that CHMI addresses.

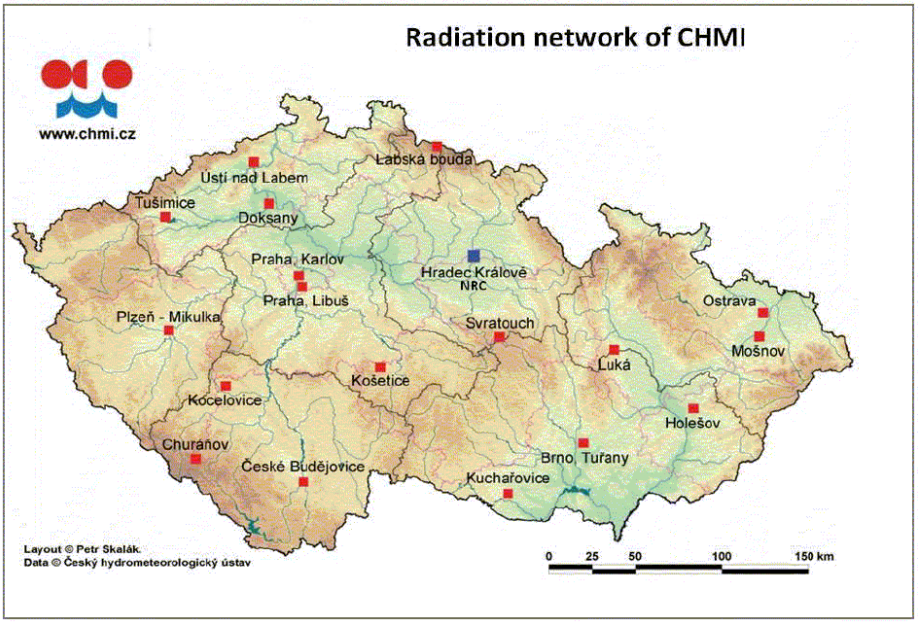

Figure 1. CHMI radiation network stations within the Czech Republic (as of October 2013) (source: http://portal.chmi.cz).

Validation studies of the satellite-generated data were conducted. Naturally, there were prior validation studies conducted directly by the CMSAF staff [4–9]. However, to ensure a convincing confirmation of the quality of the CMSAF data, a comparison was needed with the solar radiation data measured directly in the Czech Republic.

In the beginning of 2015, a new set of long-term data records of surface incoming shortwave radiation, SARAH (Surface Solar Radiation Data Set-Heliosat), was released [10]. This set provides data for the period of 1983 to 2013, including the monthly, daily, and even hourly averages in a regular longitude/latitude grid at a resolution of 0.05° × 0.05°. The accuracy of these data relative to surface measurements is 5.5 m for the monthly SIS averages [11]. It should be noted that SARAH includes not only SIS but also the direct normal radiation and effective cloud albedo.

In the following sections, several applications of CMSAF solar radiation and its usage are described. Because of a partial interconnection between the solar radiation and cloudiness data, we have also focused on selected cloudiness products provided by CMSAF. Sometimes it is more convenient and even precise to work with the sunshine duration to establish the average cloudiness during the day than directly using the cloudiness measurement. The reason for this is the large subjectivity regarding the cloud cover (and its types) in the human observation-based measurement at weather stations. For this reason, we have also paid special attention to cloudiness products of the cloud fractional cover (CFC) and cloud type (CTY) [12].

2. Use and Application of CMSAF Solar Data

2.1. Verification of SIS in the CHMI

As mentioned above, the validation of SIS data was conducted by CMSAF climatologists as well as by other authors. However, before the use of the data for climatological applications, we had to check the data to obtain convincing proof of their reliability, both for us and other potential users. Because the highest demand from users was for monthly data, the comparison was made for this time scale only. The verification was performed similarly to the Validation Report of CMSAF [13]. For 10 stations measuring SIS since 1984, SIS data from the CMSAF dataset from the period of 1989–2009 (based on AVHRR (Advanced Very High Resolution Radiometer) Global Area Coverage data) was extracted for points closest to the stations. Basic statistical parameters (bias, standard deviation, and the number of months with a difference between surface and satellite data over 15 W/m^2) were computed. The results can be seen in Table 1. The values of the bias are approximately 4–5 W/m^2. Although there is generally no substantial difference between various locations, the stations located in the northwestern part of Bohemia (with a stronger aerosol pollution) have slightly higher values. This is consistent with other studies focusing on Central Europe [4] that found a bias of 5.3 W/m^2 for the Hradec Králové station for the period of 1983–2005. This suggests a slight radiation overestimation in CMSAF data compared to the surface measurements. The portion of months with differences exceeding 15 W/m^2 is approximately 11%. The highest bias was found at the Churanov station, located in the mountains in the southwestern Czech Republic; this can be related to the complex terrain in the region, with fog and stratus clouds often forming in the valleys (see [14]). The annual course of SIS radiation sums is similar for both types of data (Figure 2). Generally, it may be concluded that the SIS data from CMSAF are very similar to those measured at the surface, with only slight overestimations compared to surface stations (with the largest bias in April); thus, it is acceptable to use them for various climatological applications.

Table 1. Basic statistics of comparison between SIS (surface incoming shortwave) data from CMSAF (Satellite Application Facility on Climate Monitoring) (SIS product) and the surface station observations at a monthly time scale.

Station (and Type)	Altitude (m a.s.l.)	Bias (W/m^2)	Ratio of Months with Difference over 15 W/m^2	Standard Deviation (W/m^2)	Number of Cases
Hradec Králové (lowland)	285	4.1	10%	8.1	252
Churáňov (mountainous)	1122	4.7	14%	8.8	252
Kocelovice (hilly, countryside)	519	4.6	8%	8.8	252
Košetice (hilly, countryside)	470	4.4	9%	8.3	252
Kuchařovice (lowland, countryside)	334	4.5	10%	8.5	252
Luká (hilly, countryside)	510	4.5	9%	8.4	252
Mošnov (lowland, countryside)	242	4.2	9%	8.3	252
Praha-Karlov (city, centre)	254	4.3	11%	8.2	252
Svratouch (hilly, countryside)	737	4.2	10%	8.1	252
Tušimice (industrial region)	322	4.5	13%	8.6	252
Ústí nad Labem (industrial region)	375	4.6	12%	9.2	252

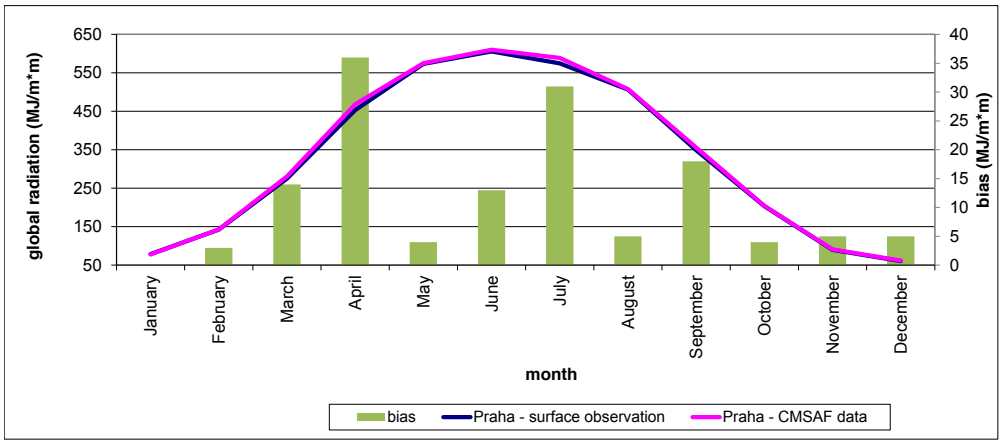

Figure 2. Average annual course (1989–2009) of average monthly sums of SIS radiation (MJ = mega-joules, m = metre) for Prague both for the surface station-and satellite-derived data (SIS product of CMSAF); the bias is also shown.

2.2. Solar Radiation Maps and Graphs—on Monthly and Long Term Bases

The surface incoming shortwave radiation is of great interest to solar power plant operators [5]. However, the information on solar radiation is often also required by banks (providing credit to the operators) and state bodies, such as the Energy Regulatory Office of the Czech Republic. They either require the measured data (which is, however, limited due to the small number of stations observing the global radiation) or sometimes maps. To process maps of SIS, it is necessary to interpolate the observations, but when only measured values are used, the resulting map has limited values due to errors originating from the interpolation. A possible method of improving these maps is the use of a special regression model with the relative sunshine duration values measured at meteorological stations because this parameter is observed more often. Another way is combining both the measured values of SIS from the surface measurements and the SIS data of CMSAF (operational data, see [15] for details). This was conducted by extracting satellite data into a regular grid at a resolution of 15 × 15 km over the Czech Republic area. The extracted values are placed in the centers of the satellite pixels. Further measured values are added where available (in their real positions) and then the values are interpolated with the help of the inverse distance weighting (IDW) method spatial interpolation. The IDW method was selected because the field of solar radiation over the Czech Republic is quite homogeneous, and the input data are fairly equally distributed; otherwise, the kriging method would probably be preferable. Additionally, grids outside the Czech Republic can also be used in constraining the values for the border regions to more realistic estimates. These maps are available with a few weeks' delay compared to the surface data, but their complexity offsets this negative aspect. An example of such a map prepared from an operational product can be seen in Figure 3 (with the indication of utilized locations). It should be noted that due to the customer requests, the values are calculated and presented not in the intensity values but in the amount values (mega-joules per square meter).

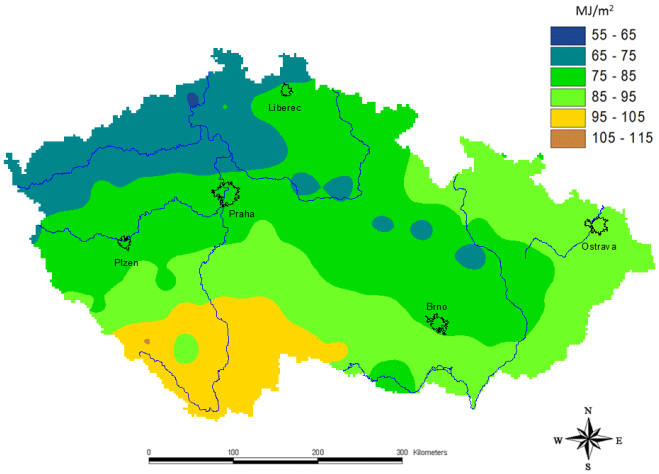

Figure 3. Monthly sum of SIS in December 2013. Example of a product combining the surface measured data and CMSAF data.

From the times series data, long-term averages were also constructed. The resulting maps can facilitate assessment of the solar radiation availability for solar panels in the given region. An example for the whole yearly sum (1989–2009) is shown in Figure 4.

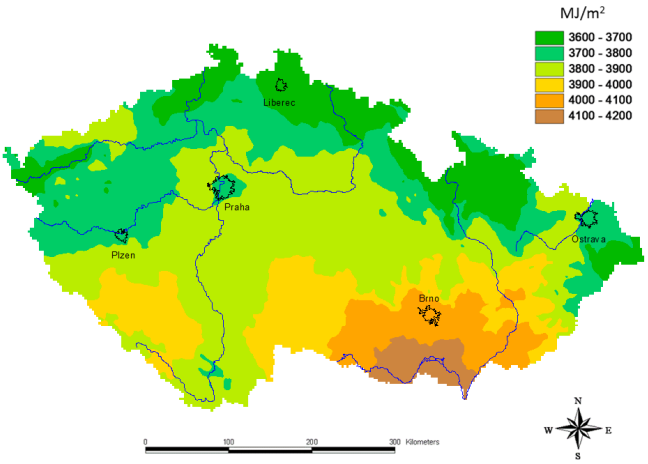

Figure 4. Long-term average of the annual sum of SIS constructed by the combination of measured and CMSAF data (1989–2009).

2.3. Long-Term Changes of Surface Solar Radiation in the Czech Republic

There are various reasons why the long-term changes of SIS are also of some interest. In addition to the aforementioned solar power plant development possibilities, they may be useful, for example, in

agriculture or the tourism industry. In the preceding part of this paper, the SIS CMSAF dataset covering the 20-year period of 1989–2009 was used (the seven years from 1982–1988 might possibly be used as well as auxiliary data), but in climatology, longer periods are better. Usually a period lasting at least 30 years is required for further analyses. Nevertheless, all of this changed in the beginning of 2015 when the SARAH dataset was released. It contains a 31-year period from 1983–2013, which perfectly suits the climatological requirements. Due to the limited time since the data were released, only few analyses could be conducted, the first of which was to capture the trend, if any, of SIS in the Czech Republic. A map was constructed for this period based solely on SIS CMSAF data (Figure 5). It can be seen that while almost no trend is observed in the southern and northeastern parts of the Czech Republic, clear positive trends occur in the northern and northwestern parts of Bohemia. There might be two explanations for this occurrence: (1) The northwestern part of Bohemia was particularly heavily industrialized and substantially polluted in the 1980s (with many brown coal power plants lacking desulphurization). During the 1990s, desulphurization was carried out, and economic changes led to a reduction of the chemical industry and a decrease in aerosol pollution; this had a reducing effect on fog and low-level cloud occurrence [14]. (2) Naturally, climate change might have had an impact, e.g., the lower frequency of Atlantic cyclones (less cloudiness), thus allowing a higher amount of solar radiation to reach the surface [16]. In general, point (1) has had a greater impact. When comparing trends measured at surface stations with those derived from CMSAF, very similar values can be seen (Table 2), and this is in line with previous studies [11].

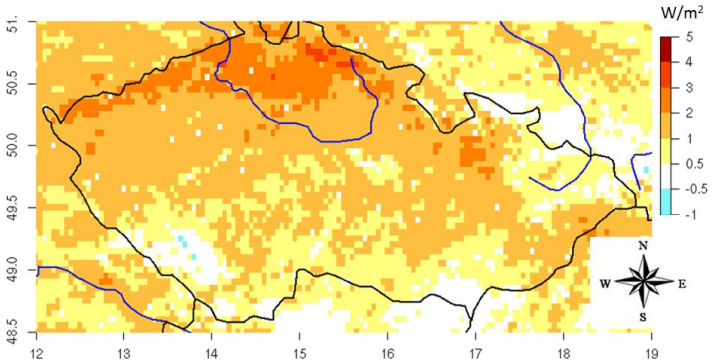

Figure 5. Map of the decadal trend of SIS in the Czech Republic from the SARAH dataset (1983–2013).

Table 2. Decadal trends of SIS for selected stations in the 1983–2013 period. Values for surface stations and for the closest points were derived from SARAH data.

Station (and Type)	Altitude (m a.s.l.)	Trend of Surfaced Data (W/m²)	Trend of Satellite Data (W/m²)
Hradec Králové (lowland)	285	1.6	1.7
Churáňov (mountainous)	1122	1.1	0.8
Ústí nad Labem (industrial region)	375	4.8	4.0
Ostrava (lowland, city)	242	1.2	0.9

Table 2. *Cont*.

Station (and Type)	Altitude (m a.s.l.)	Trend of Surfaced Data (W/m²)	Trend of Satellite Data (W/m²)
Kocelovice (hilly, countryside)	519	0.6	0.4
Košetice (hilly, countryside)	470	1.2	1.2
Kuchařovice (lowland, countryside)	334	1.3	1.1
Luká (hilly, countryside)	510	1.6	1.7
Praha-Karlov (city, centre)	254	1.5	1.9
Svratouch (hilly, countryside)	737	1.6	1.8
Tušimice (industrial region)	322	3.3	2.8

2.4. Weather Test Reference Year

Weather Test Reference Year (TRY) represents a typical course of meteorological elements during the year and has been constructed and used in many countries [17]. However, in the Czech Republic, it was first constructed approximately six years ago [18] using the data from 1990–2005, so it is perfectly covered by the SIS dataset. Since its preparation, it has been used in many application fields, especially in civil engineering. It contains 10 meteorological elements, including temperature, precipitation, humidity, wind, and SIS. Due to limited SIS measurements, it was computed based on the relative sunshine duration. However, the data are not available everywhere, as there are parts of the Czech Republic with a limited number of stations measuring the sunshine duration. This is why a correction of TRY was tested. For these regions, 'fictitious' points were created in selected locations, which differ in climate from the surrounding regions (and have no surface solar radiation observation). These additional points create a denser network of input data. An interpolation based on this network was conducted. We present the results for the southwestern part of Bohemia because this is a region with a complex orography and with different climate features in the immediate neighboring regions. The average May values are given in Figure 6 (a comparison between the original values and the state after adding SIS data from CMSAF). The resultant field of SIS reflects the climate features in the studied area better than the previous approximation.

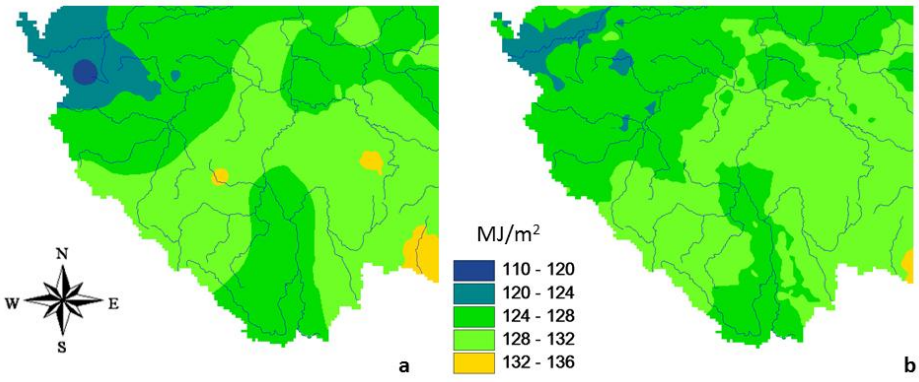

Figure 6. Example of SIS map used for TRY computation (southwestern part of Bohemia) for May ((**a**) based on station data only, (**b**) combination of both station and CMSAF data).

2.5. Solar Radiation and Cloudiness Data

As previously mentioned in the introduction, we focused on selected cloudiness products provided by CMSAF, especially the Cloud Fractional Cover (CFC). CLAAS (CM SAF CLoud property dAtAset) data have been used for this purpose [19]. The average cloudiness is one of the main climatological parameters describing cloudiness, but sometimes it is more convenient and even more accurate to work with the sunshine duration to compute the average cloudiness during the day than using the cloudiness measurement directly. The cloudiness is computed according to the relative sunshine duration for the given day. This is also a common practice in the Czech Republic [14]. Using daily data from seven years, maps of average monthly cloudiness were constructed based on the surface sunshine duration data and CFC data. The method of map construction is as follows: A regular grid of average monthly cloudiness was prepared from CFC data (monthly data from CMSAF). For surface stations measuring sunshine duration, the cloudiness was computed according to the relative sunshine duration. In this network of higher density data (more grids with cloudiness), a spatial interpolation was conducted. An example can be seen in Figure 7.

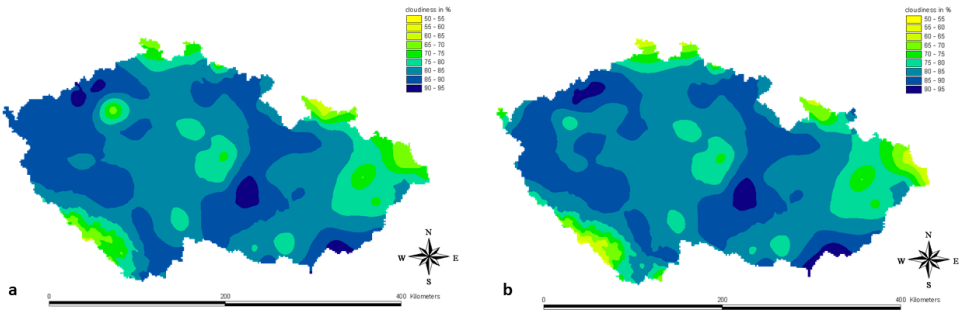

Figure 7. Average monthly cloudiness for November 2012: (**a**) Only station data based on the sunshine duration; (**b**) combination of station and CMSAF data.

2.6. Outlook

Since SARAH data were released, more climatological applications and studies have become possible because we now have a homogenized time series of radiation with a span of 31 years. Because radiation is one of the main climate features, it can be used for various applications in agriculture as well as in many climate classifications. Another potential lies in the tourism industry, e.g., the most and least sunny period for a given place can be obtained; the first results for Prague and the mountain area of Jeseníky in the northeastern part of the Czech Republic are given in Figure 8. A sunny day is defined as a day with 80% or more of available clear-sky surface solar radiation for the given day. Of course, the possibilities of model data validation seem to be promising because these data have very high time and spatial resolution and homogeneity and are freely available, which could be of great importance in the Czech Republic where only a part of the meteorological data is free of charge.

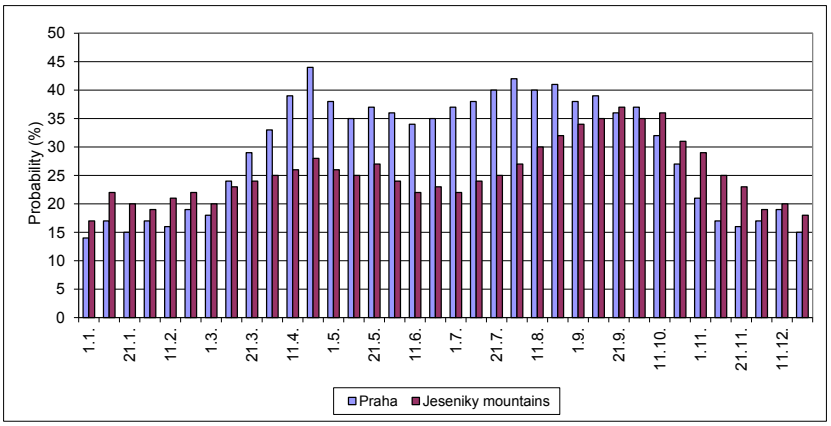

Figure 8. Probability of sunny day occurrence for a given decade for the regions of Prague and the Jeseníky mountains (from SARAH products).

3. Uncertainties, Errors, and Accuracies

As shown in Section 2, the SIS data from the CMSAF are very close to the values observed at the surface climatological stations, which is also the case for the region of the Czech Republic. The differences between these two data sources usually do not exceed 5 W/m^2 for monthly values (in terms of the average intensity of the SIS), with CMSAF data slightly overestimating the ground observations. Also, the number of months with higher differences (in excess of 15 W/m^2) seems to be reasonably small. Validation should also be performed for daily or even hourly values, particularly for the SARAH dataset, but as shown in [10], the monthly and daily mean from CMSAF SARAH have higher quality than the previous CMSAF surface radiation dataset. This is also the case for the direct surface radiation, which was additionally evaluated for the SARAH dataset to allow a comparison with the previous version of the CMSAF surface radiation dataset. Higher uncertainties of SIS are expected for regions with a long-lasting snow cover and desert regions with brighter surfaces, but this is not the case for the territory of the Czech Republic. Furthermore, based on the CMSAF team findings [10], there is no obvious inhomogeneity apparent in the SIS time series, so these time series are fit to be applied in long-term change studies. However, what still needs to be taken into account is the question of possible inhomogeneity caused by the significant decrease in aerosol load after 1989.

4. Discussion

Satellite data provide a great source of climate information and can be used in various applications within climatology, meteorology, or beyond. However, generally this also represents a source of potential problems: When we want to use satellite data instead of (or combined with) surface observations, there is an issue of locality matching (usually the satellite grid point slightly deviates from the surface station location). In the case of solar radiation data, SIS in particular, the situation is generally good. This parameter is instrumentally measured at the surface, so there is no subjective element to be considered when comparing the data with the satellite counterparts (namely CMSAF in this case). For

this reason, the use of SIS provided by CMSAF seems to be very promising and helpful in climatology. Another point that has to be mentioned here, especially regarding the Czech Republic, is the existence of a good network of SIS surface observations (taking into account its spatial variability) and a fairly large number of stations measuring the sunshine duration, a parameter that can be used for the computation of SIS as an alternative. Simultaneously, the recently released SARAH dataset also makes the direct normal radiation available to us, a parameter that is only partly measured, and therefore this element can now be extracted from this dataset for the entire Czech Republic. Another issue is cloudiness. Generally, the observer cannot see all the clouds above him/her if they are located in multiple layers overlapping each other. For example, when observing 8/8 of sky covered by stratus clouds, the observer is not able to spot any higher clouds. The satellite, in contrast, is able to capture cirrus or altostratus clouds above the stratus level. Furthermore, in summer the observers tend to report more distant clouds (in case there is no cloudiness in the station surroundings), especially if they are of convective origin such as cumulonimbus clouds, the anvil of which can be observed from 50 to 100 km or even farther. However, from the satellite's point of view, there are no clouds immediately above the observer. This means the man-performed observation from surface stations can lead to a mismatch when making comparisons with the satellite data, but this is only due to the different viewing technologies and not due to a physical inconsistency. Generally, the specifics of satellite-based observations need to be remembered when comparing them with the surface ("conventional way of") observation. The high quality of measurements from surface stations might also be one of the reasons why climatologists in the Czech Republic do not feel an urgent need to use and work with satellite data (which is not limited to CMSAF data in this respect). Finally, there is also an economic argument for using the satellite data; due to budgetary cuts, the number of stations has decreased in the Czech Republic over the last decade, making the satellite data more useful than ever.

5. Conclusions

The solar radiation data obtained from the CMSAF satellite measurements have proved to be a useful complement to conventional surface observations. They can help to create more realistic maps of the surface incoming shortwave radiation when combining CMSAF SIS data with the surface radiation network observations. These maps can then find various practical applications, for instance, in solar power plants. When the long-term version of the data is utilized, useful information about the local solar climate variability can also be obtained. This is especially the case when using the SARAH dataset data covering the 31-year period of 1983–2013. Such a period is sufficiently long to be used in climatology for various applications. For example, trends can be detected. As has been shown in the Czech Republic, these are mostly slightly positive, with the highest values in the northwestern parts of Bohemia (approximately 4 W/m^2 per 10 years). It is possible to determine the sunniest periods during the year and also during the whole period. For example, in Prague, the sunniest period during the year is the second half of April, whereas the sunniest month since 1983 was July 1994 (which was also one of the warmest months). Many more applications based on this long-term data may yet be found, especially in agriculture, but also in the construction industry. The usefulness of CMSAF solar radiation data has already been shown in the model validation [20–22], with the largest benefit lying in the data homogeneity and resolution, both spatial and temporal.

Acknowledgements

This study was supported by the Czech Science Foundation (GA ČR) through grant P209/11/0956.

Author Contributions

Michal Zak wrote the first draft. All authors planned the manuscript and provided input at all stages of writing.

Conflicts of Interest

The authors declare no conflict of interest.

References

1. EUMETSAT. Available online: http://www.eumetsat.int/website/home/Satellites/GroundSegment/Safs/index.html (accessed on 30 July 2015).
2. Schulz, J.; Albert, P.; Behr, H.-D.; Dewitte, S.; Dürr, B.; Gratzki, A.; Hollmann, R.; Karlsson. K.-G.; Manninen, T.; Müller, R.; *et al*. Operational climate monitoring from space: The EUMETSAT Satellite Application Facility on Climate Monitoring (CMSAF). *Atmos*. *Chem*. *Phys*. **2009**, *9*, 1687–1709.
3. CMSAF. http://www.cmsaf.eu (accessed on 30 July 2015).
4. Sanchez-Lorenzo, A.; Wild, M.; Trentmann, J. Validation and stability assessment of the monthly mean CMSAF surface solar radiation dataset over Europe against a homogenized surface dataset (1983–2005). *Remote Sens*. *Environ*. **2013**, *134*, 355–366.
5. Posselt, R.; Mueller, R.W.; Stöckli, R.; Trentmann, J. Remote sensing of solar surface radiation for climate monitoring—The CMSAF retrieval in international comparison. *Remote Sens*. *Environ*. **2012**, *118*, 186–198.
6. Antonanzas-Torres, F.; Cañizares, F.; Perpiñán, O. Comparative assessment of global irradiation from a satellite estimate model (CMSAF) and on-ground measurements (SIAR): A Spanish case study. *Renew*. *Sustain*. *Energy Rev*. **2013**, *21*, 248–261.
7. Sancho, J.M.; de Sanchez Cos, M.C.; Jiménez, C. Comparison of global irradiance measurements of the official Spanish radiometric network for 2006 with satellite estimated data. *Tethys* **2011**, *8*, 43–52.
8. Journée, M.; Bertrand, C. Improving the spatio-temporal distribution of surface solar radiation data by merging ground and satellite measurements. *Remote Sens*. *Environ*. **2010**, *114*, 2692–2704.
9. Bojanowski, J.S.; Skidmore, A.K.; Vrieling, A. A comparison of data sources for creating a long-term time series of daily gridded solar radiation for Europe. *Sol*. *Energy* **2014**, *99*, 152–171.
10. Müller, R.; Pfeifroth, U.; Träger-Chatterjee, C.; Trentmann, J.; Cremer, R. Digging the Meteosat Treasuer—3 decades of solar surface radiation. *Remote Sens*. **2015**, *7*, 8067–8101.
11. Müller, R.; Pfeifroth, U.; Träger-Chatterjee, C.; Cremer, R.; Trentmann, J.; Hollmann, R. *Surface Solar Radiation Data Set-Heliosat (SARAH)-Edition 1*; EUMETSAT Satellite Application Facility on Climate Monitoring: Offenbach, Germany, 2015.
12. Zak, M.; Sacha, P.; Pisoft, P. On the use of the CMSAF cloud-data in the Czech Republic. In Proceedings of First International Conference on Remote Sensing, Paphos, Cyprus, 8–10 April 2013.

13. Karlsson, K.-G.; Riihelä, A.; Müller, R.; Meirink, J.F.; Sedlar, J.; Stengel, M.; Lockhoff, M.; Trentmann, J.; Kaspar, F.; Hollmann, R.; Wolters, E. CLARA-A1: A cloud, albedo, and radiation dataset from 28 year of global AVHRR data. *Atmos*. *Chem*. *Phys*. **2013**, *13*, 5351–5367.
14. Tolasz, R.; Květoň, V.; Vaníček, K.; Richterová, D.; Němec, L.; Metelka, L.; Valeriánová, A.; Hostýnek, J.; Štěpánek, P.; Žák, M.; *et al*. *Climate Atlas of Czechia*; Czech Hydrometeorological Institute and University of Palacky: Olomouc, Czech Republic, 2007; p. 256.
15. Müller, R.W.; Matsoukas, C.; Gratzki, A.; Behr, H.D.; Hollmann, R. The CMSAF operational scheme for the satellite based retrieval of solar surface irradiance—A LUT based eigenvector hybrid approach. *Remote Sens*. *Environ*. **2009**, *113*, 1012–1024.
16. Climate Change in the Bohemia-Silesia Border Region. Available online: https://publikationen.sachsen.de/bdb/artikel/23661/documents/32551 (accessed on 30 August 2015).
17. Bilbao, J.; Miguel, A.; Franco, J.A.; Ayuso, A. Test Reference Year Generation and evaluation methods in the continental Mediterranean area. *J*. *Appl*. *Meteorol*. **2004**, *43*, 390–400.
18. Květoň, V.; Valeriánová, A.; Žák, M. Weather test reference years in the Czech Republic. *Meteorol*. *Z*. **2009**, *62*, 65–72.
19. Stengel, M.; Kniffka, A.; Meirink, J.F.; Riihelä, A.; Trentmann, J.; Müller, R.; Lockhoff, M.; Hollmann, R. Claas: CMSAF cloud property dataset using SEVIRI-edition 1-hourly/daily means, pentad means, monthly means/monthly mean diurnal cycle/monthly histograms. *Satell*. *Appl*. *Facil*. *Clim*. *Monit*. **2013**, *1*, doi:10.5676/EUM_SAF_CM/CLAAS/V001.
20. Alexandri, G.; Georgoulias, A.K.; Zanis, P.; Katragkou, E.; Tsikerdekis, A.; Kourtidis, K.; Meleti, C. On the ability of RegCM4 regional climate model to simulate surface solar radiation patterns over Europe: An assessment using satellite-based observations. *Atmos*. *Chem*. *Phys*. **2015**, *15*, 18487–18535.
21. Hagemann, S.; Loew, A.; Andersson, A. Combined evaluation of MPI-ESM land surface water and energy fluxes. *J*. *Adv*. *Model*. *Earth Sys*. **2013**, *5*, 259–286.
22. Haiden, T.; Trentmann, J. Verification of cloudiness and radiation forecasts in the greater Alpine region. *Meteorol*. *Z*. **2015**, *13*, doi: 10.1127/metz/2015/0630.

Appendix C

M Zak, P Zahradnicek, P Skalak, T Halenka, D Ales, V Fuka, M Kazmukova, O Zemanek, J Flegl, K Kiesel, R Jares, J Ressler, and P Huszar. *Pilot Actions in European Cities – Prague*, pages 373–400. Springer International Publishing, Cham, 2016. ISBN 978-3-319-10425-6. doi: https://doi.org/10.1007/978-3-319-10425-6_14

Chapter 14
Pilot Actions in European Cities – Prague

Michal Žák, Pavel Zahradníček, Petr Skalák, Tomáš Halenka, Dominik Aleš, Vladimír Fuka, Mária Kazmuková, Ondřej Zemánek, Jan Flegl, Kristina Kiesel, Radek Jareš, Jaroslav Ressler, and Peter Huszár

Abstract This chapter describes results of pilot actions in Prague. Two different pilot areas were selected (Legerova street and Bubny-Holesovice quarter) with different modelling approach. Finally, the Green belt around Prague is studied as well. Different scenarios are tested and their results discussed. The matter of air quality is also analysed.

Keywords Urban heat island of Prague • Potential equivalent temperature • Mitigation of urban heat island • Effects

M. Žák (✉)
Department of Climatology, Czech Hydrometeorological Institute,
14306 Praha 4, Prague, Czech Republic

Faculty of Mathematics and Physics, Department of Atmospheric Physics,
Charles University Prague (CUNI), Prague, Czech Republic
e-mail: michal.zak@chmi.cz

P. Zahradníček • P. Skalák
Department of Climatology, Czech Hydrometeorological Institute,
14306 Praha 4, Czech Republic

T. Halenka • V. Fuka • P. Huszár
Faculty of Mathematics and Physics, Department of Atmospheric Physics,
Charles University Prague (CUNI), Prague, Czech Republic

D. Aleš • M. Kazmuková • O. Zemánek • J. Flegl • R. Jareš
Prague Institute of Planning and Development, Prague, Czech Republic

K. Kiesel
Department of Building Physics and Building Ecology,
Vienna University of Technology, Vienna, Austria

J. Ressler
Institute of Computer Science, The Czech Academy of Sciences, Prague, Czech Republic

F. Musco (ed.), *Counteracting Urban Heat Island Effects in a Global Climate Change Scenario*, DOI 10.1007/978-3-319-10425-6_14

14.1 Urban and Environmental Framework

14.1.1 General Remarks on Prague

Prague is the capital of the Czech Republic. As the largest city in the country by its area (496 km^2) and by population (1.2 million inhabitans) faces the same environmental challenges, as the other large cities in the world. The city strives for the substantial reduction of the environmental burden as to become clean, healthy, and harmonic place for living. Prague is situated on the banks of the Vltava river and its tributaries. The complicated morphology creates limitation for a good ventilation of the area. The lowest point is in 149 m and the surrounding hills at the southwestern part of Prague are almost 400 m above sea level.

14.1.2 Prague Urban Heat Island Analysis

Prague and especially its city centre belongs to the warmest regions of the Czech Republic with annual average air temperature around 10 °C in the city centre (see Fig. 14.1). This is partly caused by the urban heat island (UHI) of Prague.

The intensity of UHI is about 1.6 °C when we use the average daily temperatures. The highest intensity occurs during June, while the lowest intensity in September. It has to be noted, that the UHI intensity of Prague is considerably higher when looking at minimum temperatures (annual average is approximately 3 °C) but smaller for maximum temperatures (annual average approx. 1 °C). The intensity of Prague's UHI has increased during the last 50 years. This increasing is caused due to the city enlargement and transport intensification.

The magnitude of this intensification is 0.15 °C/10 years for minimum temperatures, 0.07 °C/10 years for average daily temperatures and 0.02 °C/10 years for maximum temperatures. This intensification of UHI is documented on Fig. 14.2 where differences of daily air minimum temperatures between period 2001–2010 and 1961–1970 are demonstrated. While the temperature in the whole Prague area increases (due to the climate change in the Central Europe), the largest increment of the temperature can be seen in city centre, close to the Vltava river, in the densely built up part of the city.

Another point of view of the intensity of UHI can be obtained by using physiological equivalent temperature PET (Matzarakis et al. 2010). This temperature describes the temperature really felt by the human being standing outside and includes not only influence of air temperature and wind, but also humidity and radiation including the radiation coming from buildings in the streets. The average annual and daily course of PET for the Praha–Karlov stations is given in Fig. 14.3. It can be seen, that the highest values occur during summer months, July and the first half of August.

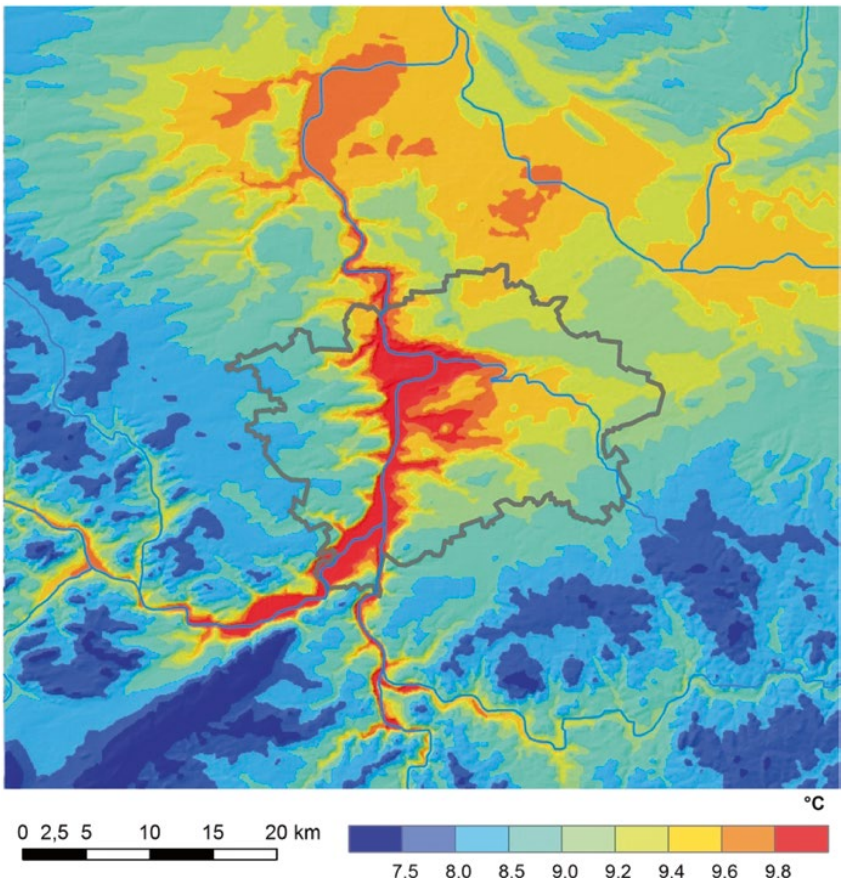

Fig. 14.1 Annual average air temperature for Prague and surrounding, period 1961–2010

The differences of PET values between Praha–Karlov station located in the city centre and Praha–Ruzyně station situated on the periphery of the city (Fig. 14.4) show the highest values in the summer half of the year starting after the sunset and vanishing during the morning hours. Few hours after the sunrise this differences can be even negative indicating lower PET values in the city centre. Regarding long term changes, there is positive trend in PET values in Prague during spring and summer indicating greater human stress during the warm summer half-year. It should be noted that PET was computed for the location with ideal horizon without obstacles – this is also the case of the following case study of a hot day.

The largest UHI negative effects (in the sense of bioclimatic discomfort) usually occur during the summer months. For demonstration, case study of hot day, the day of 28th July 2013 has been chosen. Maximum air temperature on that day reached

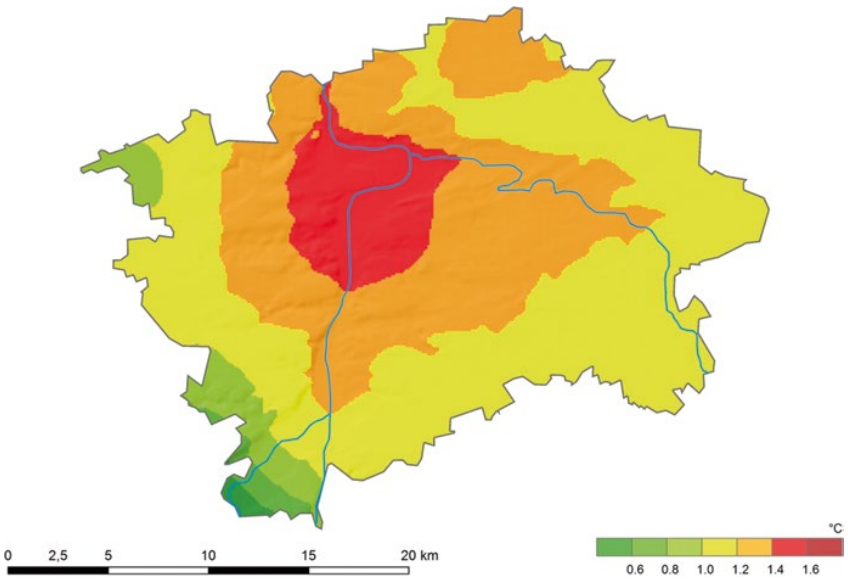

Fig. 14.2 Difference of daily air minimum temperature between period 2001–2010 and 1961–1970

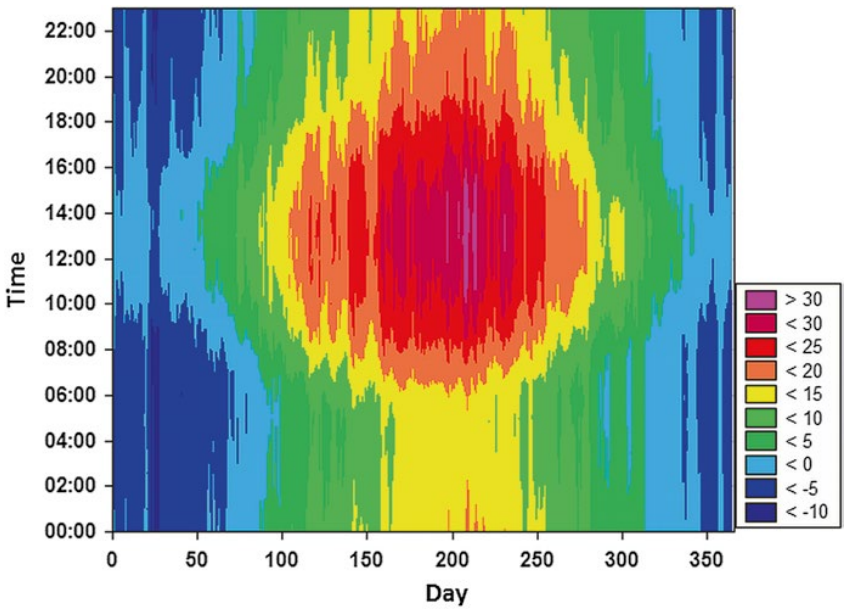

Fig. 14.3 Annual course of PET for Praha-Karlov station, period 2005–2013

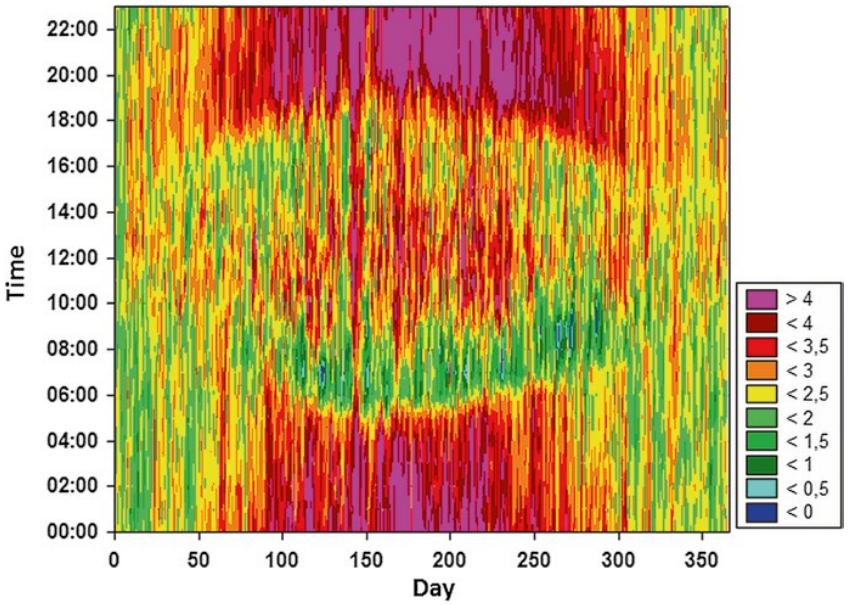

Fig. 14.4 Annual course of PET of differences between stations Praha-Karlov and Praha-Ruzyně, period 2005–2013 (positive values mean Karlov is warmer than Ruzyne)

values around 37 °C (Fig. 14.5), with differences among different parts of the city being maximal about 2 °C. PET values (Fig. 14.6) on that day reached over 46 °C in the city centre, with difference through the city being a bit higher compared to the differences in the air temperatures. Values of PET over 40 °C started already around 9 in the morning and continued to 5 in the afternoon. Especially in the evening, the differences between city centre and periphery exceeded 8 °C.

14.1.3 Air-Quality Issues

Mária Kazmuková
Prague Institute of Planning and Development, Prague, Czech Republic

Peter Huszár and Tomáš Halenka
Faculty of Mathematics and Physics, Department of Atmospheric Physics,
Charles University Prague (CUNI), Prague, Czech Republic

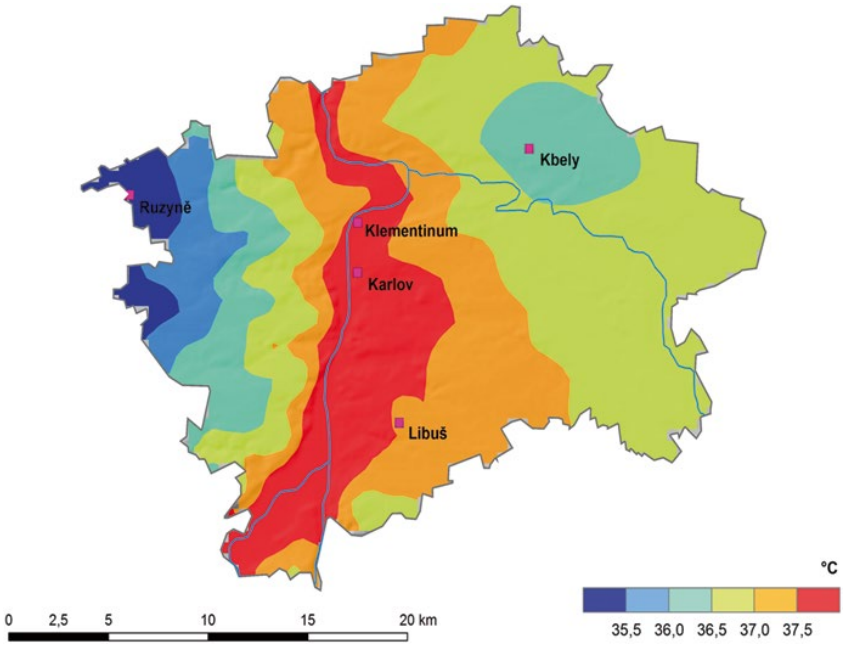

Fig. 14.5 Maximum air temperature in Prague on 28th July 2013

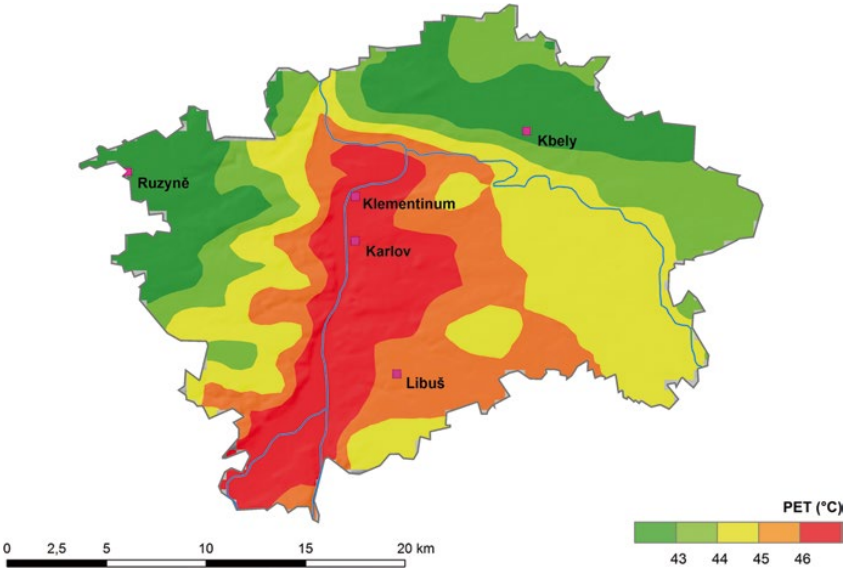

Fig. 14.6 Maximum PET in Prague on 28th July 2013

Despite the substantial reduction of the emissions from industrial sources in the past years, air quality is still influenced by the emissions from automotive traffic, as a main source of air pollution. In the suburban residential areas air quality is influenced by the emissions from local heating burning solid fuels.

In the agglomeration of Prague the limits for air quality are exceeded, especially for particular matter PM10, NO2, O3 and benzo(a)pyren. The majority of exceedances is connected with the high traffic loads in Prague, but also with the domestic heating in family houses in the residential areas in Prague.

The share of mobile sources on the total of PM emissions is more than 85 %, on the total of NO_x ca 75 %. The contribution of the household heating to PM emissions is almost of 16 %.

In the last years the ambient air quality has been improved. The annual limit concentration NO_2 (40 $\mu g.m^{-3}$) has been exceeded only on two traffic monitoring stations in Prague, however it can be supposed that the exceeding could occur in other areas with a similar traffic volume.

Also the PM_{10} concentrations dropped significantly, nevertheless the average 24 h PM_{10} concentrations are exceeding the limit at the 13 monitoring stations.

The concentrations of benzo(a)pyren measured at two monitoring stations in Prague were exceeded only at one of theme, the results of monitoring fluctuates around the limit of 1 $ng.m^{-3}$.

The concentrations of O_3 are regularly exceeded only at the one background station in the suburb over years.

The rest of the air quality limits are usually met in the area of Prague (Figs. 14.7 and 14.8).

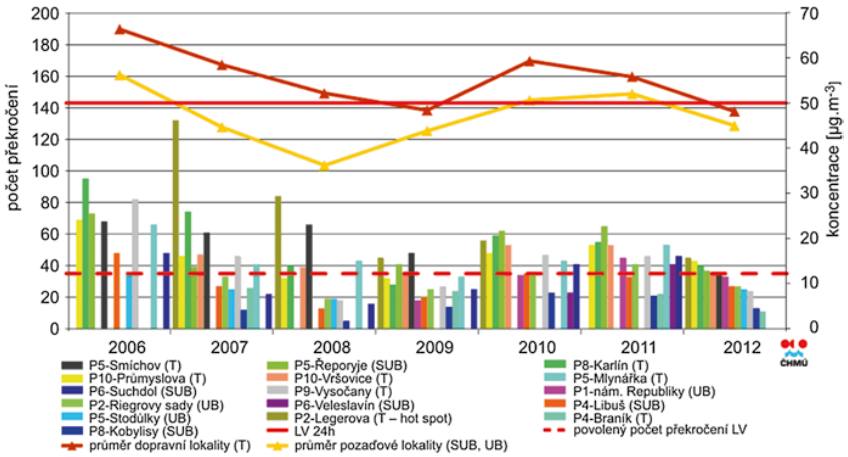

Fig. 14.7 Trends in yearly characteristics of the fraction PM_{10} and the 36th highest 24-h PM_{10} concentration in selected monitoring stations in Prague

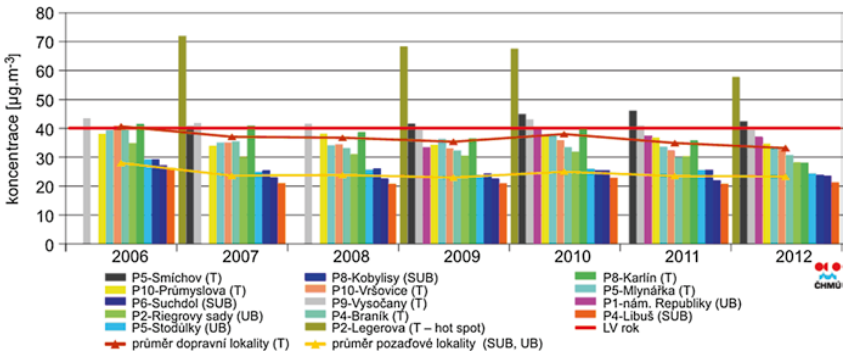

Fig. 14.8 Trends in yearly characteristics of NO_2 in selected monitoring stations in Prague

14.2 Pilot Areas Identification Methodology

The pilot areas in Prague were selected with the aim to enable the simulation of UHI mitigation strategies in different scales.

For the scale of a street canyon the Legerova street was selected, representing one of the streets with a very high traffic volume crossing the residential area.

For the Pilot Area 2 was chosen the brownfield Bubny – Holešovice, an abandoned railway area, which aspires to be a new city quarter. Microclimatic simulations were performed for the central part measuring 500 m by 500 m.

The Pilot Area 3 as the whole territory of Prague has been chosen to enable simulations of the mitigation effects as a green belt around Prague or traffic emission reduction in all Prague agglomeration.

14.3 UHI Phenomena in the Pilot Area and Connection with Specific Aspects of Urban Form and Built Environment

14.3.1 Pilot Area 1 Legerova street

Dominik Aleš and Mária Kazmuková
Prague Institute of Planning and Development, Prague, Czech Republic

Vladimír Fuka
Faculty of Mathematics and Physics, Department of Atmospheric Physics,
Charles University Prague (CUNI), Prague, Czech Republic

Michal Žák and Pavel Zahradnicek
Department of Climatology, Czech Hydrometeorological Institute,
Prague, Czech Republic

Fig. 14.9 Prague

Legerova Street represents a corridor with the width of 25 m, surrounded by 21 m high buildings. The traffic density is approximately 45 000 cars per day in 4 lines. The street leads through a residential area in north-south direction. During summer months it is fully open to sunshine and the incoming solar energy is largely absorbed by asphalt and concrete as well as by facades of the buildings. There are only a few sparse parts of grass beds and no availability for shade (Figs. 14.9 and 14.10).

Implementation of tree alleys was assessed as a mitigation measure. Three different scenarios varying the form and position of the alleys were tested in cooperation of Prague Institute of Planning and Development, Czech Hydrometeorological Institute, and the Department of Meteorology and Environment at Faculty of Mathematics and Physics, Charles University in Prague.

Besides the thermal comfort, also the air pollution concentrations were taken in mind. The initial NO_x concentrations in Legerova Street could reach ca. 33 $\mu g/m^3$ on the east windward sidewalk and even around 160 $\mu g/m^3$ on the west leeward sidewalk due to the prevailing west wind direction which causes this unbalanced air pollution dispersion.

The thermal comfort was simulated by using of the microclimate model RayMan (Matzarakis et al. 2010). The ventilation conditions for air pollution were simulated by a model developed at the Department of Meteorology and Environment, CUNI Prague.

Fig. 14.10 Aerial view of Legerova street in Prague

A mild summer day of 21st June 2013 was chosen for the simulation of all proposed scenarios. Temperature effect was also modelled on a tropical day of 18th June (Fig. 14.11).

The simulation results for all scenarios in the mild summer day ($T_{A,max} = 26$ °C) show a possible effect of PET reduction of 2.3° in shade. During the tropical day ($T_{A,max} = 37$ °C) the reduction can reach 3.5°. However, all scenarios show also more or less negative impact on the ventilation conditions for air pollutants.

In the scenario with small trees positioned densely along the sidewalks, there is quite short time period of shade provided to one assessed point. On the other hand, the street canyon ventilation in not worsened noticeably (Fig. 14.12).

The effect of PET reduction in the scenario with large trees along the sidewalks lasts for a longer afternoon period due to a larger shade. However, the large crowns significantly impact the air flow and cause a serious concentrations increase on the windward sidewalk (Fig. 14.13).

The simulation of the scenario with an axial position of small trees in one row in the centre of the street shows no impact on PET, providing no shade on the sidewalks. At the same time, this arrangement constitutes an obstacle to the vortex and thus causes additional increase of already worse high concentrations on the leeward sidewalk (Fig. 14.14).

High trees in the street bring more shade with a positive effect on PET, but also create less favourable ventilation conditions. The scenario with the small trees planted densely along the sidewalks seems to be the optimal solution for UHI mitigation for Legerova Street. This scenario does not have such a negative effect on ventilation conditions and provides shade and a positive effect on PET.

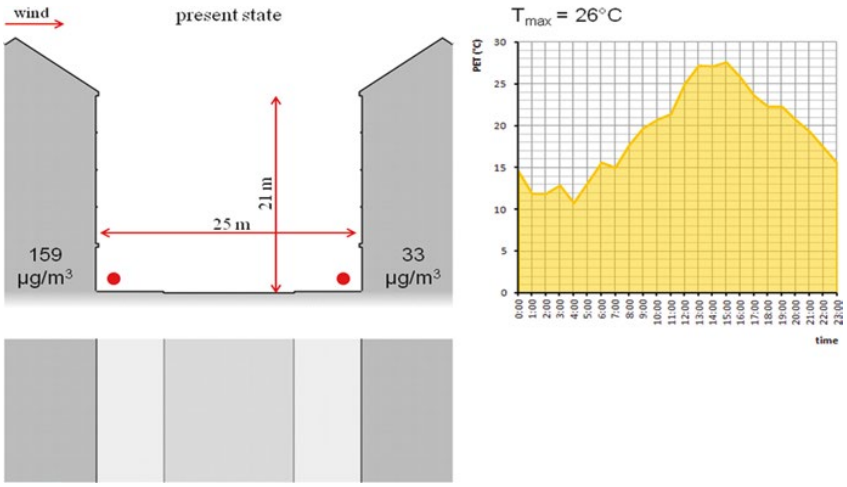

Fig. 14.11 Mild summer day scenario

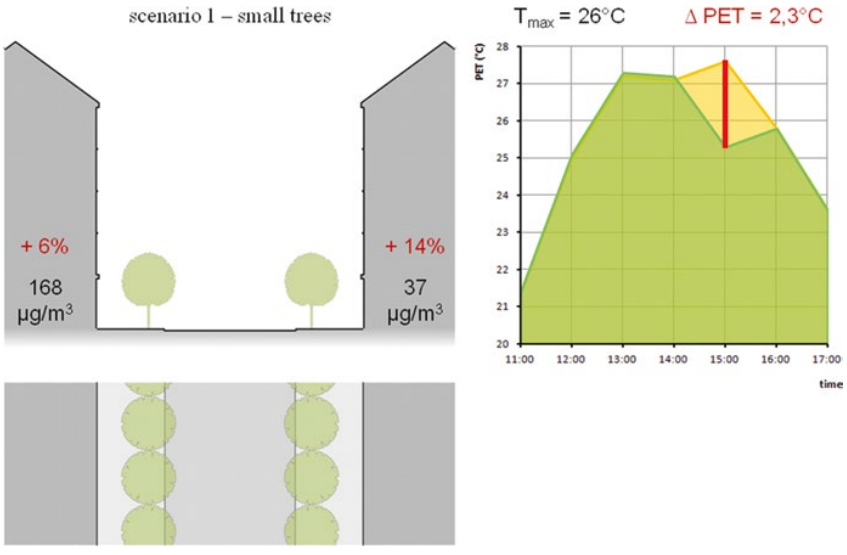

Fig. 14.12 Effect of PET reduction

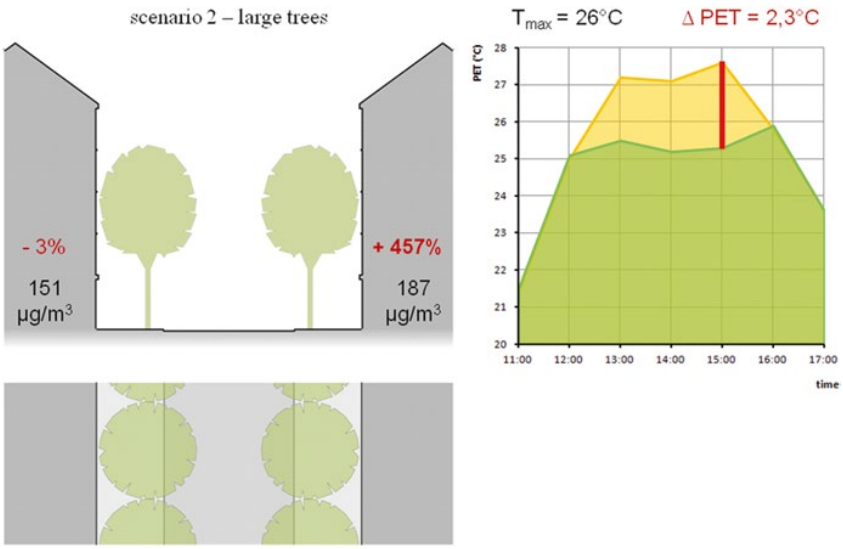

Fig. 14.13 Scenario 2

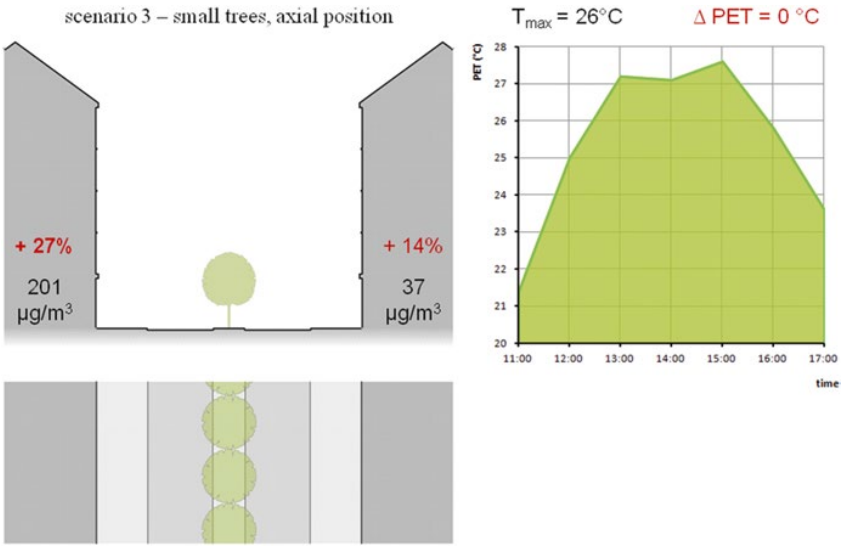

Fig. 14.14 Scenario with the small trees planted densely along the sidewalks

14.3.2 Pilot Area 2 Holešovice – Bubny

Mária Kazmukova, Ondrej Zemánek, Jan Flegl, and Radek Jareš
Prague Institute of Planning and Development, Prague, Czech Republic

Michal Žák
Department of Climatology, Czech Hydrometeorological Institute,
Prague, Czech Republic

Faculty of Mathematics and Physics, Department of Meteorology
and Environment Protection, Charles University Prague (CUNI),
Prague, Czech Republic

Pavel Zahradníček
Department of Climatology, Czech Hydrometeorological Institute,
Prague, Czech Republic

Kristina Kiesel
Department of Building Physics and Building Ecology,
Vienna University of Technology, Vienna, Austria

Lokalita Holešovice – Bubny

Holešovice – Bubny was chosen to be one of the Prague's pilot areas due to its strong development potential and proximity to the city centre. Once used as a freight station the site is nowadays a brownfield that aspires becoming a living city quarter. A significant part of the area is occupied by the transport infrastructure, the rest is scattered with isolated buildings and fragments of block structure. Existing greenery is not properly maintained. In the east and west the site is adjoining various urban structures and the Vltava River in the north and south. The selected pilot area is about 82.5 ha large (Fig. 14.15).

The site is considered to be the future residential and commercial district. According to the current urban study the area shall be converted into a block structure, accompanied by small-scale parks and alley-like streets. Mean building height (between 25 and 26 m) shall be pierced with several landmarks (height from 50 up to 70 m). These adjoin to park areas as well as to the northern river bank. Existing railway tracks shall be reduced and elevated to enable streets to pass beneath (Fig. 14.16, 14.17 and 14.18).

The aim of the research was to examine the benefits of the current study (scenario 1) and to compare it with alternative urban studies proposing different urban structures and larger park areas (scenarios 3 to 6) (Fig. 14.19, 14.20 and 14.21).

In terms of land use, greenery types and building characteristics the following GIS models were performed:

Scenarios 3 and 4 propose a massive east-west oriented park strip located in the middle of the pilot area. A loose urban structure with high buildings of small footprints adjoin to the park in the north (Fig. 14.22).

This arrangement should leave more space for greenery and enable better ventilation of the area.

Fig. 14.15 Future residential and commercial district

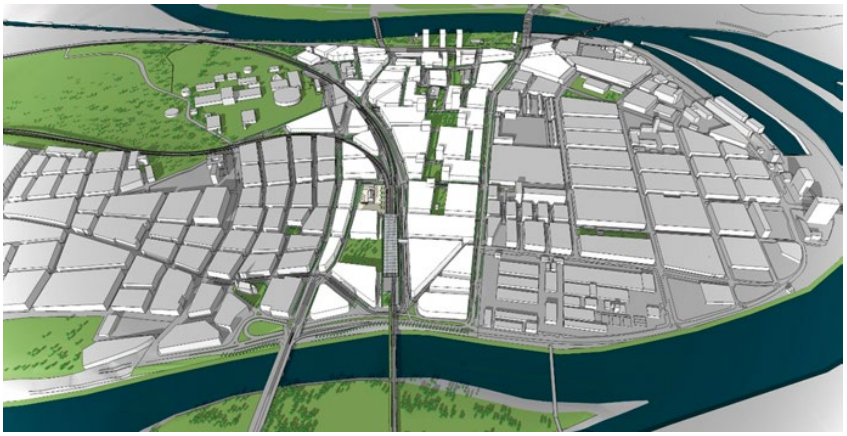

Fig. 14.16 Series of small-scale parks shall by hooked up through alley-like streets

Fig. 14.17 Inside yards of housing blocks shall be used for greenery and be walkthrough

Fig. 14.18 Scenario 1

Fig. 14.19 Scenario 2

Similarly to the current study scenarios 5 and 6 propose a block structure combining it with another arrangement of the central park: (Figs. 14.23 and 14.24)

In collaboration with the Meteorological Institute of the University of Freiburg and ATEM Prague following microclimate models were carried out with use of the ENVI-met software. The models simulate life conditions 1.5 m above the ground level during the day with the strongest insolation on June 20th at 3.00 PM.

We are conscious that the following conclusions are badly one-sided. For acquiring more realistic climatic conditions it would be necessary to perform a higher number of simulations.

Street canyons shaded by buildings have cooling effect (depending on the aspect ratio): (Figs. 14.25 and 14.26)

Wide streets not surrounded by buildings and not shaded by trees have a desiccating effect:

Fig. 14.20–14.21 (Scenario 3 and Scenario 4)

Busy streets have a warming effect due to the heat output from motor transport (see the bottom Fig.). Still water basins have no cooling effect: (Figs. 14.27, 14.28, 14.29, 14.30 and 14.31)

As mentioned above the block structure offers better day time conditions than the loose urban structure. However further research should explore the cooling effect of the parks during the night time.

14.3.3 Green Belt

Mária Kazmukova and Radek Jareš
Prague Institute of Planning and Development, Prague, Czech Republic

Tomáš Halenka
Faculty of Mathematics and Physics, Department of Meteorology and Environment Protection, Charles University Prague (CUNI), Prague, Czech Republic

Jaroslav Ressler
Institute of Computer Science, The Czech Academy of Sciences, Prague, Czech Republic

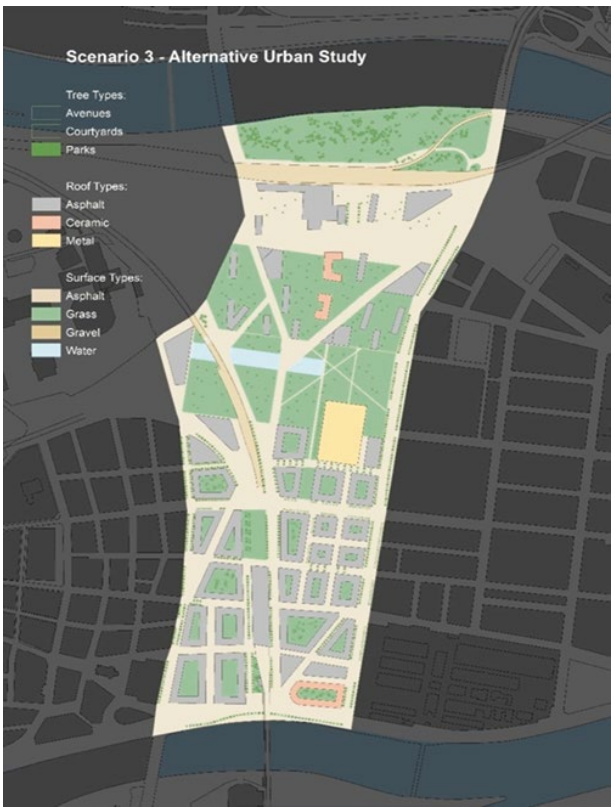

Fig. 14.22 Better ventilation scenario

The assessment was focused on the issue of modelling of meteorological fields and air quality in conditions of conurbation with regard to presence of urban heat island phenomenon. Within the project framework, modelling tools for air quality evaluation were tested while meteorological parameters and chemistry of the atmosphere were taken into account. Based on the acquired findings from the base state, the horizon of fulfilment of land use plan in its present form and the variants of urban and traffic concept were assessed.

The project assessed the following scenarios: baseline state, fulfilment of the land use plan, low-emission zone and implementation of a green belt. In addition, sensitivity to the expected climate change was studied.

In terms of UHI, the most important was evaluation of green belt scenario, i.e. state when the transport concept and vehicle fleet composition corresponds to the year 2020 and fulfilment of the land use plan is presumed with the exception of areas defined as green belt whose land use is assumed to be changed into forest area or forest park.

Fig. 14.23–14.24 Scenario 5 and Scenario 6

The method used for modelling of transport of chemical substances required to include a large territory in which boundary conditions were modelled, influencing meteorological quantities and concentrations of pollutants within the area of interest. The entire modelled area covered Europe, i.e. area measuring 4 644 × 3 294 km with its centre being located in Prague. Assessment with the finest resolution was carried out for Prague and its surroundings where grids of 1 km and 333 m were used.

Input data for the project were prepared in such detail that has not yet been realized. For this purpose, data from regularly updated study Evaluation of Air Quality in the Territory of the Capital City of Prague Based on Mathematical Modelling as well as data about the area of interest provided by the IPR institute and available databases from other sources were utilized.

The project involved both modelling of meteorological fields using the WRF model and modelling of air pollutant dispersion using the CMAQ model. The meteorological model was con Fig.d with an urban surface impact model; the emission flux model contained an anthropogenic emission model, a biogenic emission model, a chemical transport model and modules of data post processing and statistical processing of the outputs. For long term experiments, urbanized RegCM was used with 10 km resolution, allowing SUBBATS (Pal, J. S., F. Giorgi, X. Bi, N. Elguindi, F. Solomon, X. Gao, R. Francisco, A. Zakey, J. Winter, M. Ashfaq, F. Syed, J. L.

Fig. 14.25–14.26 Scenari

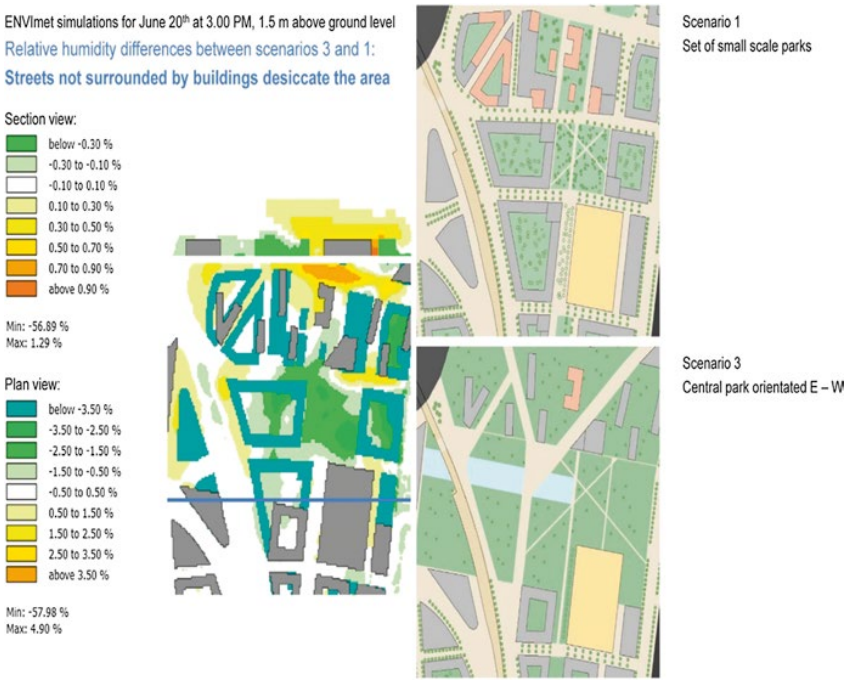

Fig. 14.27 Scenari 1/3

Bell, N. S. Diffenbaugh, J. Karmacharya, A. Konare, D. Martinez, R. P. da Rocha, L. C. Sloan and A. Steiner, 2007: The ICTP RegCM3 and RegCNET: Regional Climate Modeling for the Developing World, B. Am. Meterol. Soc., 88, 1395–1409) in 2 km.

Both meteorological parameters (temperature, humidity, wind speed) and concentration of pollutants were modelled.

Outcomes of the assessment allow evaluating not only long-term indicators (annual average) but also characteristics that have not yet been assessed sufficiently accurately, such as exceedance period of an air pollution limit and n^{th} highest values of short-term average values in accordance with legislation. Also ozone concentrations can be evaluated. The results are available both for current state, for future scenario of land use plan and other scenarios being assessed.

The evaluation points out the following:

By 2020 or by the horizon of land use plan fulfilment, respectively, reduction of concentrations of pollutants in Prague can be expected with the exception of vicinity of large transport structures where the impact of newly introduced car traffic outweighs.

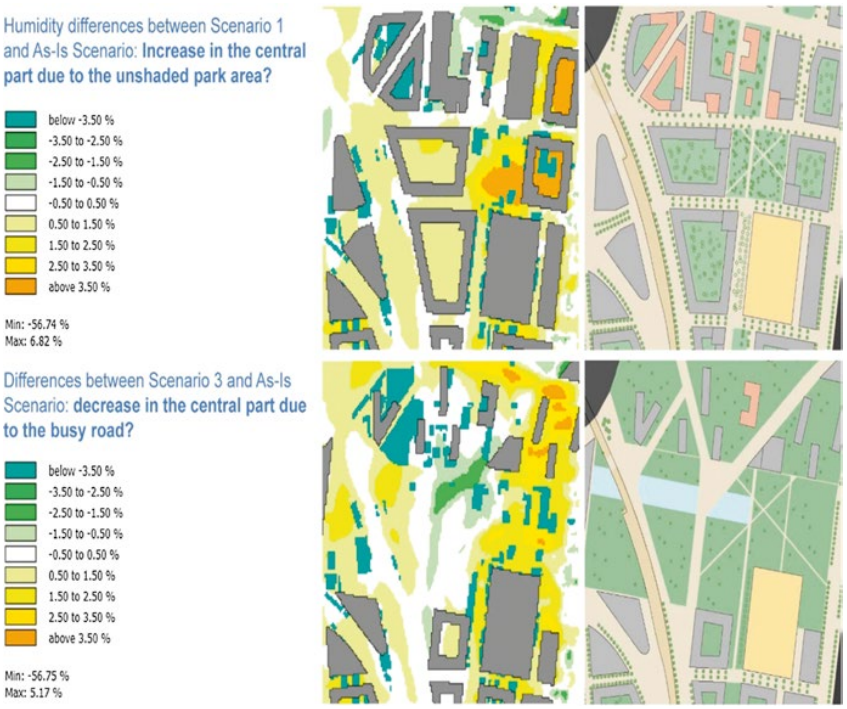

Fig. 14.28–14.29 Humidity differences

Improvement in vehicle fleet composition has a positive effect on NO_2 and suspended particulate matter concentrations and also on benzene (but less). In the case of ozone, the peak concentrations (which are limited in terms of health) decrease and average annual concentrations increase (higher concentrations at night time).

The evaluation showed that secondary aerosols have a relatively high contribution to air pollution load by suspended particulate matter. This issue requires further specification because higher concentrations of PM_{10} are one of the major problems of air quality protection in the capital city of Prague.

The influence of the green belt is rather small; it affects only few sites by small decrease in temperature and consequent change in concentrations of pollutants

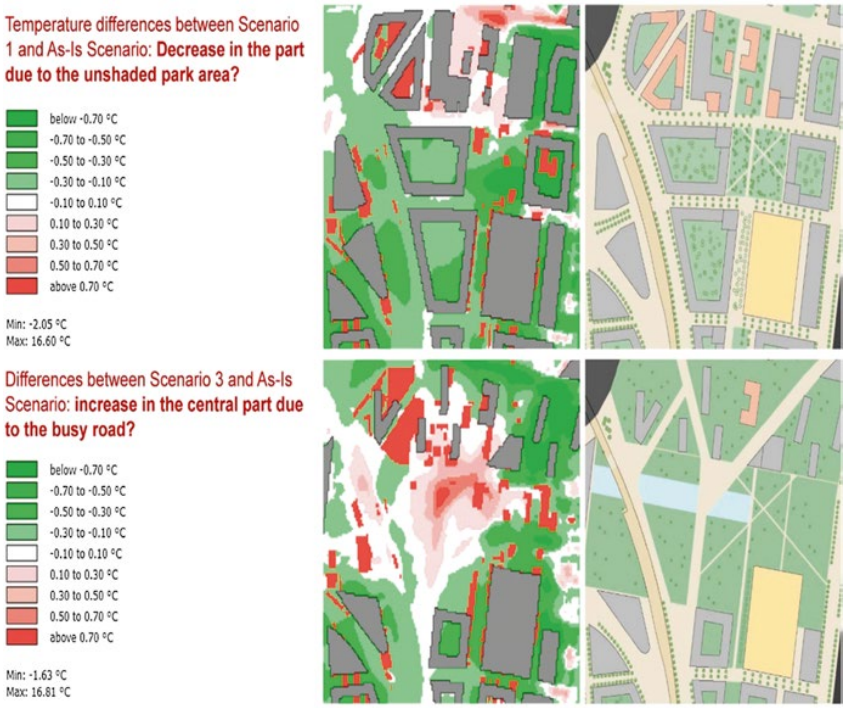

Fig. 14.30 The cooling effect of green roofs is negligible

caused by a change in biogenic emissions production and by a change in chemical reactions in the atmosphere. Certain changes can be seen in long term simulation, with small temperature decrease, especially in summer night. Remote effects are rather climatic noise. Changes in the future go with the overall temperature change, but they are again rather small.

The presented project practically verified the potential use of chemical transport models for air quality and UHI assessment in a small scale. The fine resolution that reaches up to 333 m for the innermost domain allows assessing air quality and UHI effect in cities in detail.

Proposed green belt around Prague (Figs. 14.32, 14.33, and 14.34).

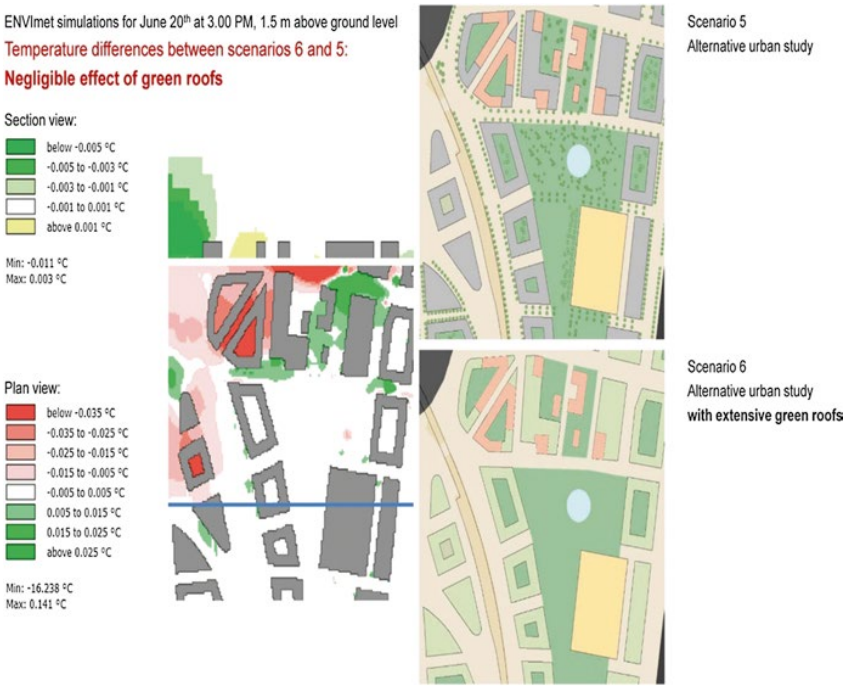

Fig. 14.31 The block structure offers better day time conditions

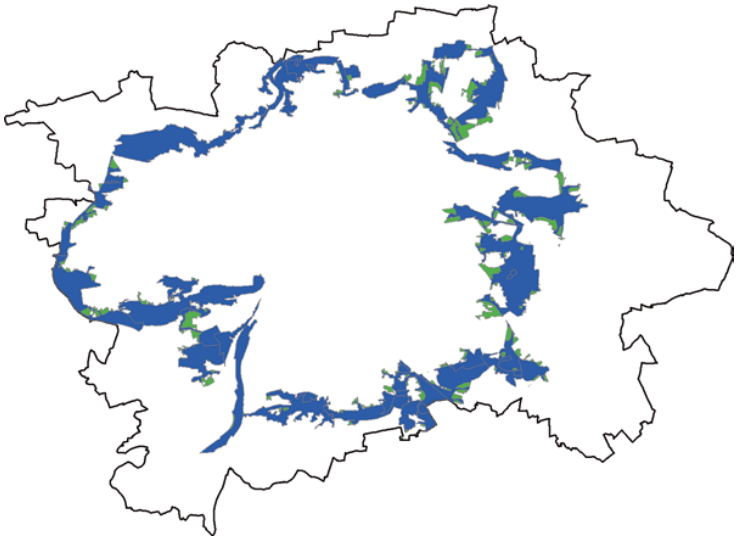

Fig. 14.32 Temperature shift caused by green belt in a hot July day

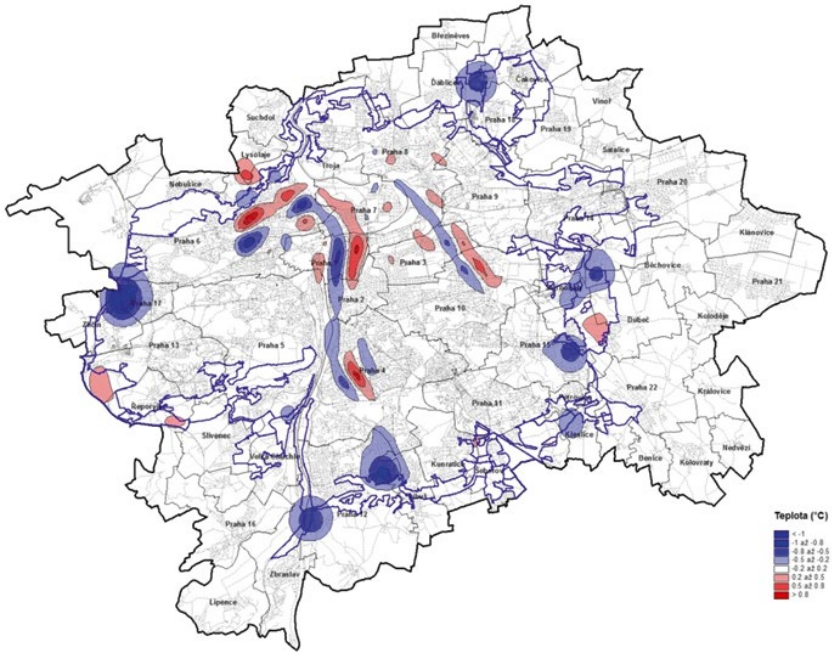

Fig. 14.33–14.34 Temperature changes in long term simulation of 2001–2010 (JJA, night) caused by green belt

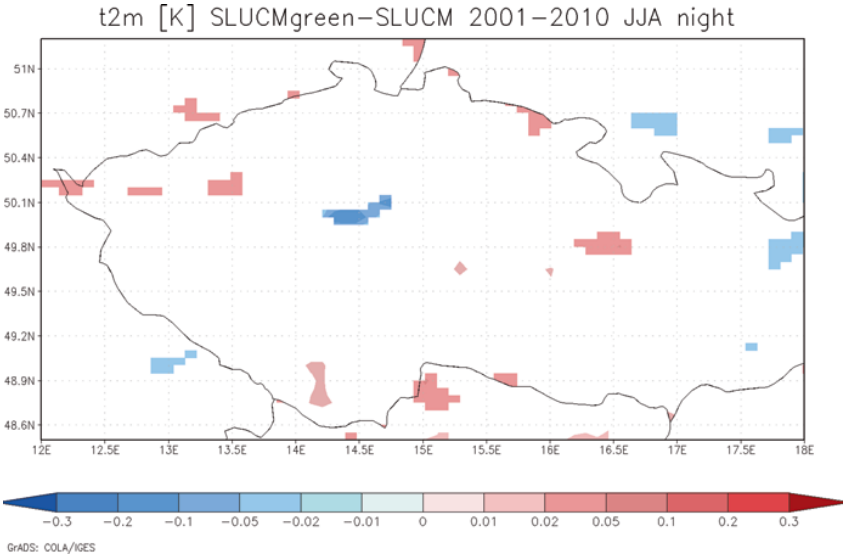

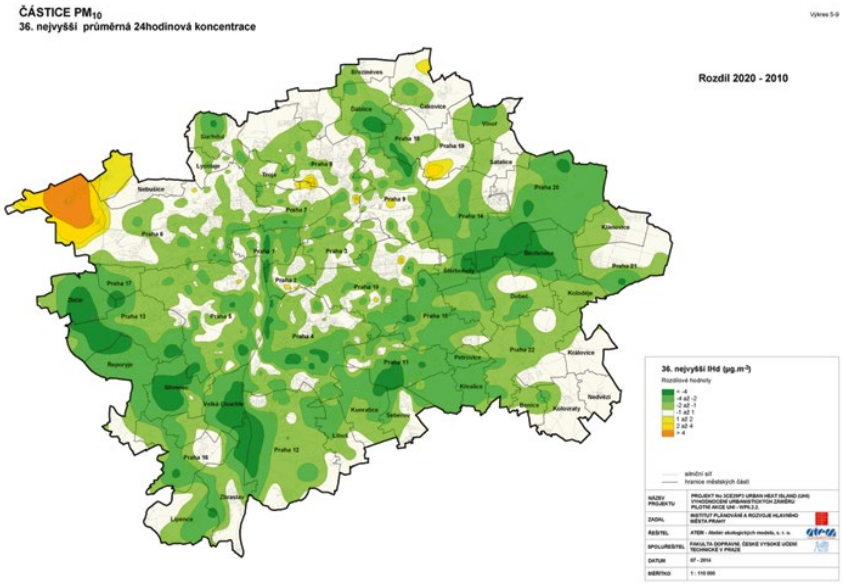

Fig. 14.35 Differences in 24-h-averaged PM_{10} concentrations

Differences in 24-h-averaged PM_{10} concentrations between years 2010 and 2020 (Fig. 14.35).

14.4 General Strategic Vision to Mitigate UHI Effects-Counteracting Measures

14.4.1 Street Canyons

As a result of the simulations, the scenario with the small trees planted densely along the sidewalks seems to be the optimal solution for UHI mitigation for Legerova Street and other similar street canyons with a heavy traffic volume. This scenario does not have such a negative effect on ventilation conditions and provides shade and a positive effect on PET.

14.4.2 Development Areas

The aim of the research was to examine the benefits of the different scenarios compared with alternative urban studies proposing different urban structures and larger park areas.

The simulations have shown that the block structure offers better day time conditions than the loose urban structure. However further research should explore the cooling effect of the parks during the night time.

14.4.3 Green Belt

The assessment of the effect of a proposed green belt as a scenario for UHI mitigation in Prague was focused on the issue of modelling of meteorological fields and air quality in conditions of conurbation with regard to presence of urban heat island phenomenon.

Within the project framework, modelling tools for air quality evaluation were tested while meteorological parameters and chemistry of the atmosphere were taken into account.

In terms of UHI, the most important was evaluation of green belt scenario, i.e. state when the transport concept and vehicle fleet composition corresponds to the year 2020 and areas defined as green belt are assumed to be changed into forest area or forest park.

The method used for modelling of transport of chemical substances required to include a large territory in which boundary conditions were modelled, influencing meteorological quantities and concentrations of pollutants within the area of interest

The project assessed the following scenarios: baseline state, fulfilment of the land use plan, low-emission zone and implementation of a green belt.

The presented project practically verified the potential use of chemical transport models for air quality and UHI assessment in a small scale. The fine resolution that reaches up to 333 m for the innermost domain allows assessing air quality and UHI effect in cities in detail.

As a result of the recent modelling, the influence of the green belt showed to be rather small; it affects only few sites by small decrease in temperature and consequent change in concentrations of pollutants caused by a change in biogenic emissions production and by a change in chemical reactions in the atmosphere. Further simulations with traffic modifications are needed. It should be pointed out, that the effect of climate change for the year 2020 is negligible compared to the effects by changes in land-use and transport concepts with vehicle fleet changes.

Adaptation strategies to contrast bioclimatic emergencies were included in a proposition for the Prevention plan in cooperation with the State Institute of Health. The proposition of the Prevention Plan includes the instructions for people, especially for sensitive groups how to react and what measures to take in extreme hot periods in cities.

The proposed HEAT Warning System will help to coordinate adaptative strategies and the reaction of City Authoritities to the extreme weather phenomena as to protect citizens against the harmful effects of heat and the UHI.

Reference

Matzarakis, A., Rutz, F., & Mayer, H. et al. (2010). Modelling radiation fluxes in simple and complex environments – Basics of the RayMan model. *International Journal of Biometeorology, 54*, 131–139.

Appendix D

J Karlicky, P Huszar, T Halenka, M Belda, N Zak, P Pisoft, and J Miksovsky. Multi-model comparison of urban heat island modelling approaches. *Atmospheric Chemistry and Physics*, 18(14):10655–10674, 2018. doi: https://doi.org/10.5194/acp-18-10655-2018.

Atmos. Chem. Phys., 18, 10655–10674, 2018
https://doi.org/10.5194/acp-18-10655-2018

Atmospheric Chemistry and Physics
Open Access
EGU

Multi-model comparison of urban heat island modelling approaches

Jan Karlický, Peter Huszár, Tomáš Halenka, Michal Belda, Michal Žák, Petr Pišoft, and Jiří Mikšovský

Department of Atmospheric Physics, Faculty of Mathematics and Physics, Charles University, V Holešovičkách 2, 180 00 Prague 8, Czech Republic

Correspondence: Jan Karlický (jan.karlicky@mff.cuni.cz)

Received: 2 January 2018 – Discussion started: 18 April 2018
Revised: 19 June 2018 – Accepted: 10 July 2018 – Published: 26 July 2018

Abstract. Cities are characterized by different physical properties of surface compared to their rural counterparts, resulting in a specific regime of the meteorological phenomenon. Our study aims to evaluate the impact of typical urban surfaces on the central European urban climate in several model simulations, performed with the Weather Research and Forecasting (WRF) model and Regional Climate Model (RegCM). The specific processes occurring in the typical urban environment are described in the models by various types of urban parameterizations, greatly differing in complexity. Our results show that all models and urban parameterizations are able to reproduce the most typical urban effect, the summer evening and nocturnal urban heat island, with the average magnitude of 2–3 °C. The impact of cities on the wind is clearly dependent on the urban parameterization employed, with more simple ones unable to fully capture the wind speed reduction induced by the city. In the summer, a significant difference in the boundary-layer height (about 25 %) between models is detected. The urban-induced changes of temperature and wind speed are propagated into higher altitudes up to 2 km, with a decreasing tendency of their magnitudes. With the exception of the daytime in the summer, the urban environment improves the weather conditions a little with regard to the pollutant dispersion, which could lead to the partly decreased concentration of the primary pollutants.

1 Introduction

From a global point of view, cities represent small and separated areas with significantly different surface properties compared to the surrounding rural ones. Considering the fact that more than half of the human population lives in cities and the number is still increasing (United Nations, Department of Economic and Social Affairs, 2014), the investigation of the impact of urbanized areas on environment, especially on atmospheric conditions, becomes of crucial importance (Folberth et al., 2015). There are many ways in which urban areas influence the atmosphere: from directly impacting the air composition and consequently the radiative balance and climate (Huszar et al., 2016; Huszár et al., 2016) to the meteorological forcing cities represent, best known in terms of the urban heat island effect. The concept of the urban heat island (UHI) was introduced many decades ago (Oke and Maxwell, 1975) and embodies that, due to different thermal, radiative, hydrological and mechanical properties of urban surfaces and due to anthropogenic thermal resources, temperatures in the city centres are a few degrees higher than in the city surroundings. This is true for averaged temperature difference, but the impact is not uniformly distributed across the day, and at specific times of day (typically evening and night), the difference can exceed 10 °C (Oke, 1982).

Other observation- and model-based studies (e.g. Lee et al., 2011; Huszar et al., 2014; Theeuwes et al., 2015) describe that not only is temperature affected by urban surfaces, but the wind speed is also significantly altered (Roth, 2000; Klein et al., 2001; Hou et al., 2013). Urban surfaces further influence the structure of the boundary layer as well (Angevine et al., 2003), along with the height of the planetary boundary layer (PBLH), which is very important from an air-quality perspective. It was also shown by Huszar et al. (2014) that whole regions can be affected by urban meteorological effects, and the magnitude of the temperature increase can be compared to the magnitude caused by the climate change. It was also of interest to investigate the possible modifications of UHI in a changing climate. In the future, due to the fact that global temperature is predicted to

Published by Copernicus Publications on behalf of the European Geosciences Union.

rise, together with cities growing and cities population rising, their inhabitants could be affected by more intensive, frequent and longer heat waves, as described by Meehl and Tebaldi (2004). To prevent these dangerous scenarios, many mitigation measures are proposed and tested using climate models (e.g. Fallmann et al., 2016), but the climate models are still, despite their steady advancement, burdened by many uncertainties and inaccuracies, so further development, evaluation and inter-model comparisons are still needed.

Last decade, many validation studies appeared where numerical weather prediction and/or regional climate models are coupled to various types of urban canopy models (UCMs; e.g. Chen et al., 2011; Lee et al., 2011; Liao et al., 2014) in order to capture different urban processes on local and regional scale with an effort to describe especially the urban heat island more accurately. These studies applied one of the wide range of approaches to parameterize the urban meteorological phenomenon, from simply modifying the surface parameters to represent an average value corresponding to urban surface – so-called bulk parameterization (described, e.g. in Chen et al., 2011), over models considering a single urban layer and an idealized street canyon (e.g. Single-Layer Urban Canopy Model – SLUCM; Kusaka et al., 2001), to more sophisticated multi-layer models of urban environment with ability to include different heights of buildings in the city and to resolve the vertical structure of the urban canyon (e.g. Building Environment Parameterization – BEP; Martilli et al., 2002).

Due to the fact that not only the temperature is affected by different urban surface, but also other variables, including ones important from the air-quality perspective (e.g. boundary-layer structure, turbulence), it is necessary also to study the impact of the urban-induced meteorological changes on air quality. Studies, evaluating this impact, usually use coupled meteorological, urban canopy and chemical-transport models (Liao et al., 2014; Fallmann et al., 2016; Huszár et al., 2018), and they conclude that inclusion of the urban meteorological effects has an important impact on final species concentrations, both primary and secondary ones.

Despite the urban canopy parameterization progress, and how often they are implemented in the surface schemes, there are still large uncertainties in modelling the mesoscale meteorological conditions within the urban environment. These primarily emerge from the uncertainties given by the choice of the urban canopy scheme. Moreover, additional sources of uncertainties include the driving surface model and the meteorological model itself, uncertainties in the driving meteorological data and the uncertainty of the choice of the urban parameters. Urban models differ in the processes considered and in the way they are implemented. It is widely accepted that complex urban parameterizations that include more processes are able to capture the urban phenomenon more accurately. However, recently Best and Grimmond (2015) showed that this is not a general rule. They concluded that there is a "need to balance the requirement for complexity within models against what is actually required for a model to be fit for purpose" and even a simple approach suffices if the most relevant processes are included. This implies that the general goal should not only be the continuous development of more complex urban modelling approaches but also their intercomparison and contrasting with simpler techniques. Such intercomparisons are important in terms of driving models and meteorological conditions as well. Finally, as background climate is a strong factor influencing the UHI and other urban effects (Zhao et al., 2014), long-term simulations are necessary to reveal the long-term variability of these effects.

Our study aims to contribute to the abovementioned works by looking at the uncertainty of UHI modelling associated with selection of the driving meteorological model and the underlying UCM. Another goal is to investigate the benefits of more sophisticated urban parameterizations with respect to simple approaches in light of the conclusions of Best and Grimmond (2015). The work will focus not only on averaged values but on variability and extreme values as well that are crucial in assessing the urban impact on environment and human life. The work also presents the urban impact on poorly observed or immeasurable variables in the city and its surroundings, e.g. temperature and wind profiles or boundary-layer height. Lastly, it evaluates also air-quality-related meteorological quantities that directly influence pollutant dispersion, which is an important precondition for urban air quality. All these issues will be evaluated in a long-term perspective using 10-year long simulations.

2 Methods

2.1 Models, urban parameterizations

In our study, two meteorological models are used, the Weather Research and Forecasting (WRF) model and the Regional Climate Model version 4 (RegCM4). The WRF model (Skamarock et al., 2008) is a mesoscale, non-hydrostatic limited area meteorological model, developed originally for weather prediction, but also widely used as a regional climate model. All simulations used in this study are performed by WRF version 3.7.1, which enables connection with bulk, SLUCM, BEP and BEP/Building Energy Model (BEM) urban parameterizations (description below).

The second model used in this study, RegCM4, is described in detail by Giorgi et al. (2012). RegCM4 is a mesoscale, non-hydrostatic (hydrostatic dynamics included) limited area regional climate model developed at the International Centre for Theoretical Physics (ICTP). Simulations performed for this study were executed by RegCM model version 4.4, which offers connection with two different models of land-surface processes: Biosphere–Atmosphere Transfer Scheme (BATS; Dickinson et al., 1993) and the more detailed scheme called the Community Land Model version 4.5 (CLM4.5; Lawrence et al., 2011; Oleson et al., 2013). Both

land-surface schemes include parameterizations of the urban canopy detailed further.

The simplest way to capture the impact of urban surfaces is to adapt values of parameters representing surface characteristics such as roughness length, surface albedo, heat capacity, soil thermal conductivity and green-vegetation fraction for urban environment conditions, which represent a zero-order effect of urban surfaces (Chen et al., 2011). By default, the WRF model uses values of these parameters obtained by Liu et al. (2006). This approach is most often called bulk parameterization (Chen et al., 2011; Lee et al., 2011), sometimes also referred to as a slab model (Kusaka et al., 2001; Kusaka and Kimura, 2004). Further, we will refer to it as the bulk parameterization.

SLUCM (Kusaka et al., 2001; Kusaka and Kimura, 2004) represents the next level of model approximation of the urban meteorological phenomena. Here, the city is assumed as an infinitely long street canyon with different prescribed orientations. This enables to include shadowing, reflections and trapping of radiation. Further, this model distinguishes temperatures of roofs, walls and roads, and profiles within these surfaces. For wind, an exponential profile is assumed. The total sensible heat flux from all surfaces, the total momentum flux and friction velocities are then returned back to the land-surface and boundary-layer schemes of the driving models. The CLMU (Community Land Model Urban) urban parameterization (Oleson et al., 2008), implemented in the RegCM model under the CLM4.5 land-surface scheme, is also based on canyon representation of urban areas and is conceptually very similar to SLUCM.

The most sophisticated urban parameterization used in this study is the multi-layer urban canopy model (BEP; Martilli et al., 2002). Its main benefits lie in allowing the computation of vertical profiles of temperature, momentum and turbulent kinetic energy within urban canyon explicitly, taking into account the vertical distribution of the sources and sinks of heat, momentum and moisture, and its direct interactions with the boundary-layer parameterization.

The BEP urban model can be improved by using a scheme that computes the energy exchange between the atmosphere and the interior of the building. The WRF model implements such a scheme, called BEM, developed by Salamanca et al. (2009). In contrast to SLUCM, which enables only simple inclusion of the anthropogenic heat (AH) with constant daily profiles and annual profiles, the BEM allows both double-sided energy exchange and computing of the AH depending on specific weather conditions, which makes the AH flux more realistic. To achieve this, the BEM takes into consideration the following processes: heat and radiation transfer between indoor and outdoor areas, heat and radiation transfer between indoor walls and floors, indoor heat generation by human bodies and machines, and finally ventilation, heating and air conditioning (Chen et al., 2011).

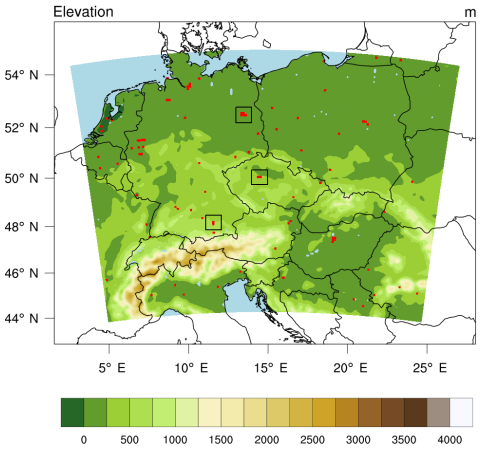

Figure 1. Position of the model domain with model topography in 10 km resolution (m). Grid boxes with dominant urban land use are marked in red colour. From the bottom, the cities of Munich, Prague and Berlin are marked.

2.2 Experimental setups

All simulations performed within this study were run on a 160×120 domain centred over central Europe, with 10 km $\times$ 10 km horizontal resolution (Fig. 1). In vertical direction, 30 and 23 levels are considered for WRF and RegCM, respectively. The model top is 50 hPa in both cases. The simulation time span is 10 years (2001–2010), without any restart or nesting procedure. It has to be noted that using finer resolution, the entire terrain, land cover and urban features would be captured much better than is shown in Fig. 2, but it is not possible to run long-term simulations on such large domain because of high computational cost. Moreover, as seen from these two figures, the main urban areas (which are analysed here) are well resolved even at 10 km resolution. As meteorological boundary conditions, the ERA-interim (Dee et al., 2011) dataset is used. For static geographic data, standard WRF and RegCM input USGS-based data are used. The standard WRF land-use input includes only one urban category type. In the case of RegCM experiments with CLM4.5, urban land-use percentage was derived from the 0.05° resolution LandScan2004 data described by Jackson et al. (2010). They provide urban canyon parameters and surface characteristics. For the RegCM with the BATS/SLUCM, a 2 km $\times$ 2 km sub-grid was applied for surface processes. Each sub-grid box is considered to be covered by one land-use type. Urban and suburban categories are considered. In order to have consistent land-use data for both RegCM setups, we set the number of urban and suburban sub-grid boxes to correspond to the fraction defined in the case of the CLM4.5 urban setup. Ur-

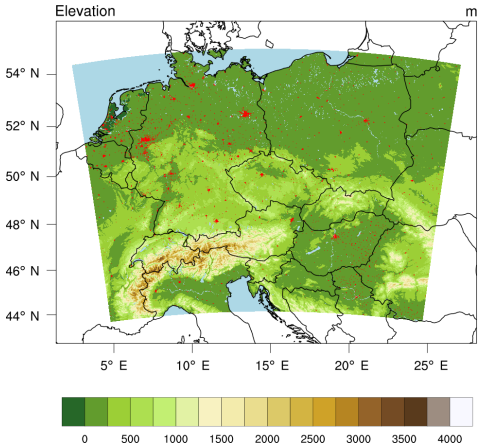

Figure 2. Same as Fig. 1 but with model topography and land use in 1 km resolution (m), for comparison.

ban canopy parameters used by urban schemes are adapted to urban environment in Prague and are listed in Table 1.

For the WRF model, simulations were performed with its hydrostatic version. For the radiation transfer, the Rapid Radiative Transfer Model for General Circulation Models (RRTMG) scheme (Iacono et al., 2008) is used for both long- and short-wave spectrums. Microphysical processes are resolved by the Morrison double-moment scheme (Morrison et al., 2009). Further, the Noah land-surface model (Chen and Dudhia, 2001) is chosen for the description of the land-surface processes, surface layer processes are parameterized according to Janjić (1994), planetary boundary layer is resolved by the Mellor–Yamada–Janjic scheme (Janjić, 1994), and the Tiedtke scheme (Tiedtke, 1989) for convection is used.

In the case of the RegCM model, also the hydrostatic version is used. Radiation transfer is resolved by NCAR Community Climate Model Version 3 (CCM3; Kiehl et al., 1996). The Holtslag scheme (Holtslag et al., 1990) is applied to planetary-boundary-layer processes. For large-scale precipitation and convection, the SUBBEX (Pal et al., 2000) and the Grell schemes (Grell, 1993) are used, respectively. As already noted, the RegCM model includes two different parameterizations of land-surface processes, specifically the more simple and older BATS (connected with SLUCM urban scheme), which is configured with 2 km × 2 km sub-grid setting, and the more detailed CLM4.5 (connected with the CLMU urban scheme).

The aim of this study is to determine the impact of cities on climate. To this end, two types of simulations are performed: firstly, simulations with cities (or urban surfaces in general) using the unaltered geographic data and, secondly, simulations where urban surfaces are removed from geographic data and replaced by the dominating land-use category in its surroundings (crops in the majority of cases). Unfortunately, the models adopted do not allow for connection with all listed urban models. However, all allowed and meaningful combinations are considered. The summary of the simulations performed is provided by Table 2.

2.3 Observational data

For the basic validation of model outputs, the E-OBS (v. 12.0) dataset (Haylock et al., 2008) is used. E-OBS includes a 0.25° × 0.25° resolution gridded data of temperature and precipitation for the whole modelled period. The ECAD (European Climate Assessment and Dataset) data (Klein Tank et al., 2002) including station-based temperature means, maxima and minima are used for evaluating the temperature differences between city centres and their vicinity. Additionally, data supplied by the Czech Hydro-Meteorological Institute (CHMI) provide hourly temperatures as well as their daily averages and extremes for stations in both the centre and the vicinity of the Czech capital, Prague. Finally, radiosonde observations, provided by the Department of Atmospheric Science of the University of Wyoming and freely downloadable from its website (http://weather.uwyo.edu/upperair/sounding.html, last access: 30 May 2018), are used for basic evaluation of vertical profiles of the temperature and wind speed above the chosen cities.

3 Results

3.1 Model validation

Figure 3 shows the seasonal model biases for temperature means, maxima, minima and daily precipitation means (compared to the E-OBS data). In general, model biases depend mainly on the model type, eventually on the land-surface scheme; the choice of different urban parameterizations and the inclusion/exclusion of urban surfaces have only minor effect on the overall bias as only a small fraction of grid points in the whole domain is covered by urban land-use type. The temperature means are reproduced by the WRF model with a bias up to around 1 °C. For the RegCM model coupled to BATS, biases are mostly 1–2 °C, but for the RegCM model combined with CLM4.5 land-surface model, they reach 2–4 °C. Temperature extremes are generally captured with even higher biases. In terms of average daily precipitation, the WRF model captures the annual cycle more accurately; the RegCM simulations exhibit large winter positive bias contrasting the E-OBS annual cycle. The values are also substantially overestimated in RegCM simulations, mainly in the ones with the CLM4.5 land-surface model.

Figure 4 shows the spatial distribution of precipitation biases for all seasons and for WRF–SLUCM, RegCM–SLUCM and RegCM–CLM4.5 simulations. It is clearly visi-

Table 1. Urban canopy parameters used in simulations. Values in brackets indicate different parameters used in RegCM simulations with the SLUCM scheme, in which urban and suburban categories are considered.

Parameter	Unit	Value	Used in
Building height	m	17.5 (20.0, 15.0)	SLUCM
Roof width	m	17.5 (20.0, 15.0)	SLUCM, BEP + BEM
Road width	m	17.5 (15.0, 20.0)	SLUCM, BEP + BEM
Anthropogenic heat	$W\,m^{-2}$	35.5 (50.0, 20.0)	SLUCM
Urban fraction	–	0.8 (0.9, 0.7)	SLUCM, BEP + BEM
Heat capacity of roof	$J\,m^{-3}\,K^{-1}$	0.776×10^6	SLUCM, BEP + BEM
Heat capacity of building wall	$J\,m^{-3}\,K^{-1}$	1.02×10^6	SLUCM, BEP + BEM
Heat capacity of ground (road)	$J\,m^{-3}\,K^{-1}$	1.7×10^6	SLUCM, BEP + BEM
Thermal conductivity of roof	$J\,m^{-1}\,s^{-1}\,K^{-1}$	0.8	SLUCM, BEP + BEM
Thermal conductivity of building wall	$J\,m^{-1}\,s^{-1}\,K^{-1}$	1.28	SLUCM, BEP + BEM
Thermal conductivity of ground (road)	$J\,m^{-1}\,s^{-1}\,K^{-1}$	0.6	SLUCM, BEP + BEM
Surface albedo of roof	–	0.30	SLUCM, BEP + BEM
Surface albedo of building wall	–	0.27	SLUCM, BEP + BEM
Surface albedo of ground (road)	–	0.16	SLUCM, BEP + BEM
Surface emissivity of roof	–	0.70	SLUCM, BEP + BEM
Surface emissivity of building wall	–	0.88	SLUCM, BEP + BEM
Surface emissivity of ground (road)	–	0.92	SLUCM, BEP + BEM
Thickness of each roof layer	m	0.05, 0.05, 0.05, 0.05	SLUCM
Thickness of each building wall layer	m	0.05, 0.05, 0.05, 0.05	SLUCM
Thickness of each ground (road) layer	m	0.05, 0.25, 0.50, 0.75	SLUCM
Roughness length for momentum over roof	m	0.01	BEP + BEM
Coefficient of performance of the A/C systems	–	3.5	BEP + BEM
Coverage area fraction of windows in the walls of the building	–	0.2	BEP + BEM
Thermal efficiency of heat exchanger	–	0.75	BEP + BEM
Target temperature of the A/C systems	K	298 (±0.5)	BEP + BEM
Target humidity of the A/C systems	$Kg\,Kg^{-1}$	0.005 (±0.005)	BEP + BEM
Peak number of occupants per unit floor area	person m^{-2}	0.01	BEP + BEM
Peak heat generated by equipments	$W\,m^{-2}$	18.00	BEP + BEM
Street direction	degrees from north	0, 90	BEP + BEM
Building heights	m	10, 15, 20, 25	BEP + BEM
Building heights' percentage	%	10, 40, 40, 10	BEP + BEM
Diurnal AH profile		0.16 0.13 0.08 0.07 0.08 0.26 0.67 0.99 0.89 0.79 0.74 0.73 0.75 0.76 0.82 0.90 1.00 0.95 0.68 0.61 0.53 0.35 0.21 0.18	
Diurnal heating profile of heat generated by equipment		0.25 0.25 0.25 0.25 0.25 0.25 0.25 0.5 1.0 1.0 1.0 1.0 1.0 1.0 1.0 1.0 1.0 0.5 0.25 0.25 0.25 0.25 0.25	

Table 2. Summary of simulation experiment setups.

Experiment	Abbreviation	Model	Urban inclusion	Urban scheme	Land-surface model
WRF–woU	W–woU	WRF	No	–	Noah LSM
WRF–BULK	W–B	WRF	Yes	Bulk	Noah LSM
WRF–SLUCM	W–S	WRF	Yes	SLUCM	Noah LSM
WRF–BEP + BEM	W–BB	WRF	Yes	BEP + BEM	Noah LSM
RegCM–SLUCM–woU	R–S–woU	RegCM	No	–	BATS
RegCM–SLUCM	R–S	RegCM	Yes	SLUCM	BATS
RegCM–CLM4.5–woU	R–C–woU	RegCM	No	–	CLM4.5
RegCM–CLM4.5	R–C	RegCM	Yes	CLMU	CLM4.5

ble that great winter overall biases in RegCM precipitation originate from mountainous regions (Alps). However, this overestimation does not occur in the summer season, leading to flipped annual cycle of domain-averaged precipitation

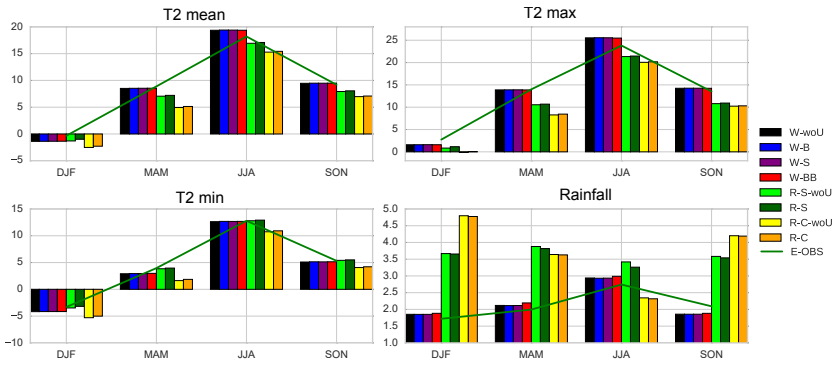

Figure 3. Averaged seasonal modelled temperatures (in °C) and precipitation (mm) for individual model simulations: black – WRF–woU, blue – WRF–BULK, purple – WRF–SLUCM, red – WRF–BEP+BEM, light green – RegCM–SLUCM–woU, dark green – RegCM–SLUCM, yellow – RegCM–CLM4.5–woU, orange – RegCM–CLM4.5. The green curve indicates the seasonal values given by E-OBS.

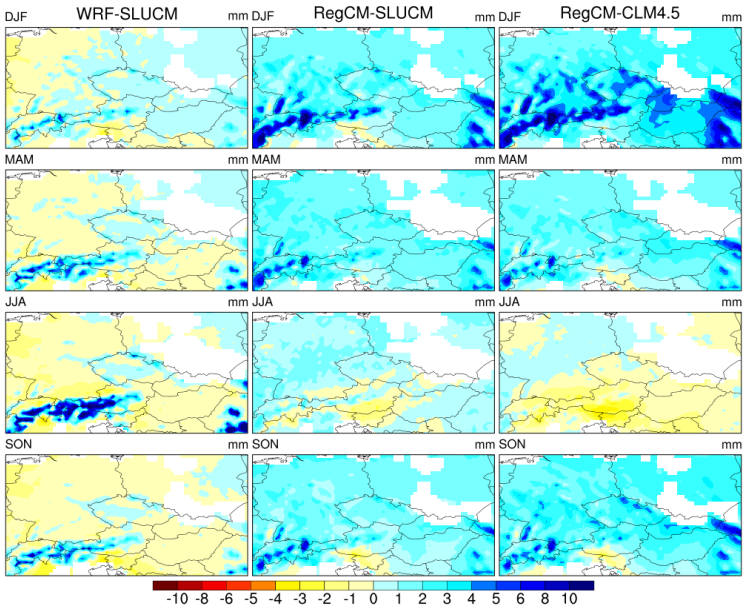

Figure 4. Spatial distribution of averaged daily precipitation biases (mm) for individual seasons and simulations. The white colour indicates missing reference data.

in RegCM simulations, compared to the E-OBS precipitation cycle. On the other hand, WRF simulations tend to overestimate mountain area precipitation particularly in the summer season.

Another important question is how the models are able to predict the temperature difference between urban area and its non-urban vicinity. To evaluate this, we chose three big cities, Berlin, Munich and Prague, as they are located inland

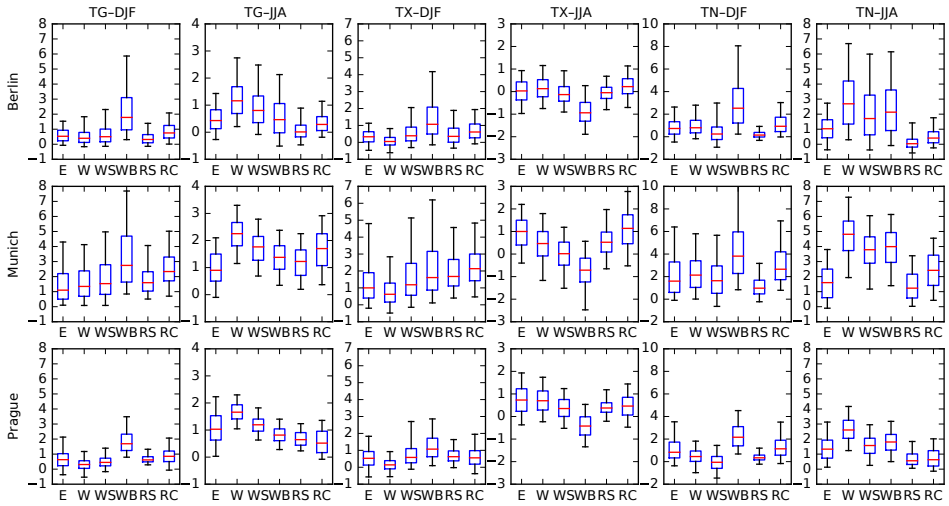

Figure 5. Distributions of temperature differences (°C) between city centres and their surroundings in winter and summer seasons given by station data (E), WRF–BULK (W), WRF–SLUCM (WS), WRF–BEP + BEM (WB), RegCM–SLUCM (RS) and RegCM–CLM4.5 (RC) model simulations. TG denotes temperature means; similarly, TX and TN stand for maxima and minima, respectively. Whiskers indicate 5th and 95th percentiles.

without significant orographic variation that would mask the urban canopy effects. We took one station from each city centre (Berlin Mitte, Munich Bogenhausen and Prague Karlov) and one from its surroundings (Berlin Schönefeld, Munich Flughafen and Prague Ruzyně). To prevent the impact of different altitudes of the listed stations and grid points, adjustment was performed using a standard temperature moist adiabatic gradient of $0.65 \times 10^{-2}\,\mathrm{K\,m^{-1}}$. As written above, the urban versus rural temperature difference can vary substantially depending on the specific weather conditions, time of the day and year. We therefore focus on the distribution of these differences (Fig. 5). The range between the 5th and the 95th percentiles is mostly well captured but often overestimated in the simulation using the most sophisticated urban model (WRF–BEP+BEM). Also, the distribution of differences is often substantially different for the W–BB simulation compared to the rest of the analysis setups. On the other hand, in terms of summer temperature minima, all WRF simulations give distributions with the median significantly shifted to higher values.

Over Prague, hourly temperature data are available for both the city centre and from a station in the surrounding area, which enables a detailed comparison of daily temperature cycles. Again, the adjustment of temperature to the sea level was performed using the standard temperature lapse rate. Results are shown in Fig. 6. Modelled values are often significantly biased (e.g. winter minima and summer maxima by WRF, daily means by RegCM in spring, summer and autumn). Furthermore, the diurnal temperature range is evidently overestimated by the WRF model with the exception of winter and underestimated by the RegCM model, which is consistent with the domain-averaged temperature biases (Fig. 3).

We are also interested in temperature differences between the city centre and its surroundings. From this perspective, models are qualitatively able to capture the evening and nighttime city centre temperature increase in warmer seasons. While the RegCM model tends to underestimate this effect, WRF rather overestimates it in all simulations. Nearly all simulations show a zero temperature difference for the morning hours, in line with the station data. However, the W–BB simulation manifests the UCI (urban cool island) in the morning, occasionally observed during this part of the day in Prague but not on average over each day. In the winter season, the W–BB simulation also overestimates the temperature difference during the whole day. From the perspective of temperature differences, we can conclude that all urban schemes give qualitatively good results and there is no significant improvement from using the more sophisticated urban model, in comparison to the simple BULK scheme.

Because of the fact that we are also interested in the impact of urban surfaces on the temperature and wind speed profiles, we need evaluate also the model performance at higher levels. Radiosonde observations are used for this pur-

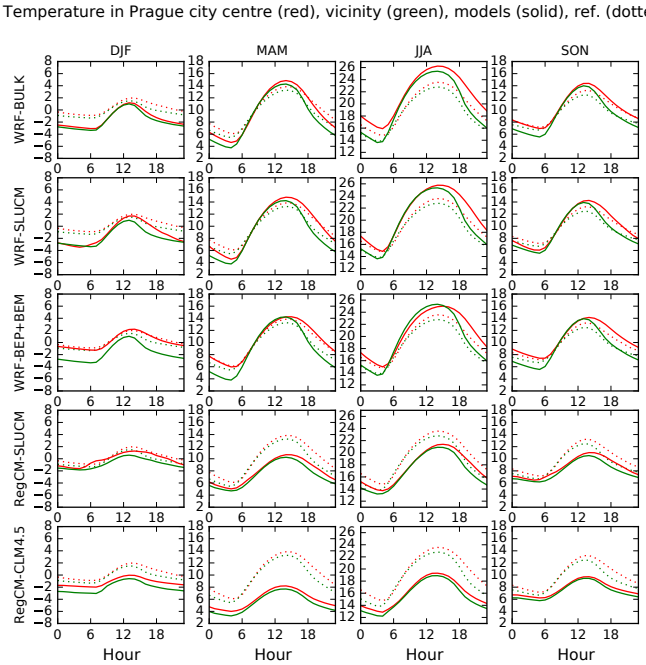

Figure 6. Averaged daily temperature cycles (°C) in the Prague city centre (station Karlov, red) and its surroundings (station Ruzyně, green). The comparison shown is of modelled (solid) and measured values (dotted). The time axis corresponds to UTC.

pose, although they have limitations; e.g. they do not provide data for city centre and its vicinity but only a single measurement per city, which makes it impossible to evaluate the difference between the profiles over the city centre and its surroundings. The simple comparison of the averaged model profiles with observed values for winter and summer is shown in Figs. 7 (temperature) and 8 (wind speed). Given the fact that substantial differences between specific model performances occur only in the bottom part of the atmosphere below 2 km (see further Figs. 12 and 13), the comparison is performed for these altitudes only. Models generally capture both of the main features – the temperature decrease and wind speed increase with the altitude. Individual WRF simulations are close to each other and larger differences are modelled only below 200 m, where the different urban parameterizations have strong influence. In summer, surface temperatures of WRF simulations are significantly higher than observed ones, probably caused by the fact that model data are taken from an urban grid box (i.e. where urban land-use type is dominating), in contrary to the character of the land use where radiosonde measurements were obtained. RegCM simulations are about 2 °C underestimated in the first kilometre, in summer. In winter, an underestimation in the range of 1–2 °C occurs in all experiments, except of the first 100 m. Wind speed biases occur most often between 1 and 3 m s^{-1}. In summer, models perform with a higher accuracy, and the spread of values is much smaller.

3.2 Benefits of more complex approaches of urban parameterizations

In this section, we will show the long-term impact of urban surfaces on meteorological conditions both near the surface and at higher altitudes. This can give us an insight into the impacts of urban environment on selected immeasurable meteorological variables. At the same time, we will evaluate the benefits and/or disadvantages of the specific model approaches. First, the impact of urban surface on the temperature is shown (Fig. 9). Daily temperature cycles pertain to the city of Prague and its surroundings. More specifically, the city centre value is taken from a grid point with a position closest to the actual city centre and containing the urban land use. The surroundings are defined as a square ring of grid points with a distance of two grid points around the central

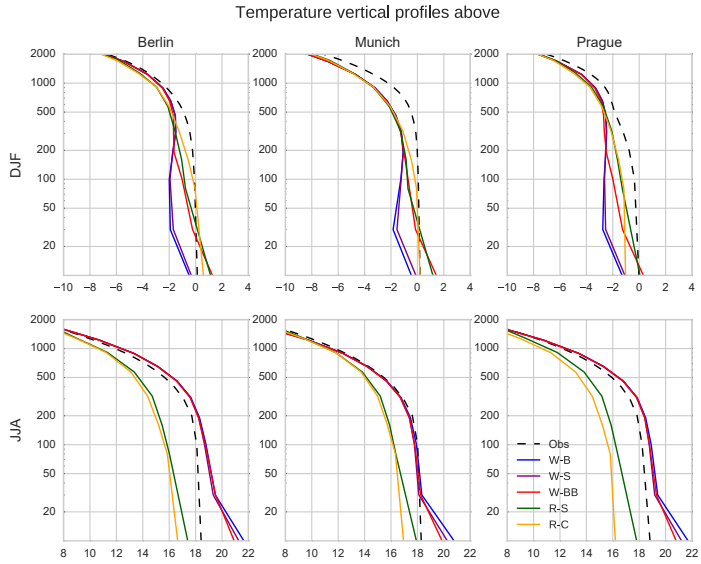

Figure 7. The averaged temperature vertical profiles (in °C) over selected cities, given by models and radiosonde observations. The y axis indicates the altitude in metres.

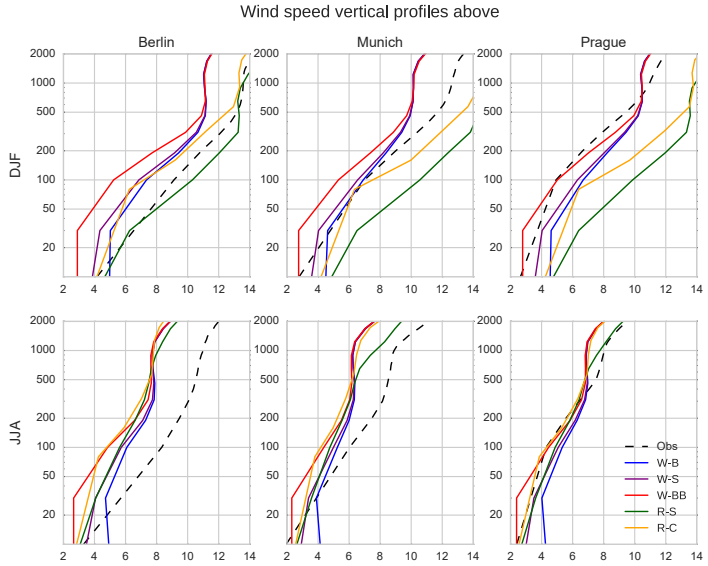

Figure 8. The averaged wind speed vertical profile ($\mathrm{m\,s^{-1}}$) over selected cities, given by models and radiosonde observations. The y axis indicates the altitude in metres.

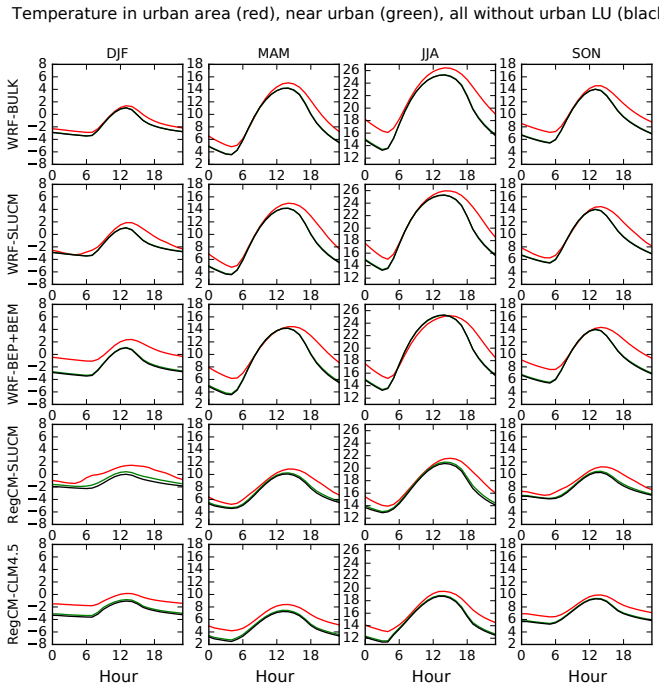

Figure 9. Averaged daily temperature cycles (°C) in the Prague city centre (red), in its surroundings (green) and those simulated with the urban surface removed (black).

grid point. For comparison, values from the simulations with urban land use removed are also taken into consideration, in this case from both the central grid point and the square ring.

As stated in the previous section, all model approaches are able to capture evening and nocturnal UHI in the warm season, although the magnitudes differ. The BULK model increases summer temperature maxima more than the urban canopy models, which is probably caused by disregarding the three-dimensional character of urban areas. The winter temperature cycles differ more between each other, which is consistent with the substantial differences in the implementation of the anthropogenic heat production. The differences between the temperature profiles and profiles given by non-urban simulations over city surroundings are very low, indicating that the impact of the city on its surroundings over a distance of a few tens of kilometres is minor.

The impact of urban surfaces on the PBLH is plotted in Fig. 10. It could be expected that the PBLH will be increased by higher intensity of friction in the urban environment and by increased buoyancy due to temperature increase. Model results indeed show PBLH increase during the whole day except morning hours, when temperature increases are minimal, too. In winter, model results differ much more than in the rest of the year, in agreement with the temperature profiles. Again, impact of the city to its surroundings is mostly negligible, though in winter in the RegCM simulations, the value is about a few tens of metres. There is a significant difference in the PBLH between the two models; e.g. the PBLH is about 25 % lower in the RegCM model in comparison to the WRF model in summer.

In terms of the urban surface impact on wind speed (Fig. 11), the results show significant differences between individual models and urban schemes. Only a minor impact is detected in the WRF–BULK simulation, while much higher impacts are detected in the WRF–SLUCM and WRF–BEP + BEM simulations. On the other hand, impacts on the RegCM simulations are low (especially in summer), despite using the urban canopy model. There is a clearly visible wind speed increase during daytime in all WRF simulations, caused probably by thermal processes and convection. In the evening, when the UHI manifests, these processes have higher intensity in cities than in their surroundings. During

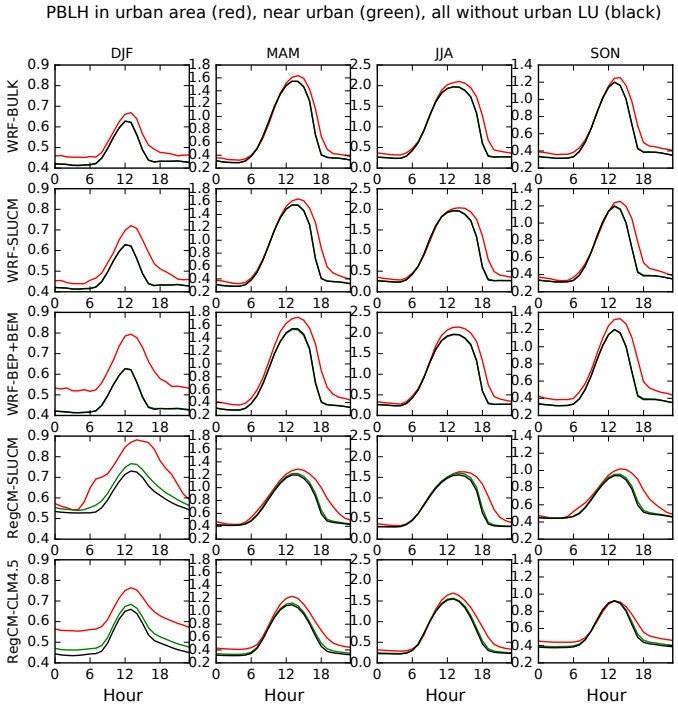

Figure 10. Averaged daily cycles of the PBLH in the Prague city centre (red), in its surroundings (green) and as simulated with the urban surface removed (black) in kilometres.

the evening, the differences in wind speed between city centres and their surroundings are also lower. In the RegCM simulations, summer wind speed daily amplitude is rather small with hardly visible hourly variation.

Similarly to their effects on surface variables, the impacts of urban surfaces on vertical profiles of meteorological variables are computed from the difference between simulations with and without urban land use. In Fig. 12, the impact of the urban surfaces on vertical distribution of temperature is shown over three selected cities (Berlin, Munich and Prague). In most of cases, this impact is visible up to the altitude of approximately 1 km in winter and 2 km in summer. In general, the urban effects in simulations with RegCM propagate to higher altitudes; however, the magnitudes close to the surface are usually smaller than in WRF. In winter, they are mostly between 1 and 2 °C on average. The W–BB simulation seems to be the warmest over cities but as said, over higher altitudes, the impact in RegCM is higher. In summer, the spread between models and urban parameterizations is smaller, mainly due to the fact that anthropogenic heat (which is not included in all experiments) plays a smaller role here. During this season, the effects in WRF sharply become small over the altitude of 200 m, while in the RegCM (in the R–S) experiment, urban-induced temperature warming can be as much as 0.5 °C at such altitudes.

Figure 13 shows the impact of the urban surfaces on the vertical profile of the horizontal wind speed for Berlin, Munich and Prague. Again, the impact is distinct up to 1 or 2 km and the highest impact is simulated in the WRF–BEP + BEM experiment (decrease of the wind speed over 2 m s^{-1}), where the impact increases with height in the first model layers. The remaining WRF simulations indicate less wind speed decrease in the overall profile, with about 1.5 m s^{-1} in the W–S and about 0.5 m s^{-1} in the W–B simulation in winter, and about 1 m s^{-1} in the W–S and up to 0.5 m s^{-1} (but with a small wind speed increase at the surface up to 0.3 m s^{-1}) in the W–B simulation in summer, respectively.

The RegCM simulations, in general, generate smaller impacts compared to WRF. The CLMU scheme gives an impact between 0.5 and 1.5 m s^{-1}. The RegCM simulation with the

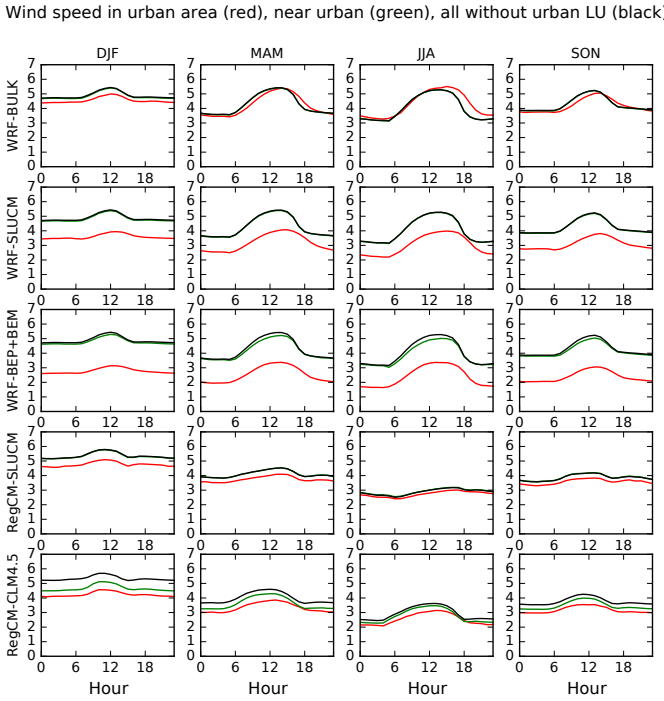

Figure 11. Averaged horizontal wind speed daily cycles ($\mathrm{m\,s^{-1}}$) in the Prague city centre (red), in its surroundings (green) and as simulated with the urban surface removed (black).

SLUCM scheme shows, however, a very small surface wind speed reduction (up to $0.5\,\mathrm{m\,s^{-1}}$).

3.3 Consequences to pollutant dispersion

Although this study is not investigating the impact of the urban surfaces on air quality, e.g. by using a coupled meteorological and chemical-transport model, we would like to outline a basic concept of how the urban surfaces impact the air quality due to modified weather and climate conditions. To achieve this, we will evaluate impacts of the urban surfaces on variables which describe the ability of the atmosphere to disperse pollutant plumes. First, this ability is given by the cleaning effect of the wind in the boundary layer, and secondly by convection and thermally inducted turbulence. To quantify these effects, we chose two indexes used by CHMI. The cleaning effect of the wind is described by the Ventilation Index (VI; Hardy et al., 2001):

$$\mathrm{VI} = \mathrm{PBLH} \cdot \overline{v}, \tag{1}$$

where $\overline{v}$ is the mean (in vertical) wind speed within the boundary layer. The dispersion effect of convection and turbulence is quantified by the Stability Index (SI; Bubník et al., 1998), which indicates the vertical stability of the atmosphere:

$$\mathrm{SI} = \frac{T_{2\,\mathrm{m}} - T_{850\,\mathrm{hPa}}}{H_{850\,\mathrm{hPa}}}, \tag{2}$$

where $T_{2\,\mathrm{m}}$ is the ground temperature, $T_{850\,\mathrm{hPa}}$ the temperature at the 850 hPa level and $H_{850\,\mathrm{hPa}}$ the mean altitude of the 850 hPa level.

Due to the fact that the wind speed is decreased by cities and conversely the PBLH is increased, it is not possible to simply infer the impact of cities on the VI. Its magnitude depends on the specific weather situation and the time of eventual coincidence between small or high values of the relevant variables. The time series of the VI does not follow the Gaussian distribution, so mean values may not be sufficiently representative and an entire distribution of the VI has to be shown. Distributions of all simulations are plotted separately, instead of relative changes between urban surface included

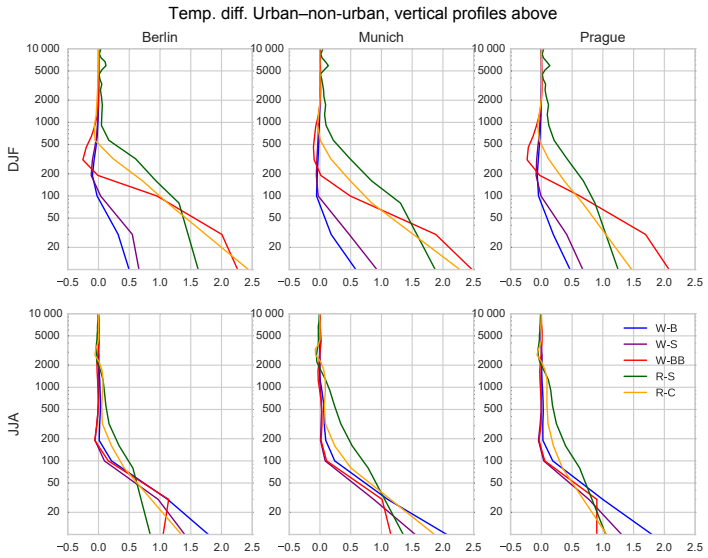

Figure 12. The impact of the urban surface inclusion on the temperature vertical profile (in °C) over selected cities. The *y* axis indicates the altitude in metres.

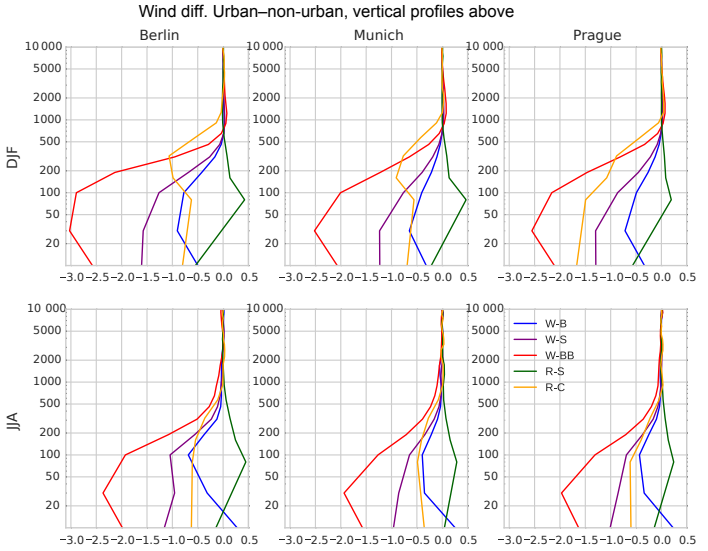

Figure 13. The impact of the urban surface inclusion on the wind speed vertical profile ($m\,s^{-1}$) over selected cities. The *y* axis indicates the altitude in metres.

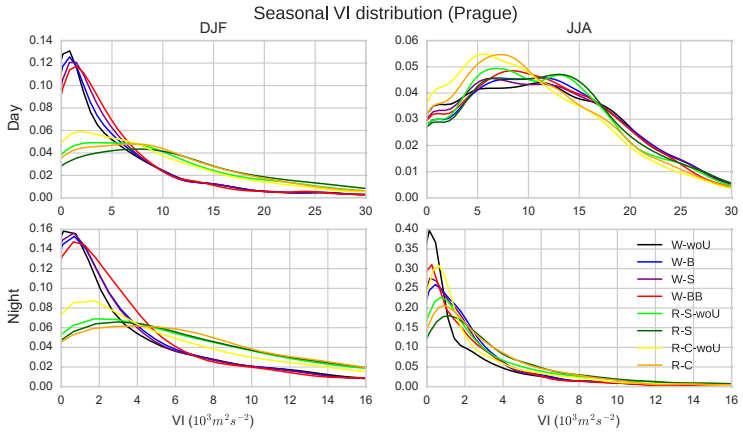

Figure 14. Seasonal distributions of the Ventilation Index (VI; in $10^3\,\mathrm{m}^2\,\mathrm{s}^{-2}$) for the city of Prague, given by all simulations. The day represents the time between 11:00 and 16:00 UTC; the night represents the time between 23:00 and 04:00 UTC. The y coordinate marks values of the estimated density function of the distribution.

or excluded simulations, because of density function values decreasing to zero. Seasonal distributions of the VI for the city of Prague are displayed in Fig. 14. In winter, there is a significant difference between the VI distributions given by the WRF and RegCM simulations. The RegCM model gives much flatter distributions and thus more favourable from the perspective of the pollutant dispersion. However, despite this great difference, all simulations indicate that the urban inclusion has a small positive impact on the VI. In summer, the differences between WRF and RegCM are smaller. Here, the inclusion of urban canopy effects increases the VI too, leading again to more favourable dispersion conditions.

The seasonal distributions of the SI for the city of Prague are shown in Fig. 15. Again, entire distributions for all simulations have to be plotted, because of the non-Gaussian distribution of the SI and its low values outside the main peaks. The negative values of the SI indicate the temperature inversion, i.e. a highly stable state of the atmosphere, with adverse conditions for the pollutant dispersion. Higher values of the SI imply more dispersive conditions. Values of the SI greater than $1 \times 10^{-2}\,\mathrm{K\,m}^{-1}$ indicate unstable state, the best from the perspective of pollutant dispersion. The winter SI distributions show a very sharp local maximum for zero SI, which is probably related to frequent occurrence of elevated temperature inversions. The position of the second maximum depends on the specific simulation. Generally, simulations with the urban surfaces shift the maximum towards higher values, indicating a positive impact of urban surfaces on the winter SI. In summer, a local maximum around zero also appears. During the summer nights, the inclusion of the urban surfaces increases the value of the SI, but in the daytime, the effect is only minor or negative (for the W–BB simulation). In summary, the urban surfaces slightly increase the SI and improve the meteorological conditions to favour pollutant dispersion.

For the other cities considered, the VI and SI distributions are almost the same as over Prague, so only the Prague data are shown and discussed.

4 Discussion

The WRF simulations are characterized by the mean temperature biases lower than 1 °C (Fig. 3), making them a reasonable basis for the analysis of the effects of urban surfaces. Mar et al. (2016), using the WRF model over Europe, reached lower temperature biases for their domain, but these values are highly dependent on the chosen physical parameterizations, domain parameters and the area of interest, as described by Katragkou et al. (2015). This is true for both temperature and precipitation biases. The RegCM simulations with the BATS land-surface scheme give temperature biases that are comparable to Huszar et al. (2016), who also employed the RegCM model with the BATS scheme. The highest temperature biases from all simulations were detected for the RegCM model with the CLM4.5 scheme. The precipitation is captured much better by the WRF model than by the RegCM model, which exhibits high precipitation overestimation. The annual cycle given by the RegCM simulation with the BATS is distinctly different from the cycle presented by Huszár et al. (2016), with the precipitation maxima occurring in winter instead of summer, given by Huszár et al. (2016) as well as the observational E-OBS data. For the CLM4.5 scheme, the precipitation characteristics are sim-

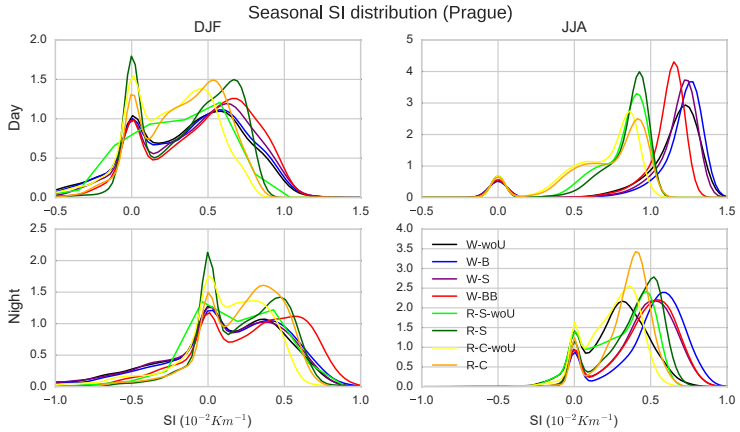

Figure 15. Seasonal distributions of the Stability Index (SI; in 10^{-2} K m^{-1}) for the city of Prague, given by all simulations. The day represents the time between 11:00 and 16:00 UTC; the night represents the time between 23:00 and 04:00 UTC. The y coordinate marks values of the estimated density function of the distribution.

ilar in shape, with strongly expressed biases. Torma et al. (2011) and Zanis et al. (2015), using an earlier version of the RegCM and performing experiments with similar resolution, concluded that the Grell convective scheme tends to overestimate precipitation over mountainous regions. Another contributing factor can be the too-wet model atmosphere caused by increased evaporation, which is indeed observed in the BATS scheme (Winter et al., 2009). Thirdly, overestimation of precipitation can be attributed to the autoconversion and raindrop evaporation rate – these parameters were tuned by Torma et al. (2011), who tried to reduce the precipitation bias in the RegCM. However, even with this tuning, some positive precipitation still remained. The observed temperature bias links to the precipitation bias: a too-wet model atmosphere leading to increased cloudiness and/or precipitation resulting in lower insolation reducing the surface temperatures. In terms of the WRF model, probably the neglect of the realistic temporal and spatial distributions of aerosols caused the summer temperature maxima overestimation, because the radiation scheme in the WRF uses values of scattering properties based on constant aerosol profiles, which is far from those over highly polluted urban areas.

The histograms of temperature differences between city centres and their surroundings (Fig. 5) show that models are able to capture the different intensity of the UHI, depending on the specific weather conditions. Model ranges of temperature differences are often even higher compared to the reference data. The urban parameters (Table 1) were chosen to describe the urban environment corresponding to the city of Prague. This can be one of the reasons why the UHI was captured with the highest agreement for this city and this stresses the importance of accurately setting urban canopy parameters. While Sarkar and De Ridder (2011) showed that the summer UHI intensity is underestimated by simple urban model in the city of Paris (by 0.5 °C), an equivalent WRF–BULK simulation indicates clear overestimation of the averaged summer UHI intensity. Trusilova et al. (2016) and Sharma et al. (2017) arrived at the same conclusion that suggests our results. Our results are well in line with the urban-canopy-induced temperature increases modelled by Trusilova et al. (2008) for central Europe, who used a single-layer urban canopy model, although our WRF–SLUCM simulation, which is closest to their setup, shows rather overestimation. The W–BB simulation has a slightly different character in this regard, exhibiting oversensitivity to the urban canopy forcing as it reacts to urban surface with a much stronger increase of the winter temperature, the summer UCI and winter minima compared to other models. This feature can be partly seen in Liao et al. (2014), where the BEP + BEM also gives the highest summer temperature minima and increases the winter temperature mean. However, in their study, which focused on the Chinese urban environment, the BEP + BEM scheme gives daily temperature profiles that are the closest ones to the reference data. This may indicate that input data can be one of the reasons why this urban canopy model performs less accurately. Further, the too-strong response in the BEP + BEM setup can also be caused by unfulfilled preconditions in the central European cities: e.g. no air conditioning but instead use of window blinds.

In all simulations, negative winter temperature biases (Fig. 6) are consistent with biases in Fig. 5. This is also true for higher summer temperature maxima given by the

WRF model, and for lower temperatures in spring, summer and autumn given by the RegCM model, especially with the CLM4.5 scheme. The diurnal temperature range (DTR) is overestimated in the summer season similarly to Liao et al. (2014). In the RegCM model, the DTR is underestimated, contrary to Huszar et al. (2014), where the DTR is rather overestimated. In terms of differences between the city and the surrounding areas, there is a good agreement in the summer morning minimum of temperature difference, except for the W–BB simulation, in which due to the oversensitivity of the urban effects, a strong UCI occurs. The lower intensity of the evening and nocturnal summer temperature increase given by the RegCM model is very similar to Huszar et al. (2014).

In general, simulations are able to capture the summer evening and nocturnal UHI (Figs. 6 and 9), with somewhat lower intensity of this phenomenon in the RegCM simulations. The BULK model gives the highest summer temperature maximum, which is in agreement with Liao et al. (2014). Also the evening and nocturnal UHI is the most intense in the WRF–BULK simulation, same as observed in Sharma et al. (2017), who also compared urban parameterizations in the WRF model for summer episodes for different urban types. In winter, there is a more notable difference between specific simulations. The simple BULK scheme has only a small impact of the urban environment (Fig. 9), in comparison to other simulations with urban canopy schemes. This is probably caused by disregarding anthropogenic heat. Regarding the temperatures, advantages of more complicated urban environment schemes seem to be only minor; perhaps the most evident improvement occurs with the winter UHI. Our results rather indicate that the most sophisticated scheme (BEP+BEM) often overemphasizes the urban effects, e.g. the summer morning UCI, which can only appear if specific weather conditions occur (Theeuwes et al., 2015), or the increased winter UHI. This conclusion contrasts with the results of Trusilova et al. (2016), where the multi-layer scheme is the only scheme that is able to correctly capture the summer UHI daily cycle. All model simulations produce the temperature maximum time shift about 1–2 h for the Prague city centre, in all seasons. This is in agreement with idealized temperature profiles for urban and rural areas given by Oke (1982) and also with observed values for the Prague area, shown by Huszar et al. (2014) or partly in Fig. 6 (besides summer).

In terms of the urban environment impact on the planetary-boundary-layer height, the differences between specific simulations are more apparent. As expected from the underlying physics and as shown in Fig. 10, the PBLH urban increase is generated by higher intensity of friction and by increased turbulent mixing caused by temperature increase. In winter, despite the low intensity of UHI, the PBLH is increased mainly by greater friction. Conversely, in the summer mornings, when the UHI is zero, there is no PBLH increase in any simulation, because the absolute value of the PBLH is too high to be impacted by friction. The BEP + BEM simulation gives the greatest increase of the PBLH, which is consistent with Liao et al. (2014).

The impact of the urban surfaces on the wind speed in 10 m is also highly dependent on the used urban scheme and the model (Fig. 11). Only a low negative impact, mostly less than 1 m s^{-1}, is indicated in all RegCM simulations. This is consistent with the results by Huszar et al. (2014) and also by Huszár et al. (2018), with smaller impacts in summer than in winter. Except for the BULK scheme, the WRF model gives a greater wind speed reduction for the city (between 1 and 2 m s^{-1}), for all seasons and times of day. The reduction is found to be the highest in the WRF–BEP + BEM simulation, which is consistent with Liao et al. (2014), despite smaller differences between the W–S and the W–BB simulations in our experiments. Regarding the wind speeds, there are significant differences between profiles given by specific urban schemes, stressing the high uncertainty of parameterization of wind within urban environment.

Similarly to impacts of urban surfaces on the 2 m temperature, the WRF model with the BULK and SLUCM schemes produces only small changes in overall temperature profile, in winter (Fig. 12). The W–BB simulation and both RegCM simulations alter the profile more significantly. In summer, the impacts on individual simulations are much more similar to each other. A weak negative impact at higher altitudes, between 2 and 10 km, indicated by Huszar et al. (2014) in their RegCM simulation, also appears, but the magnitude is negligible. As in Fig. 5, the overestimated average winter UHI at low levels (caused probably by unfulfilled preconditions for the AH flux computation) in the WRF–BEP + BEM simulation leads to the opposite annual cycle of the UHI intensity in Prague, which contrasts with observations. The UHI annual cycle is also opposite for both RegCM simulations, which is caused by slightly overestimated winter UHI and slightly underestimated summer UHI. In RegCM, the AH was prescribed as annual mean and monthly disaggregation factors, which decompose this annual value into monthly values. From the results, we can conclude that the winter AH release is probably too high leading to the UHI overestimation in winter.

Maybe it is the impact of urban surfaces on the wind speed profile (Fig. 13) where individual models/parameterizations differ the most, and not only in the shape of the profile but also in the magnitude both near the surface and at higher elevations up to a few hundreds of metres. Correct simulation of wind profiles and the whole structure of the planetary boundary layer (PBL) in the urban environment is crucial for air-quality-oriented studies and our results indicate that large uncertainty lies in the selection of the model–UCM pair.

In terms of the impact of the urban surface on the ventilation index (Fig. 14), there is one important question: why are the winter distributions given by the RegCM model flatter than distributions given by the WRF model? One reason is that the negative impact of the urban surface on the surface

wind speed is much weaker in the RegCM model and also the averaged RegCM surface wind speeds are higher in cities as well as in their surroundings (Fig. 11). The second reason is that the PBLH computed by the RegCM model is higher during the night, when weather conditions unfavourable to pollutant dispersion usually occur. The RegCM–SLUCM simulation gives the highest winter PBLH during all times of day. The winter urban VI increase can be explained by the increased PBLH, which means that the averaged wind speed is computed from a thicker boundary layer, so the lower surface wind speed in the city impacts the VI only slightly, due to the general wind speed increase with the altitude and the low impact of cities on the wind speed profile (Fig. 13). In summer, the small increase of the urban VI is caused mainly by the PBLH urban increase, manifesting for only some parts of the day. However, during the night, when the PBLH has the lowest value, the urban PBLH increase occurs and the urban VI is also increased. Despite the prevailing positive urban surface impacts on the VI, the impact may be negative during some parts of the day. For instance, in morning hours, when the intensity of the UHI is zero, the urban PBLH is not increased, but the wind speed is decreased, leading to decreases in urban VI.

The impact of the urban environment on the SI (Fig. 15) shows several interesting features. A strong peak in the SI distribution appears for zero SI in all seasons and times of day. In winter, the frequent occurrence of elevated temperature inversions probably induces this maximum. In summer, rainy episodes are likely responsible, due to great thermal capacity of water equalizing the surface and the 850 hPa temperature. Conversely, a windy episode should cause strong mixing; the SI then falls between the values of the adiabatic gradient for dry or saturated air, i.e. between 0.6 and $1 \times 10^{-2}\,\mathrm{K\,m^{-1}}$. It is therefore not easy to explain the distribution maximum during the summer days given by all WRF simulations that occurs for SI greater than $1 \times 10^{-2}\,\mathrm{K\,m^{-1}}$ (strongly convective conditions). Perhaps the near-surface temperature increase in the afternoon could cause this strong temperature gradient. It is not evident why the R–S–woU simulation does not create the zero SI peak in winter.

The increase of the VI and SI in the city and improved weather conditions with regard to the pollutant dispersion are consistent with the results by Liao et al. (2014), who showed a decrease of PM_{10} species concentration in simulations with the BEP and BEM schemes against the single-layer urban canopy scheme, in both winter and summer. Similarly, Huszár et al. (2018) described a small NO and NO_2 decrease induced by the urban environment. Conversely, the O_3 concentration increases in the city, due to better mixing of primary pollutants caused by higher boundary layer and by greater intensity of the turbulence in the urban environment. Also, Liao et al. (2015) and Tao et al. (2015), who applied a coupled meteorological and chemical-transport model (WRF-Chem) with the SLUCM and BULK methods, found that the low-level concentrations of primary pollutants decrease and ozone increases after the inclusion of urban surfaces. We can assume that the urban environment impact on the surrounding rural VI and SI will be negligible, because the impact of cities on the rural temperature, PBLH and wind speed is also mostly negligible.

5 Conclusions

We performed series of simulations with the WRF and RegCM models, together with different descriptions of the urban environment. The simulations were focused on the area of central Europe, with 10 km horizontal resolution, over the 2001–2010 period. Effects of cities were detected from differences between results of simulations with and without urban surfaces included. The validation of urban impacts on the temperature was performed using the station data from ECAD and from the Czech Hydro-Meteorological Institute.

Our study shows that, in the long-term averages, all urban schemes are able to capture the main urban meteorological feature, the evening and nighttime city temperature increase (called UHI), which mainly occurs in the summer season with the intensity of 2–3 °C on average. Moreover, all models also reproduce the morning temperature equality of the city and its surroundings. From the perspective of the temperature, there is no significant improvement of model outcomes stemming from the use of a more complicated urban scheme. This is true not only for averaged daily temperature profiles in the city against its surroundings but also for entire distributions of their differences, including daily extremes. In winter, the city temperature increase is significantly affected by the anthropogenic heat computation process.

The impact of the urban environment on the PBLH and on the surface wind speed is more dependent on the used model and urban parameterization. For example, during summer, at noon, the PBLH is about 25 % lower in RegCM simulations than in the WRF simulations. In terms of the wind speed, the impact of the city is lower in the RegCM simulations (reduction of only about $1\,\mathrm{m\,s^{-1}}$), in comparison to the WRF simulations with the urban canopy scheme (reduction of 1–$2\,\mathrm{m\,s^{-1}}$). Temperature and wind speed profiles are impacted by cities up to approximately 2 km, with mostly decreasing tendency from the surface values to zero. The values of the urban-induced impacts on the lowest model layers mostly follow up the values of these impacts at the surface. Due to the absence of reference data for these poorly observed variables, we are unable to assess which model setup gives the best results. However, our results are mostly consistent with the outcomes of previous studies and should therefore provide a reasonable basis for the study of the effects of urban surfaces.

The evaluation of the indices describing meteorological conditions from the perspective of the pollutant dispersion showed that the urban environment slightly improves these conditions in comparison to the non-urban setup, except during the summer days. This is true for both the cleansing effect

of the wind and the dispersion effect of convection and turbulence. However, it must be stressed that only the concentration of primary pollutants can be decreased by urban effects (e.g. particulate matter, sulfur and nitride oxides), and not the secondary pollutants that are created in the atmosphere (e.g. ozone), as shown by Huszár et al. (2018).

Code and data availability. The source code of the WRF model is publicly available (after registration) at http://www2.mmm.ucar.edu/wrf/users/download/get_source.html (WRF, 2018). The modelled data used in this study can be provided upon request to the corresponding author.

Author contributions. TH designed the basic idea and organized the project team. JK and PH performed the model simulations; MB configured the models and maintained the platform the experiments were run on; MŽ and MB prepared the input and validation data. JK wrote the paper, with a contribution from PH, and PP and JM revised it.

Competing interests. The authors declare that they have no conflict of interest.

Acknowledgements. This work has been funded by the project OPPPR (Proof of Concept, no. CZ.07.1.02/0.0/0.0/16_023/0000108). Further, this work has been partly supported by Charles University projects SVV no. 260447 and PROGRES – Q47/Q16. The authors wish to express their thanks to the WRF and RegCM team communities for their development of models and urban modules used in the study. We acknowledge the E-OBS dataset from the EU-FP6 project ENSEMBLES (http://ensembles-eu.metoffice.com, last access: 7 December 2016), the data providers in the ECA&D project (http://www.ecad.eu, last access: 15 February 2017) and the Department of Atmospheric Science of the University of Wyoming. This work was supported also by the Ministry of Education, Youth and Sports from the Large Infrastructures for Research, Experimental Development and Innovations project "IT4Innovations National Supercomputing Center – LM2015070".

Edited by: Yun Qian
Reviewed by: three anonymous referees

References

Angevine, W. M., White, A. B., Senff, C. J., Trainer, M., Banta, R. M., and Ayoub, M. A.: Urban-rural contrasts in mixing height and cloudiness over Nashville in 1999, J. Geophys. Res.-Atmos., 108, 4092, https://doi.org/10.1029/2001JD001061, 2003.

Best, M. J. and Grimmond, C. S. B.: Key Conclusions of the First International Urban Land Surface Model Comparison Project, B. Am. Meteorol. Soc., 96, 805–819, https://doi.org/10.1175/BAMS-D-14-00122.1, 2015.

Bubník, J., Keder, J., Macoun, J., and Mañák, J.: SYMOS'97, Systém modelování stacionárních zdroju, Czech Hydrometeorological Institute Praha, Ekoair Praha, available at: http://fzp.czu.cz/~vachm/fluid/symos_A4.pdf (last access: 19 October 2017), 1998.

Chen, F. and Dudhia, J.: Coupling an Advanced Land Surface–Hydrology Model with the Penn State–NCAR MM5 Modeling System, Part I: Model Implementation and Sensitivity, Mon. Weather Rev., 129, 569–585, https://doi.org/10.1175/1520-0493(2001)129<0569:CAALSH>2.0.CO;2, 2001.

Chen, F., Kusaka, H., Bornstein, R., Ching, J., Grimmond, C. S. B., Grossman-Clarke, S., Loridan, T., Manning, K. W., Martilli, A., Miao, S., Sailor, D., Salamanca, F. P., Taha, H., Tewari, M., Wang, X., Wyszogrodzki, A. A., and Zhang, C.: The integrated WRF/urban modelling system: development, evaluation, and applications to urban environmental problems, International J. Climatol., 31, 273–288, https://doi.org/10.1002/joc.2158, 2011.

Dee, D. P., Uppala, S. M., Simmons, A. J., Berrisford, P., Poli, P., Kobayashi, S., Andrae, U., Balmaseda, M. A., Balsamo, G., Bauer, P., Bechtold, P., Beljaars, A. C. M., van de Berg, L., Bidlot, J., Bormann, N., Delsol, C., Dragani, R., Fuentes, M., Geer, A. J., Haimberger, L., Healy, S. B., Hersbach, H., Hólm, E. V., Isaksen, L., Kållberg, P., Köhler, M., Matricardi, M., McNally, A. P., Monge-Sanz, B. M., Morcrette, J.-J., Park, B.-K., Peubey, C., de Rosnay, P., Tavolato, C., Thépaut, J.-N., and Vitart, F.: The ERA-Interim reanalysis: configuration and performance of the data assimilation system, Q. J. Roy. Meteorol. Soc., 137, 553–597, https://doi.org/10.1002/qj.828, 2011.

Dickinson, R. E., Henderson-Sellers, A., and Kennedy, P.: Biosphere–atmosphere Transfer Scheme (BATS) version 1e as Coupled to the NCAR Community Climate Model, NCAR Technical Note NCAR/TN-387+STR, https://doi.org/10.5065/D67W6959, 1993.

Fallmann, J., Forkel, R., and Emeis, S.: Secondary effects of urban heat island mitigation measures on air quality, Atmos. Environ., 125, 199–211, https://doi.org/10.1016/j.atmosenv.2015.10.094, 2016.

Folberth, G. A., Butler, T. M., Collins, W. J., and Rumbold, S. T.: Megacities and climate change – A brief overview, Environ. Pollut., 203, 235–242, https://doi.org/10.1016/j.envpol.2014.09.004, 2015.

Giorgi, F., Coppola, E., Solmon, F., Mariotti, L., Sylla, M. B., Bi, X., Elguindi, N., Diro, G. T., Nair, V., Giuliani, G., Cozzini, S., Guettler, I., O'Brien, T. A., Tawfi, A. B., Shalaby, A., Zakey, A., Steiner, A., Stordal, F., Sloan, L., and Brankovic, C.: RegCM4: Model description and preliminary tests over multiple CORDEX domains, Clim. Res., 52, 7–29, 2012.

Grell, G. A.: Prognostic Evaluation of Assumptions Used by Cumulus Parameterizations, Mon. Weather Rev., 121, 764–787, https://doi.org/10.1175/1520-0493(1993)121<0764:PEOAUB>2.0.CO;2, 1993.

Hardy, C. C., Ottmar, R. D., Peterson, J. L., Core, J. E., and Seamon, P.: Smoke management guide for prescribed and wildland fire, National Wildfire Coordinating Group, Fire Use Working Team, availablet at: https://www.nwcg.gov/sites/default/files/products/pms420-2.pdf (last access: 19 October 2017), 2001.

Haylock, M. R., Hofstra, N., Klein Tank, A. M. G., Klok, E. J., Jones, P. D., and New, M.: A European daily high-resolution gridded data set of surface temperature and precip-

itation for 1950–2006, J. Geophys. Res.-Atmos., 113, d20119, https://doi.org/10.1029/2008JD010201, 2008.

Holtslag, A. A. M., Bruijn, E. I. F. D., and Pan, H.-L.: A High Resolution Air Mass Transformation Model for Short-Range Weather Forecasting, Mon. Weather Rev., 118, 1561–1575, https://doi.org/10.1175/1520-0493(1990)118<1561:AHRAMT>2.0.CO;2, 1990.

Hou, A., Ni, G., Yang, H., and Lei, Z.: Numerical Analysis on the Contribution of Urbanization to Wind Stilling: An Example over the Greater Beijing Metropolitan Area, J. Appl. Meteorol. Clim., 52, 1105–1115, https://doi.org/10.1175/JAMC-D-12-013.1, 2013.

Huszar, P., Halenka, T., Belda, M., Zak, M., Sindelarova, K., and Miksovsky, J.: Regional climate model assessment of the urban land-surface forcing over central Europe, Atmos. Chem. Phys., 14, 12393–12413, https://doi.org/10.5194/acp-14-12393-2014, 2014.

Huszar, P., Belda, M., and Halenka, T.: On the long-term impact of emissions from central European cities on regional air quality, Atmos. Chem. Phys., 16, 1331–1352, https://doi.org/10.5194/acp-16-1331-2016, 2016a.

Huszár, P., Belda, M., Karlický, J., Pišoft, P., and Halenka, T.: The regional impact of urban emissions on climate over central Europe: present and future emission perspectives, Atmos. Chem. Phys., 16, 12993–13013, https://doi.org/10.5194/acp-16-12993-2016, 2016b.

Huszár, P., Karlický, J., Belda, M., Halenka, T., and Pišoft, P.: The impact of urban canopy meteorological forcing on summer photochemistry, Atmos. Environ., 176, 209–228, https://doi.org/10.1016/j.atmosenv.2017.12.037, 2018.

Iacono, M. J., Delamere, J. S., Mlawer, E. J., Shephard, M. W., Clough, S. A., and Collins, W. D.: Radiative forcing by long-lived greenhouse gases: Calculations with the AER radiative transfer models, J. Geophys. Res.-Atmos., 113, D13103, https://doi.org/10.1029/2008JD009944, 2008.

Jackson, T. L., Feddema, J. J., Oleson, K. W., Bonan, G. B., and Bauer, J. T.: Parameterization of Urban Characteristics for Global Climate Modeling, Ann. Assoc. Am. Geogr., 100, 848–865, https://doi.org/10.1080/00045608.2010.497328, 2010.

Janjić, Z. I.: The Step-Mountain Eta Coordinate Model: Further Developments of the Convection, Viscous Sublayer, and Turbulence Closure Schemes, Mon. Weather Rev., 122, 927–945, https://doi.org/10.1175/1520-0493(1994)122<0927:TSMECM>2.0.CO;2, 1994.

Katragkou, E., García-Díez, M., Vautard, R., Sobolowski, S., Zanis, P., Alexandri, G., Cardoso, R. M., Colette, A., Fernandez, J., Gobiet, A., Goergen, K., Karacostas, T., Knist, S., Mayer, S., Soares, P. M. M., Pytharoulis, I., Tegoulias, I., Tsikerdekis, A., and Jacob, D.: Regional climate hindcast simulations within EURO-CORDEX: evaluation of a WRF multi-physics ensemble, Geosci. Model Dev., 8, 603–618, https://doi.org/10.5194/gmd-8-603-2015, 2015.

Kiehl, J. T., Hack, J. J., Bonan, G. B., Boville, B. A., Briegleb, B. P., Williamson, D. L., and Rasch, P. J.: Description of the NCAR Community Climate Model (CCM3), NCAR Technical Note NCAR/TN-420+STR, https://doi.org/10.5065/D6FF3Q99, 1996.

Klein, P., Fedorovich, E., and Rotach, M.: A wind tunnel study of organised and turbulent air motions in urban street canyons, J. Wind Eng. Ind. Aerod., 89, 849–861, 2001.

Klein Tank, A. M. G., Wijngaard, J. B., Können, G. P., Böhm, R., Demarée, G., Gocheva, A., Mileta, M., Pashiardis, S., Hejkrlik, L., Kern-Hansen, C., Heino, R., Bessemoulin, P., Müller-Westermeier, G., Tzanakou, M., Szalai, S., Pálsdóttir, T., Fitzgerald, D., Rubin, S., Capaldo, M., Maugeri, M., Leitass, A., Bukantis, A., Aberfeld, R., van Engelen, A. F. V., Forland, E., Mietus, M., Coelho, F., Mares, C., Razuvaev, V., Nieplova, E., Cegnar, T., Antonio López, J., Dahlström, B., Moberg, A., Kirchhofer, W., Ceylan, A., Pachaliuk, O., Alexander, L. V., and Petrovic, P.: Daily dataset of 20th-century surface air temperature and precipitation series for the European Climate Assessment, International J. Climatol., 22, 1441–1453, https://doi.org/10.1002/joc.773, 2002.

Kusaka, H. and Kimura, F.: Coupling a Single-Layer Urban Canopy Model with a Simple Atmospheric Model: Impact on Urban Heat Island Simulation for an Idealized Case, J. Meteorol. Soc. of Jpn,, 82, 67–80, https://doi.org/10.2151/jmsj.82.67, 2004.

Kusaka, H., Kondo, H., Kikegawa, Y., and Kimura, F.: A Simple Single-Layer Urban Canopy Model For Atmospheric Models: Comparison With Multi-Layer And Slab Models, Bound.-Lay. Meteorol., 101, 329–358, https://doi.org/10.1023/A:1019207923078, 2001.

Lawrence, D. M., Oleson, K. W., Flanner, M. G., Thornton, P. E., Swenson, S. C., Lawrence, P. J., Zeng, X., Yang, Z.-L., Levis, S., Sakaguchi, K., Bonan, G. B., and Slater, A. G.: Parameterization improvements and functional and structural advances in Version 4 of the Community Land Model, J. Adv. Model. Earth Sy., 3, m03001, https://doi.org/10.1029/2011MS00045, 2011.

Lee, S.-H., Kim, S.-W., Angevine, W. M., Bianco, L., McKeen, S. A., Senff, C. J., Trainer, M., Tucker, S. C., and Zamora, R. J.: Evaluation of urban surface parameterizations in the WRF model using measurements during the Texas Air Quality Study 2006 field campaign, Atmos. Chem. Phys., 11, 2127–2143, https://doi.org/10.5194/acp-11-2127-2011, 2011.

Liao, J., Wang, T., Wang, X., Xie, M., Jiang, Z., Huang, X., and Zhu, J.: Impacts of different urban canopy schemes in WRF/Chem on regional climate and air quality in Yangtze River Delta, China, Atmos. Res., 145, 226–243, https://doi.org/10.1016/j.atmosres.2014.04.005, 2014.

Liao, J., Wang, T., Jiang, Z., Zhuang, B., Xie, M., Changqin, Y., Wang, X., Zhu, J., Fu, Y., and Zhang, Y.: WRF/Chem modeling of the impacts of urban expansion on regional climate and air pollutants in Yangtze River Delta, China, Atmos. Environ., 106, 204–214, 2015.

Liu, Y., Chen, F., Warner, T., and Basara, J.: Verification of a Mesoscale Data-Assimilation and Forecasting System for the Oklahoma City Area during the Joint Urban 2003 Field Project, J. Appl. Meteorol. Clim., 45, 912–929, https://doi.org/10.1175/JAM2383.1, 2006.

Mar, K. A., Ojha, N., Pozzer, A., and Butler, T. M.: Ozone air quality simulations with WRF-Chem (v3.5.1) over Europe: model evaluation and chemical mechanism comparison, Geosci. Model Dev., 9, 3699–3728, https://doi.org/10.5194/gmd-9-3699-2016, 2016.

Martilli, A., Clappier, A., and Rotach, M. W.: An Urban Surface Exchange Parameterisation for Mesoscale

Models, Bound.-Lay. Meteorol., 104, 261–304, https://doi.org/10.1023/A:1016099921195, 2002.

Meehl, G. A. and Tebaldi, C.: More Intense, More Frequent, and Longer Lasting Heat Waves in the 21st Century, Science, 305, 994–997, https://doi.org/10.1126/science.1098704, 2004.

Morrison, H., Thompson, G., and Tatarskii, V.: Impact of Cloud Microphysics on the Development of Trailing Stratiform Precipitation in a Simulated Squall Line: Comparison of One- and Two-Moment Schemes, Mon. Weather Rev., 137, 991–1007, https://doi.org/10.1175/2008MWR2556.1, 2009.

Oke, T. and Maxwell, G.: Urban heat island dynamics in Montreal and Vancouver, Atmos. Environ., 9, 191–200, https://doi.org/10.1016/0004-6981(75)90067-0, 1975.

Oke, T. R.: The energetic basis of the urban heat island, Q. J. Roy. Meteorol. Soc., 108, 1–24, https://doi.org/10.1002/qj.49710845502, 1982.

Oleson, K., Lawrence, D. M., Bonan, G. B., Drewniak, B., Huang, M., Koven, C. D., Levis, S., Li, F., Riley, W. J., Subin, Z. M., Swenson, S. C., Thornton, P. E., Bozbiyik, A., Fisher, R., Heald, C. L., Kluzek, E., Lamarque, J.-F., Lawrence, P. J., Leung, L. R., Lipscomb, W., Muszala, S., Ricciuto, D. M., Sacks, W., Sun, Y., Tang, J., and Yang, Z.-L.: Technical Description of version 4.5 of the Community Land, https://doi.org/10.5065/D6RR1W7M, 2013.

Oleson, K. W., Bonan, G. B., Feddema, J., Vertenstein, M., and Grimmond, C. S. B.: An Urban Parameterization for a Global Climate Model, Part I: Formulation and Evaluation for Two Cities, J. Appl. Meteorol. Clim., 47, 1038–1060, https://doi.org/10.1175/2007JAMC1597.1, 2008.

Pal, J. S., Small, E. E., and Eltahir, E. A. B.: Simulation of regional-scale water and energy budgets: Representation of subgrid cloud and precipitation processes within RegCM, J. Geophys. Res.-Atmos., 105, 29579–29594, https://doi.org/10.1029/2000JD900415, 2000.

Roth, M.: Review of atmospheric turbulence over cities, Q. J. Roy. Meteorol. Soc., 126, 941–990, https://doi.org/10.1002/qj.49712656409, 2000.

Salamanca, F., Krpo, A., Martilli, A., and Clappier, A.: A new building energy model coupled with an urban canopy parameterization for urban climate simulations – part I. formulation, verification, and sensitivity analysis of the model, Theor. Appl. Climatol., 99, 345–356, https://doi.org/10.1007/s00704-009-0142-9, 2009.

Sarkar, A. and De Ridder, K.: The Urban Heat Island Intensity of Paris: A Case Study Based on a Simple Urban Surface Parametrization, Bound.-Lay. Meteorol., 138, 511–520, https://doi.org/10.1007/s10546-010-9568-y, 2011.

Sharma, A., Fernando, H. J., Hamlet, A. F., Hellmann, J. J., Barlage, M., and Chen, F.: Urban meteorological modeling using WRF: a sensitivity study, Int. J. Climatol., 37, 1885–1900, https://doi.org/10.1002/joc.4819, 2017.

Skamarock, W. C., Klemp, J. B., Dudhia, J., Gill, D. O., Barker, D. M., Duda, M., Huang, X.-Y., Wang, W., and Powers, J. G.: A Description of the Advanced Research WRF Version 3, NCAR Technical Note, National Center for Atmospheric Research, Boulder CO, USA, https://doi.org/10.5065/D68S4MVH, 2008.

Tao, W., Liu, J., Ban-Weiss, G. A., Hauglustaine, D. A., Zhang, L., Zhang, Q., Cheng, Y., Yu, Y., and Tao, S.: Effects of urban land expansion on the regional meteorology and air quality of eastern China, Atmos. Chem. Phys., 15, 8597–8614, https://doi.org/10.5194/acp-15-8597-2015, 2015.

Theeuwes, N. E., Steeneveld, G.-J., Ronda, R. J., Rotach, M. W., and Holtslag, A. A. M.: Cool city mornings by urban heat, Environ. Res. Lett., 10, 114022, https://doi.org/10.1088/1748-9326/10/11/114022, 2015.

Tiedtke, M.: A Comprehensive Mass Flux Scheme for Cumulus Parameterization in Large-Scale Models, Mon. Weather Rev., 117, 1779–1800, https://doi.org/10.1175/1520-0493(1989)117<1779:ACMFSF>2.0.CO;2, 1989.

Torma, C., Coppola, E., Giorgi, F., Bartholy, J., and Pongrácz, R.: Validation of a High-Resolution Version of the Regional Climate Model RegCM3 over the Carpathian Basin, J. Hydrometeorol., 12, 84–100, https://doi.org/10.1175/2010JHM1234.1, 2011.

Trusilova, K., Jung, M., Churkina, G., Karstens, U., Heimann, M., and Claussen, M.: Urbanization Impacts on the Climate in Europe: Numerical Experiments by the PSU–NCAR Mesoscale Model (MM5), J. Appl. Meteorol. Clim., 47, 1442–1455, https://doi.org/10.1175/2007JAMC1624.1, 2008.

Trusilova, K., Schubert, S., Wouters, H., Früh, B., Grossman-Clarke, S., Demuzere, M., and Becker, P.: The urban land use in the COSMO-CLM model: a comparison of three parameterizations for Berlin, Meteorol. Z., 25, 231–244, https://doi.org/10.1127/metz/2015/0587, 2016.

United Nations, Department of Economic and Social Affairs, P. D.: World Urbanization Prospects: The 2014 Revision, Highlights, NCAR Technical Note, National Center for Atmospheric Research, Boulder CO, USA, available at: https://esa.un.org/unpd/wup/publications/files/wup2014-highlights.pdf (last access: 21 September 2017), 2014.

Winter, J. M., Pal, J. S., and Eltahir, E. A. B.: Coupling of Integrated Biosphere Simulator to Regional Climate Model Version 3, J. Climate, 22, 2743–2757, https://doi.org/10.1175/2008JCLI2541.1, 2009.

WRF: Source code of the WRF model, available at: http://www2.mmm.ucar.edu/wrf/users/download/get_source.html, last access: 17 July 2018.

Zanis, P., Katragkou, E., Ntogras, C., Marougianni, G., Tsikerdekis, A., Feidas, H., Anadranistakis, E., and Melas, D.: Transient high-resolution regional climate simulation for Greece over the period 1960–2100: evaluation and future projections, Clim. Res., 64, 123–140, 2015.

Zhao, L., Lee, X., Smith, R. B., and Oleson, K.: Strong contributions of local background climate to urban heat islands, Nature, 511, 216–219, https://doi.org/10.1038/nature13462, 2014.